SPIRE SPT EMC Test Report

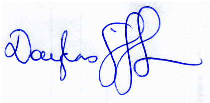

Digitally signed by Douglas Griffin
DN: cn=Douglas Griffin, o, ou=RAL-SSTD, email=D.K.Griffin@rl.ac.uk, c=GB
Date: 2009.01.26 10:03:59 Z

Change Control

Issue	Change	Date
0.1	As initially issued for discussion during JPL telecon	
1.0	Issued for IFAR Co-location meeting	17/11/2008

1. Introduction

This document reports on the analysis of the EMC tests carried out within the scope of the Herschel/SPIRE SPT tests at ESTEC from 20/08/2008 to 23/08/2008.

2. Reference and Applicable Documents

RD	Name	Doc Number
RD 1	SPIRE SPT EMC CS Pre-calibration test	SPIRE-RAL-REP-003039
RD 2	SPIRE PFM5 EMC Test Report	SPIRE-RAL-REP-002852
RD 3	SPIRE CS Test Levels for SPT	SPIRE-RAL-NOT-003041
RD 4	SPIRE IST Specific Performance Test Procedures	SPIRE-RAL-PRC-002704, Iss. 3
RD 5	Herschel FM Radiated EMC Test in Clean Room Facility Data Report	ETS-REP-EMC-2574, Iss 2
RD 6	NHSC / IPAC SPIRE wiki site https://nhscdmz1.ipac.caltech.edu/pmwiki/pmwiki.php/Spire/HomePage	N/A

3. Test Configuration

3.1 EUT Summary

Item	Description
FPU	PFM
Cryoharness	FM
WIH	FM
DCU	PFM
PSU	PFM
FCU	PFM
DPU	PFM
DPU 28V Power Harness	PFM
FCU/PSU 28V Power Harness	PFM with in-line test adaptor
SVM	PFM
PCDU	PFM

3.2 Test Equipment

Item	Description
Test Adaptor	DB01-J04 as per Figure 2 and Figure 3
BCI Clamp	8-50MHz F-130A
Current Clamp Probe	8-50MHz F-16
Signal generator	8-100MHz Agilent HP 33250
RF Amplifier	8-100MHz Amplifier Research 50WD1000
Spectrum Analyzer	HP4395A
Digital Oscilloscope	With isolated inputs

Item	**Description**
Test equipment benches / supports etc.	Sufficient bench space and/or secure locations to mount the test equipment close to the Test Adaptor
Inline power meter	R&S NRP

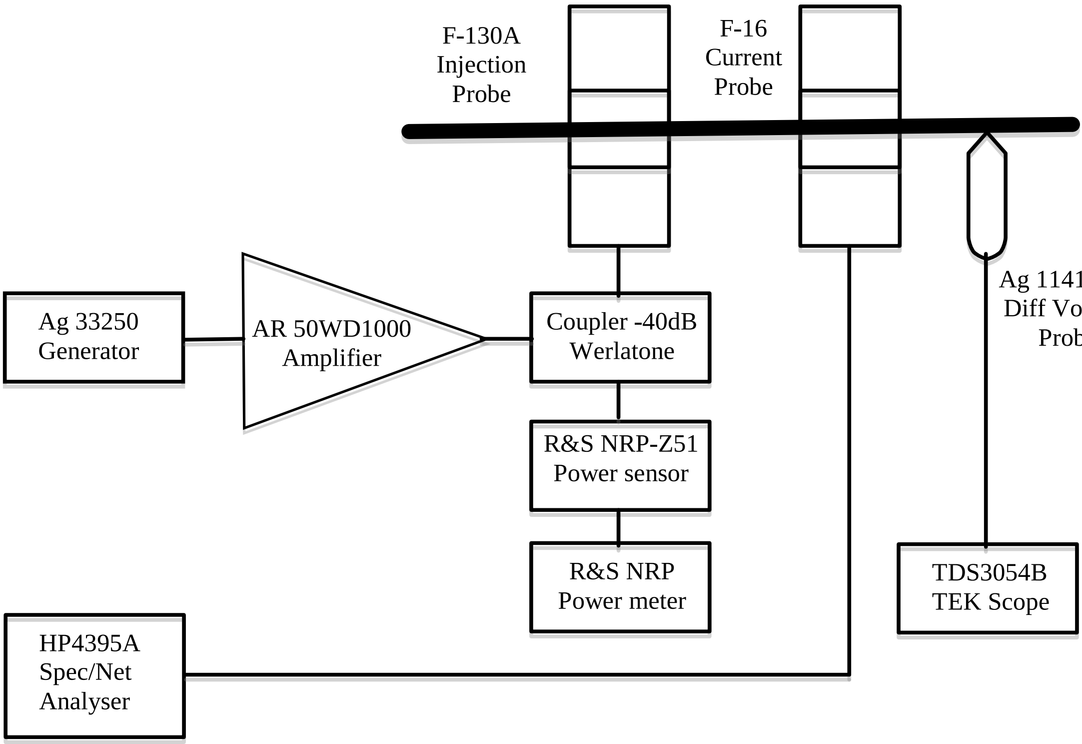

Figure 1 – Schematic of conducted susceptibility test setup

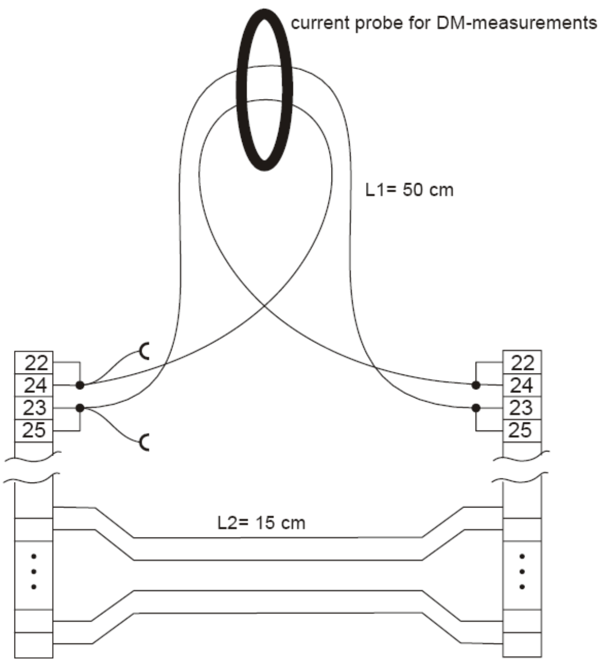

Figure 2 – Test adaptor configuration. Wires to be 20AWG

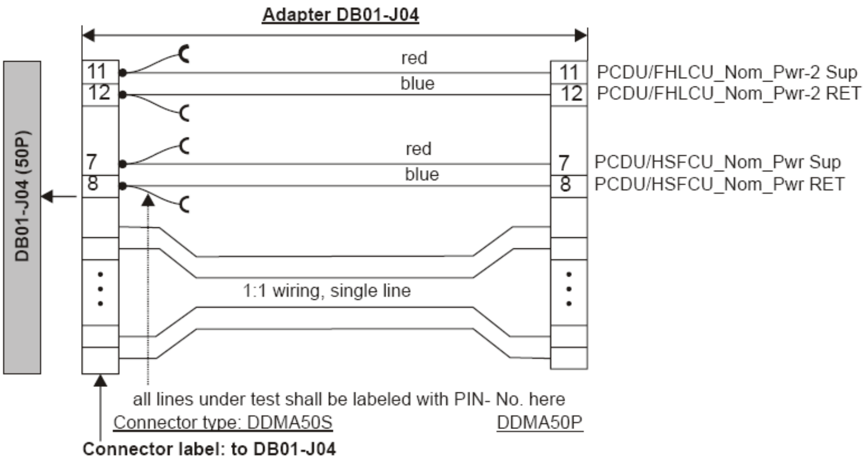

Figure 3 – Details of SPIRE test adaptor

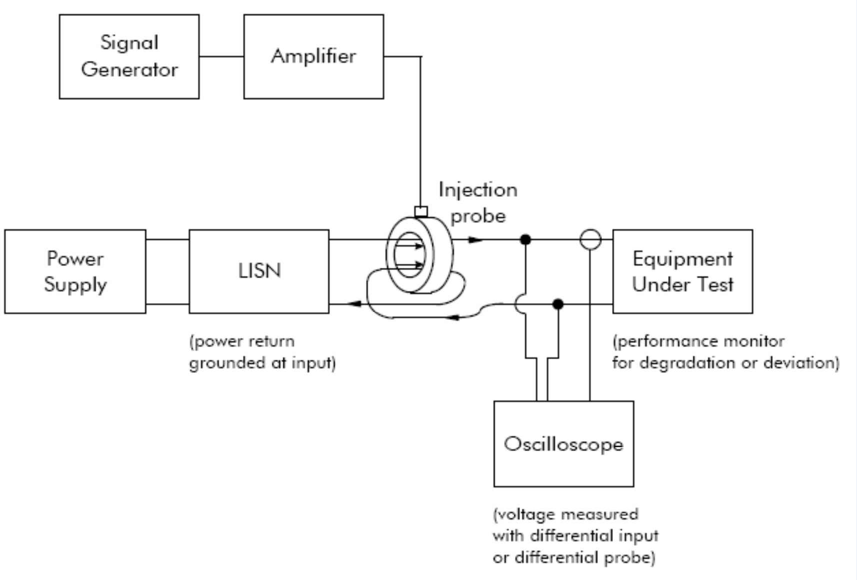

Figure 4 – DM configuration

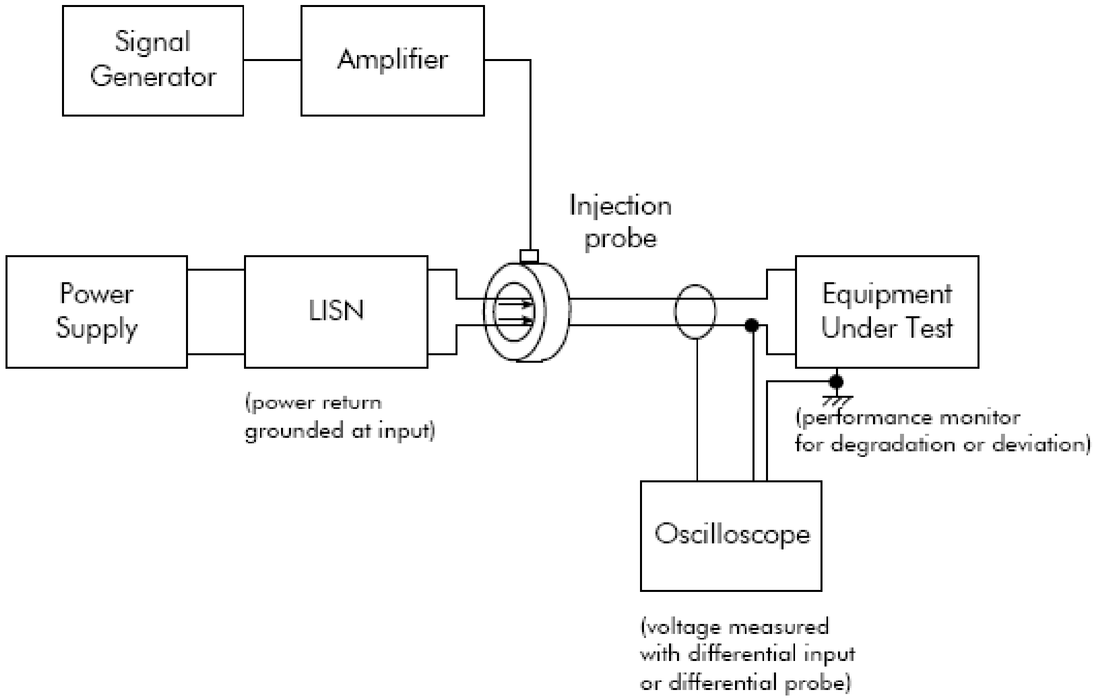

Figure 5 - CM configuration

4. Test Sequence

Test Description	ObsID
CS DM Phot. mode	0xB00014BE
CS DM Spect. Mode	0xB00014C7
CS CM Phot. Mode	0xB00014D8
CS CM Spect. Mode	0xB00014E1
RS test, Spect. Mode Vertical Polarization	0xB00014E3
RS test, Phot. Mode Vertical Polarization	0xB00014EB (Step 1)
RS test, Phot. Mode Horizontal Polarization	0xB00014EB (Step 2)

5. Discussion and Conclusions

5.1 Radiated Emissions

A measurement of the ambient E-Field in the clean room environment was added to the SPT procedure for the instruments when it was decided that there was to be no spacecraft RS testing with the Herschel instruments in their most sensitive modes in the Maxwell facility. In its place, the revised approach to RS testing of SPIRE in the Herschel cryostat foresaw that a comparison of;

1. the E-Field spectrum measured during the RE tests in the Maxwell facility with the instruments/spacecraft in their most noisy modes,
2. measurements of the ambient levels during the SPT test, and
3. measurements of the detector noise levels during the SPT with the detectors in their most sensitive mode,

would provide the necessary information to provide and indication the level of auto-compatibility of SPIRE with the rest of the Herschel spacecraft. For both test setups, the field was measured in a location close to the SPIRE Cryoharness. For information only, the results of the E-Field measurements are reported in Appendix 4. In the frequency band of 10-100MHz, where SPIRE has been found to be most susceptible to EMI in the EQM and SPT2 test, the levels are close to each other except for a narrow range around 30MHz, where the levels in the SPT tests are 10-20 dB lower than the tests in the Maxwell facility. This implies that the EM environment in the SPT was more benign in this band than the RE test in the Maxwell facility. One possible explanation for the discrepancy between the measurements in the Maxwell facility and the clean room was the presence of cryo-GSE and aluminium scaffolding which could afford a level of electromagnetic shielding/attenuation to the environment near to the SPIRE cryoharnesses at certain frequencies. The discrepancy could also be explained by subtle differences in the location and precise geometry of the measurement antennas in the two configurations.

During the SPIRE SPT, the noise performance of the instrument was measured under various bias levels and frequencies. The results are documented in RD6. For the Photometer, the noise levels as indicated by the criteria of NEP are slightly better than the levels measured during ILT (PFM5 in particular). Overall, the spectrometer noise performance is comparable with the performance seen in ILT, although the SLW array shows slightly higher noise levels. This excess noise is described as being due to “signal wiggling” in the time domain, and therefore confined to the low frequency portion of the detector response spectrum. This would give rise to an increase in the 1/f noise floor of the detectors. There is an indication from the noise measurements that there is excess optical power on some of the detectors (PSW, PMW, PLW and SSW).

The conclusions therefore from the RE and noise measurements are as follows:

- The ambient levels measured during the SPT test are slightly lower in some spectral bands (in particular around 30MHz), and therefore there is negative margin on the field amplitudes with respect to the RE test in some portions of the spectrum

• The detector noise performance does not indicate any major compliance issues and is in-line with the ILT performance results
• Within the caveats stated, SPIRE has been shown auto-compatibility with Herschel in the clean room environment.

5.2 Susceptibility Tests

The detector data collected during the radiated and conducted susceptibility tests was processed according to the following procedure:

1. The start and end times of the period during which EMI was injected was determined from the instrument housekeeping telemetry
2. The detector science data for this period was extracted from the database and separated into ten second segments.
3. A second order polynomial was fitted to each of these timelines and then subtracted from the data in an attempt to remove the DC offset and compensate for thermal drifts in the data
4. The Power Spectral Density of each of these traces was calculated and then averaged across all the ten second data segments.
5. The average PSD was estimated from the overall rms signal level and the signal bandwidth of the measurement.

The data is presented in two formats;

1. 2D X-Y Plots of the average PSD against the test frequency. These plots allow quick identification of detector channels which demonstrate an increase in the overall noise amplitude under the test.
2. 2D contour plots of the PSD with frequency on the horizontal axis, test number on the vertical axis and plot colour representing PSD.

There are several features of the detector science data need to be explained when interpreting the results.

1. The detector output occasionally shows an impulse response to an unknown stimulation. The rise time of this is less than the sampling period. The recovery time is longer, but much shorter than the thermal time constant of the bolometers. This behaviour was seen on several occasions. The effect of this is to indicate a large increase in the noise level in the detector, particularly in the X-Y noise plots. As this behaviour is know to occur randomly during nominal detector operation, it is assumed that it is not correlated with the EMI injection.
2. Temperature fluctuations within the cryostat will in general influence the thermal equilibrium of the instrument and cause temperature fluctuations in the 300-mK system. These fluctuations are identified by a change in the level and/or slope of the DC offset of all the detectors in the array.
3. Apart from the normal detectors which are sensitive to sub-mm optical sources, there are also several extra detectors in each array which are not optically sensitive. These include, (1) dark pixels which are identical to the normal detectors apart from the fact that they have no feed horns to couple radiation, (2) thermistor detectors which are directly mounted on the 300-mK bath and (3) resistor channels which have identical readout to the other detectors, but have a constant impedance and therefore no response to temperature changes. These different detector channels can be used to discriminate between different types of power coupled onto the detectors.

5.3 Conducted Susceptibility

The process results from the Differential mode tests are presented in Appendix 1 and the processed results from the Common Mode tests are presented in Appendix 2.

The following general remarks and conclusions can be made:

- In the DM test of the Photometer detectors, an apparent susceptibility appears at a test injection frequency of ~ 24 MHz. This has been identified as a being due to a change in temperature of a non-optical source, most probably the lid. In particular, it is noted that the non-optical detectors show no response to the disturbance. Furthermore, as the disturbance is identified in the PLW detector array and not, the PMW or PSW arrays, it can be concluded that the temperature of the source is less than ~ 10K, which makes the lid of the cryostat a likely candidate. It should be noted that the spacecraft thermometry of the lid is not capable of measuring these levels of temperature fluctuations.
- The spectrogrammes for the DM spectrometer tests show narrow band spectral lines at an intensity level higher than the general noise levels. This is similar to the response of the PMW detectors to a continuous, un-modulated conducted DM disturbance during the PFM5 ILT test where such a feature was seen at ~1.5Hz. Careful examination of the data reveals that the spectral features are present during the reference cases before and after the disturbance injection, and therefore the source of the features cannot be correlated with EMI. The source of the disturbance could possibly be attributed to microphonics but no definite conclusions can be made.
- Several instances of detectors suffering from impulse response have been observed. They are identified in the tables of power spectral density vs. test frequency.
- Several detectors show excess noise, but are known to have degraded performance and show no correlation with the injected EMI.
- In the Photometer CM PLW spectrogrammes show an apparent increase in the noise spectral density at low detector signal frequencies. This noise increases as the injected frequency increases. This excess noise is attributed to temperature fluctuations of an object which is optically coupled to the detector arrays. The basis for this conclusion is the fact that the disturbances are confined to the optically active detectors on the PLW array and that the band of the noise is very low (in the 100 mHz range) which corresponds to the expected periods of temperature fluctuations in the cryostat and not related to the EMI disturbance. Furthermore, the level of the amplitude of the excess noise does not change between the highest injection frequency case (50MHz) and the last reference test when the injection was switched off.
- Apart from the anomalies noted above, no correlation of the detector noise can be made with the injected CM or DM EMI.
- Given that the level of the injected disturbance was more than 6dB above the levels measured on the SPIRE FCU primary power lines during the Spacecraft CE tests and that previous susceptibilities have shown a power law dependency, it can be concluded that there is at least 12dB of margin.

5.4 Radiated Susceptibility

Three separate RS E-Field tests were carried out; two in photometer mode: one with Vertical polarization and the other in Vertical polarization. The last test was in spectrometer mode vertical polarization. The process test results are reported in Appendix 4. The following comments and conclusions are noted:

- The general comments and conclusions for the radiated tests are similar to those for the conducted test in that the excess noise seen on the detectors can be attributed to temperature fluctuations of objects optically coupled to the detectors. The exception to this is the behaviour of DP1 and DP2 which showed variations in the level of noise (in the low frequency end of the detector response spectrum).

- There is a considerable level of un-certainty in the injected levels due to the presence of cryo-GSE and aluminium scaffolding in close proximity to the radiating antenna. This could either raise or lower the local field strength in the proximity of the SPIRE cryoharness.
- Given these comments, it can be concluded that the instrument does not show any serious radiated susceptibilities.

6. Appendix 1: CS Differential Mode Detailed Results

6.1 CS Differential Mode – Photometer (0xB00014BE)

6.1.1 Noise PSD (using 49 seconds of detector data)

CS DM Photometer Mode Average PSD Across PSW, PMW and PLW Arrays
(49 Second step length)

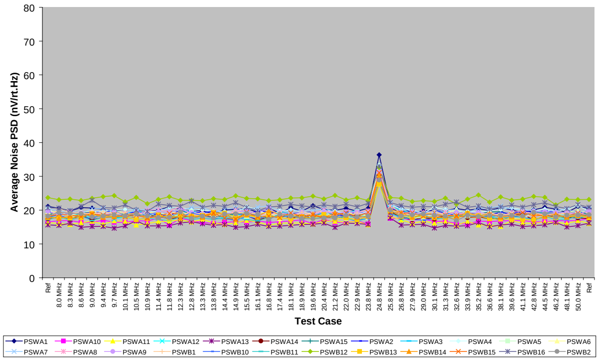

PSW

CS DM Photometer Mode Average PSD Across PSW, PMW and PLW Arrays
(49 Second step length)

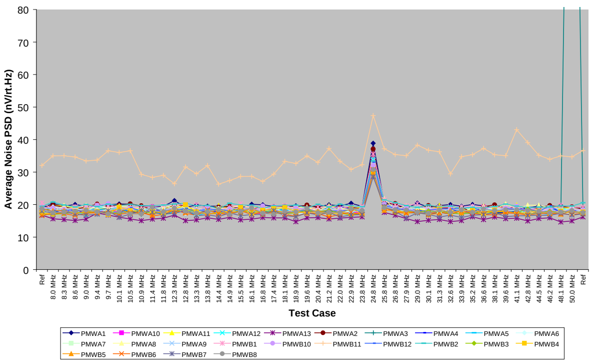

PMW B11 Noisy; PMW A3 “spikes”

6.1.2 *Noise PSD (Averaged using N 10 second “chunks” of detector data)*

CS DM Photometer Mode Average PSD Across PSW, PMW and PLW Arrays
(10 Second step length – Ensemble averaged)

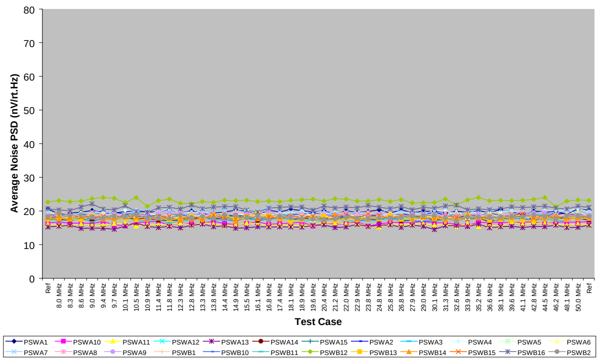

PSW

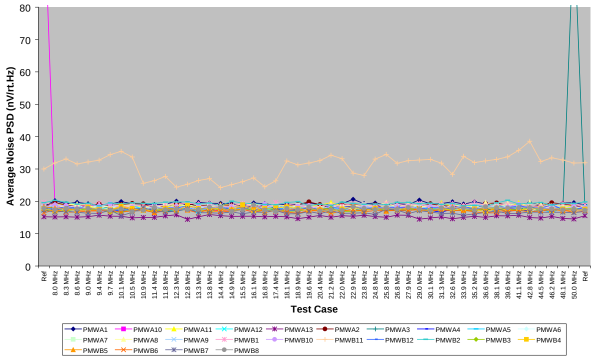

PMW B11 Noisy; PMW A10 and A3 “spike”

6.1.3 PSW Spectrogrammes

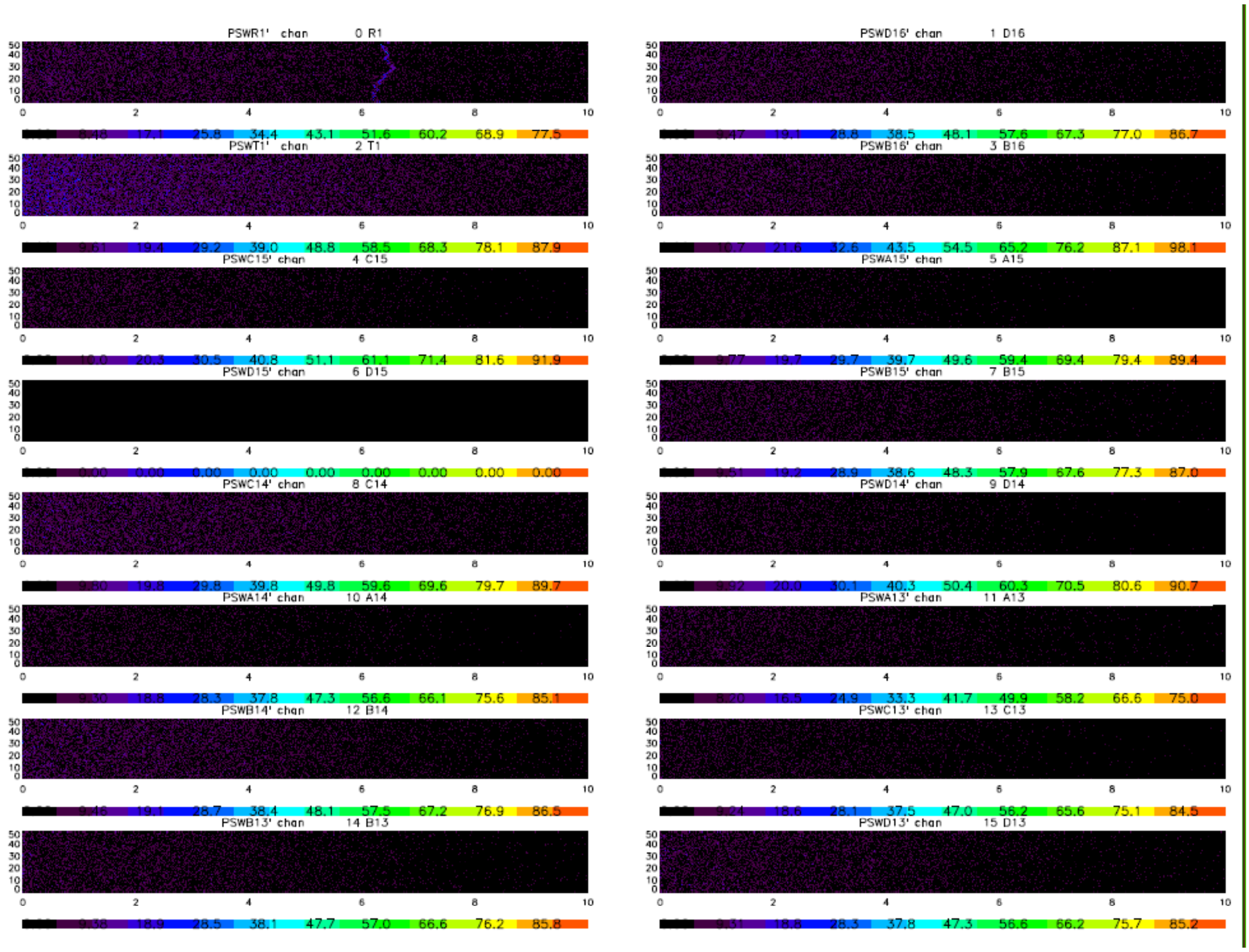

Figure 6 – PSW R1 shows spectral feature. Feature present in reference tests.

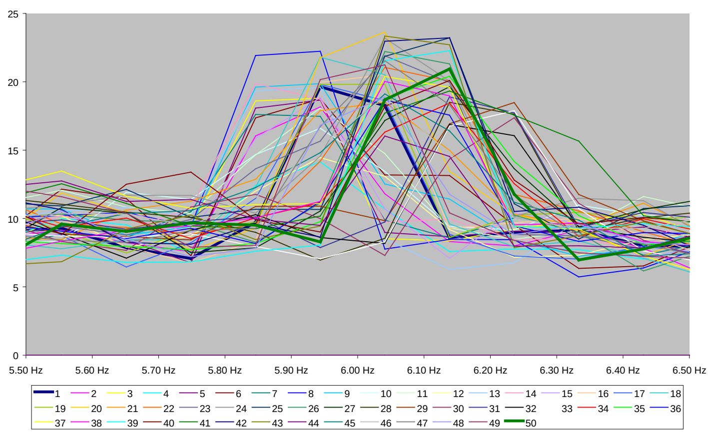

Figure 7 - PSW R1 spectra. Reference tests; Steps 1 and 50 (highlighted blue and green) show spectra feature present during the rest of the test indicating that there is no excess EMI on the detector

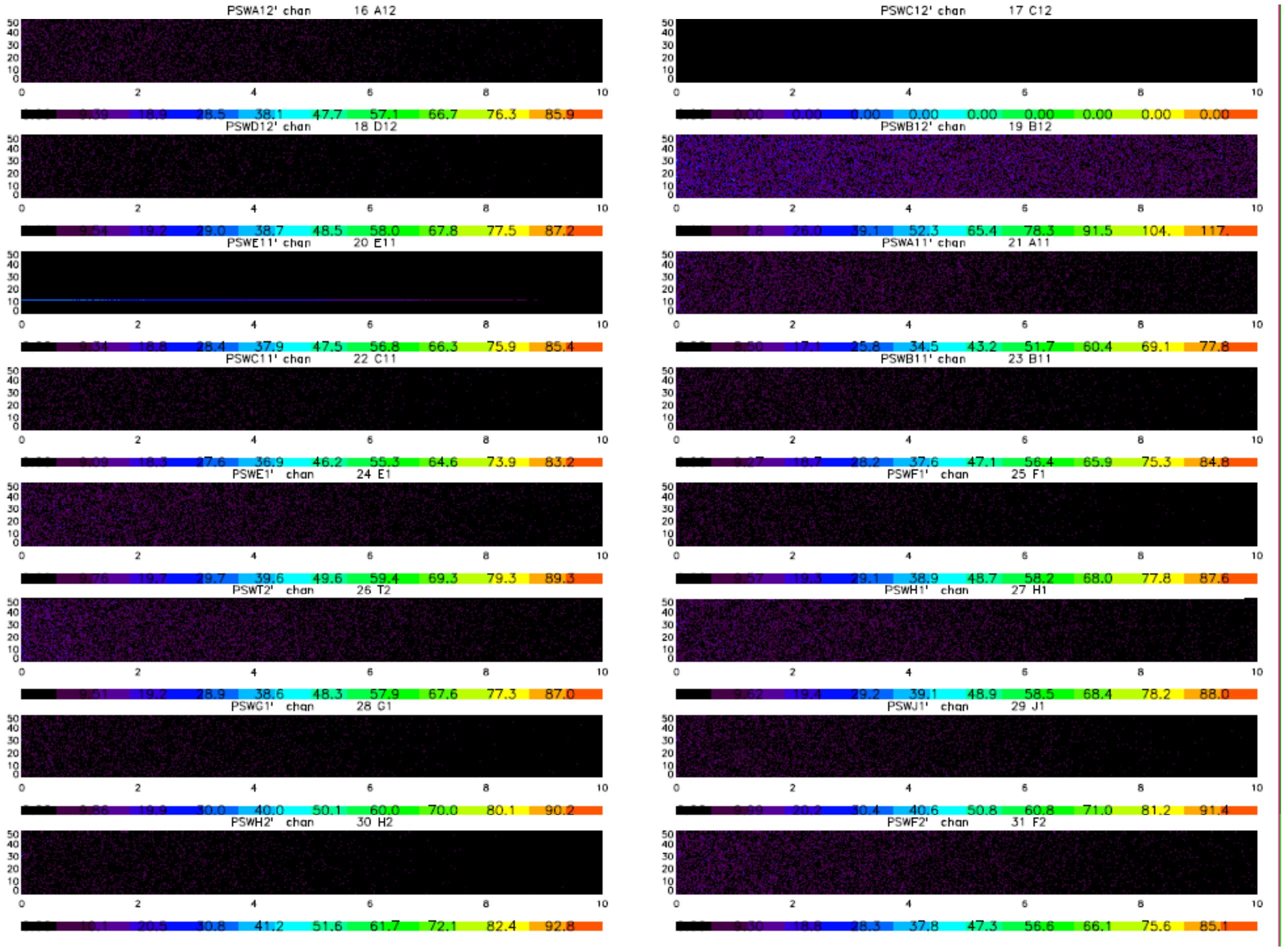

Figure 8 – Detector PSW E11"drops out"

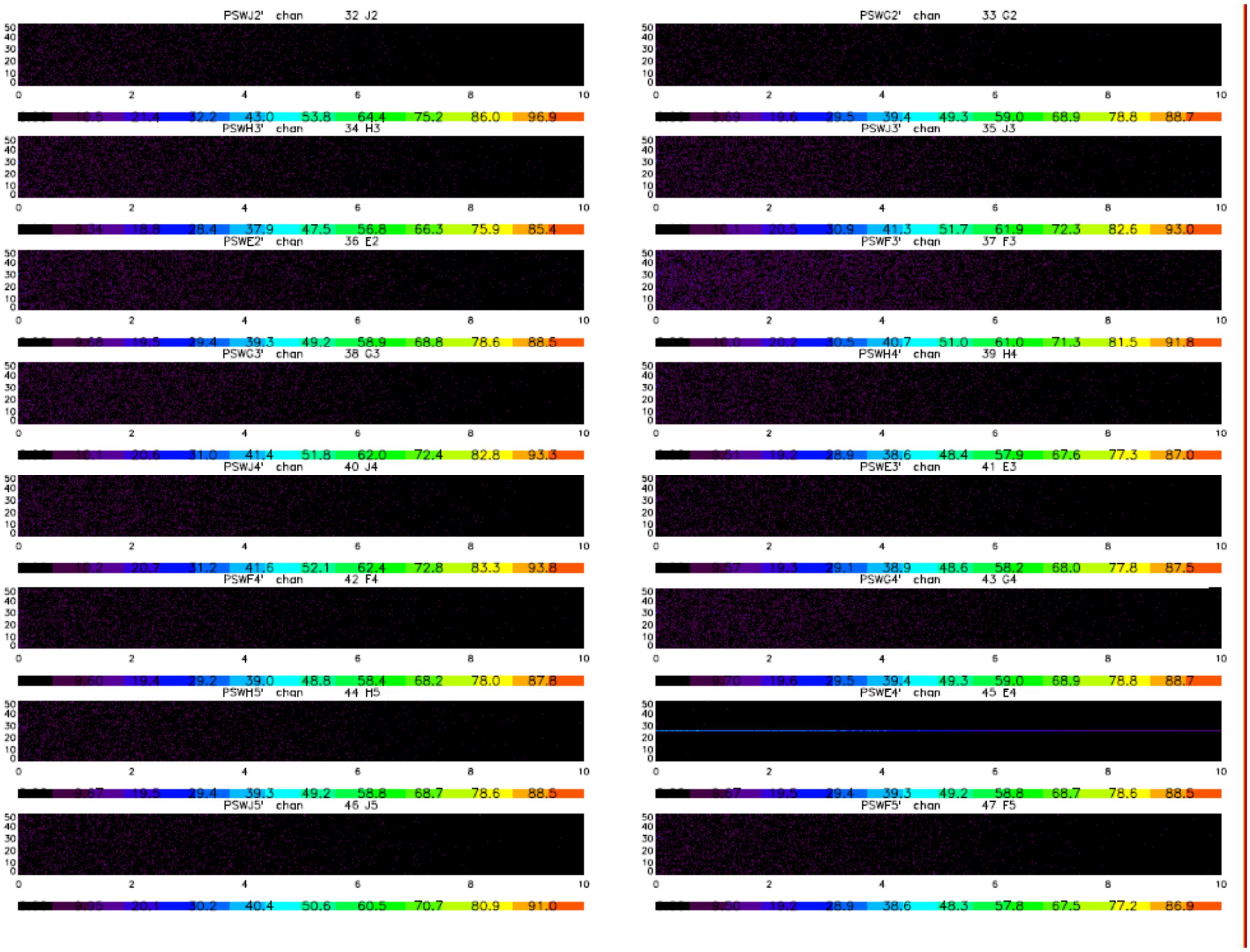

Figure 9 – PSW E4 shows a "drop out"

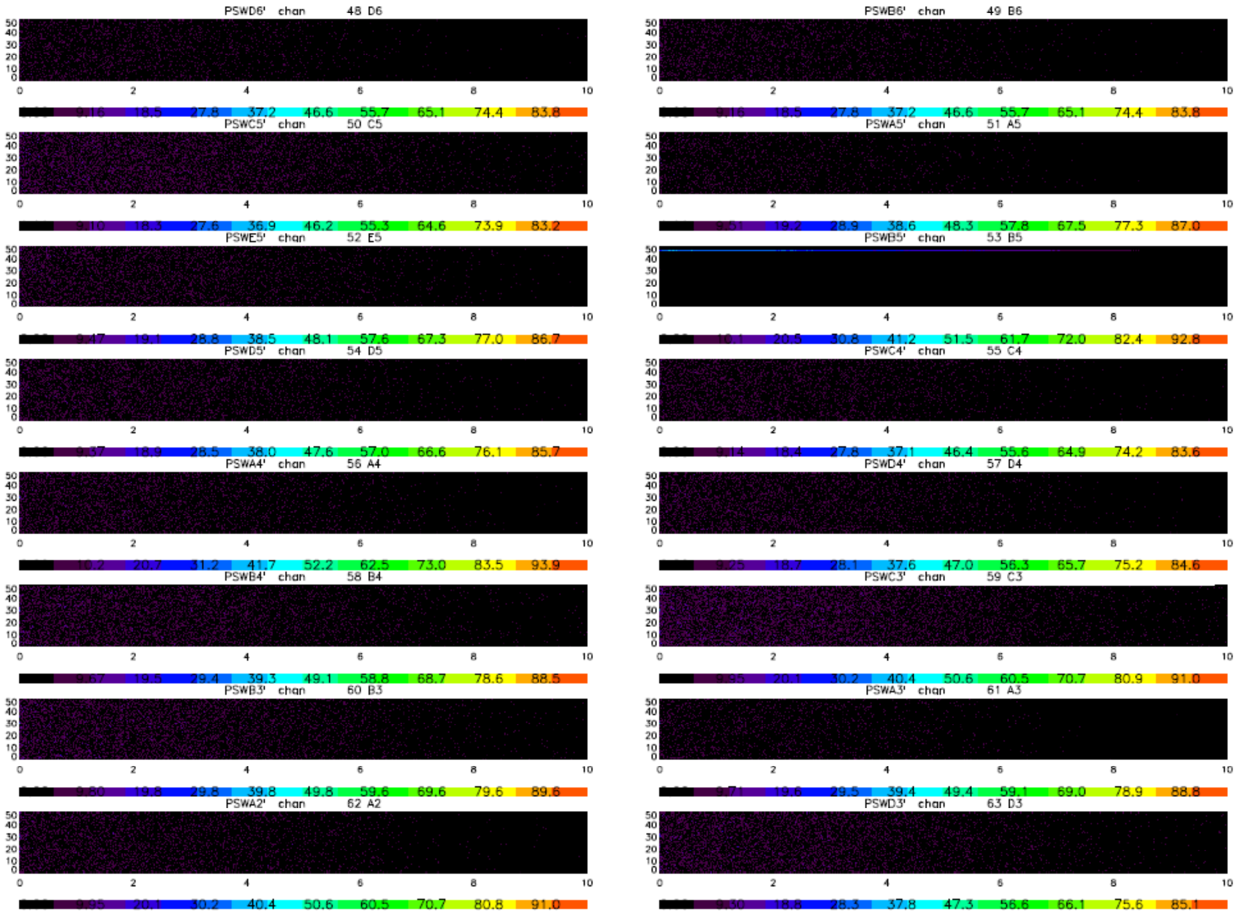

Figure 10

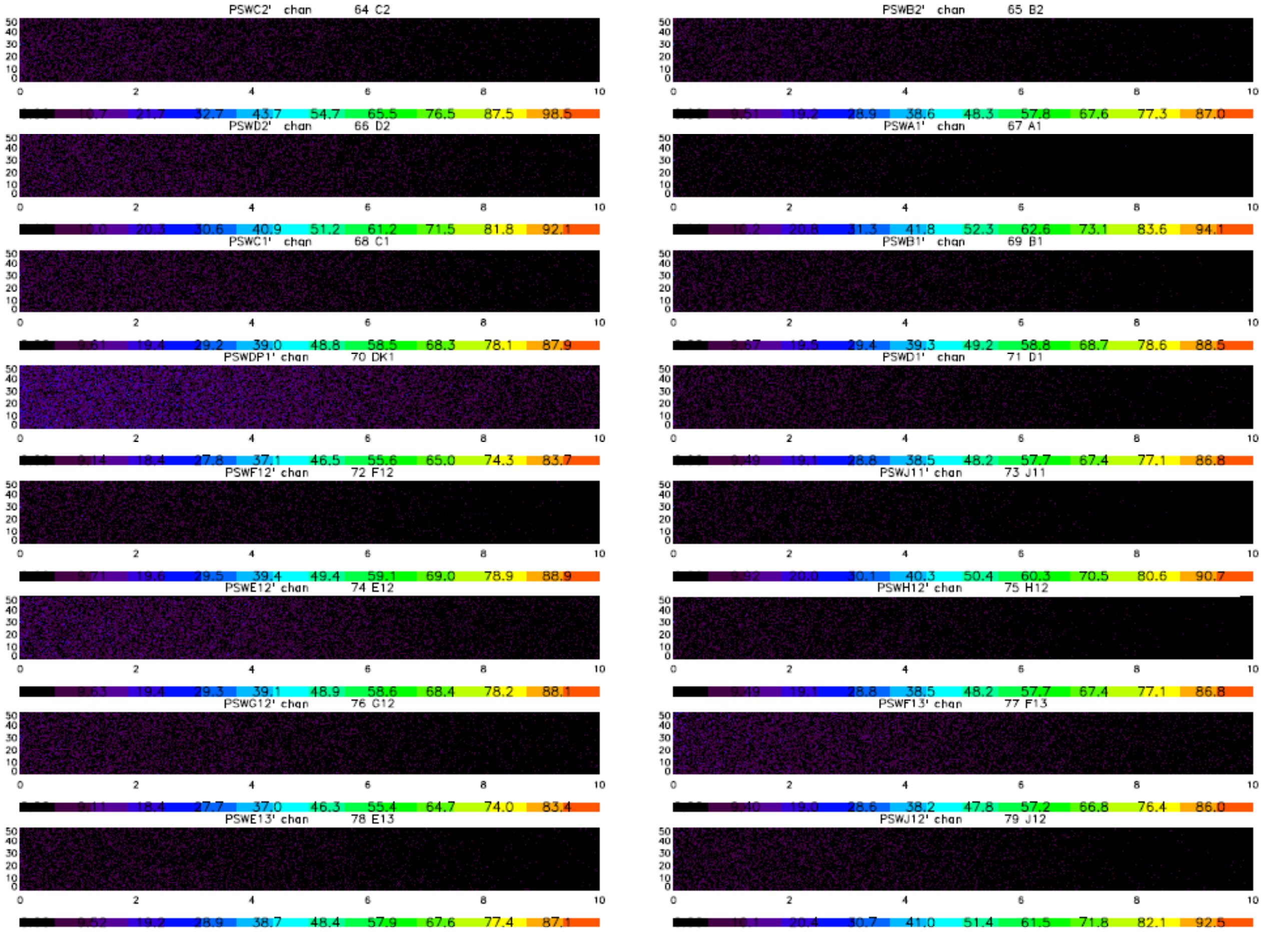

Figure 11

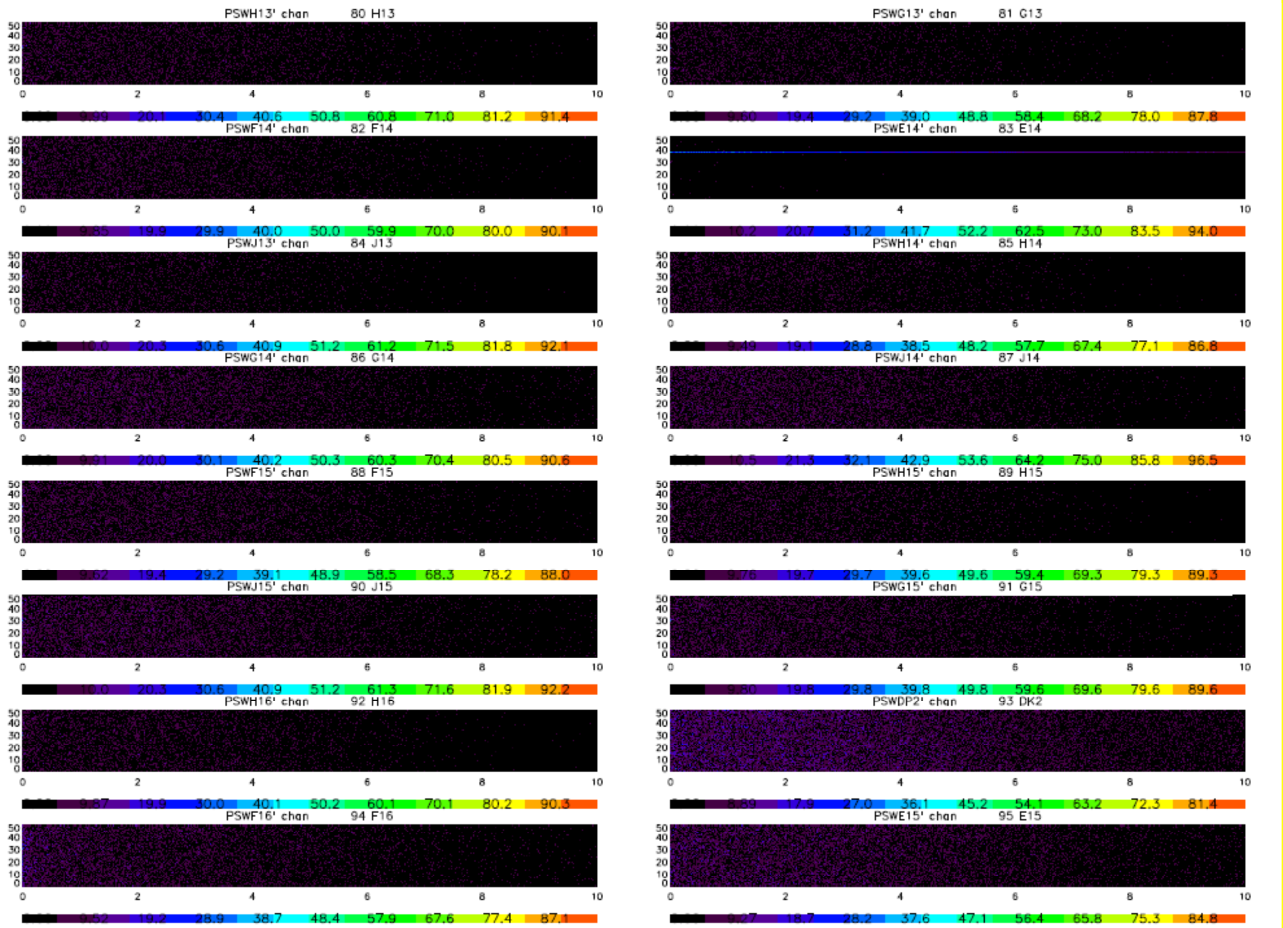

Figure 12

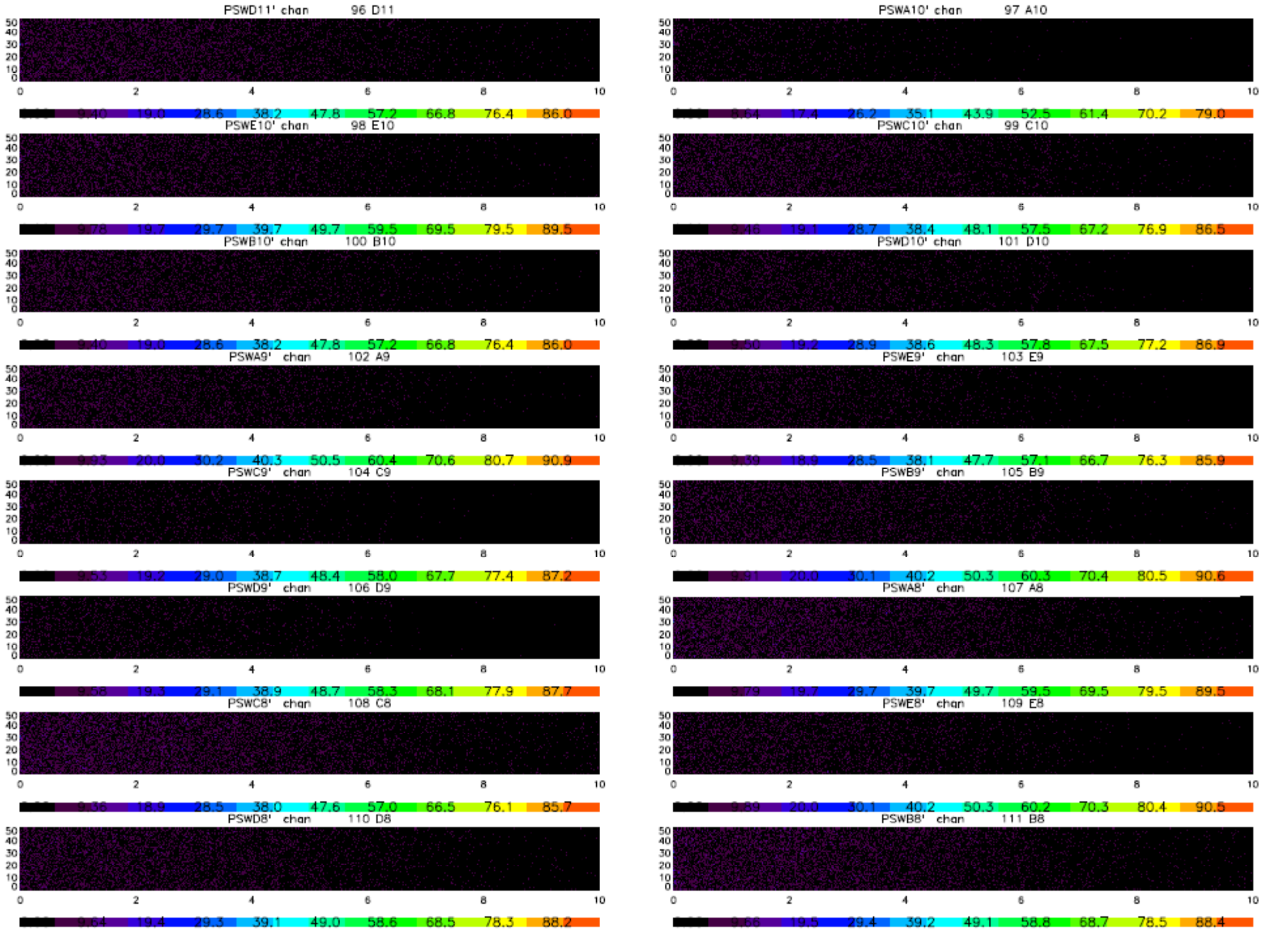
PSWD11' chan 96 D11
PSWA10' chan 97 A10
PSWE10' chan 98 E10
PSWC10' chan 99 C10
PSWB10' chan 100 B10
PSWD10' chan 101 D10
PSWA9' chan 102 A9
PSWE9' chan 103 E9
PSWC9' chan 104 C9
PSWB9' chan 105 B9
PSWD9' chan 106 D9
PSWA8' chan 107 A8
PSWC8' chan 108 C8
PSWE8' chan 109 E8
PSWD8' chan 110 D8
PSWB8' chan 111 B8

Figure 13

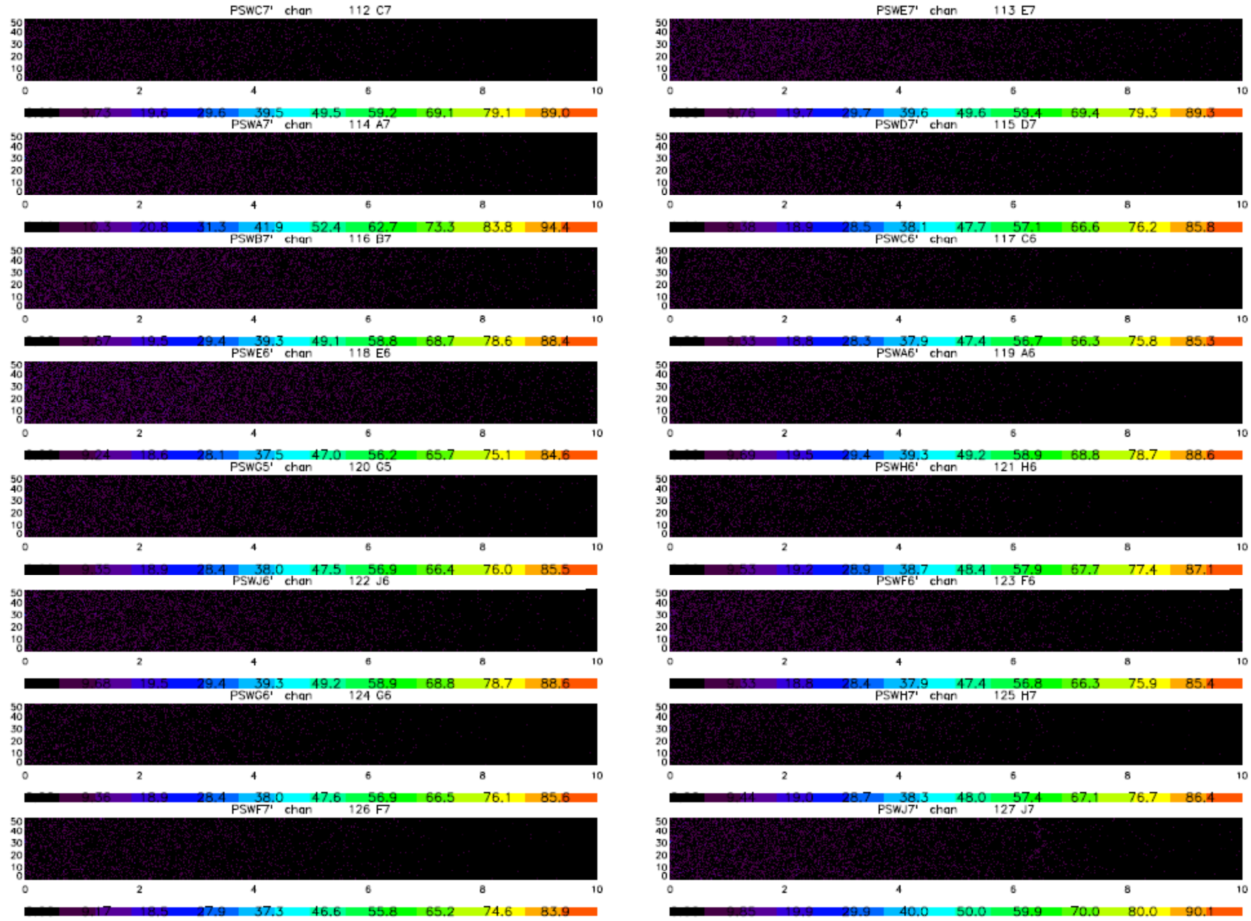
PSWC7' chan 112 C7
PSWE7' chan 113 E7
PSWA7' chan 114 A7
PSWD7' chan 115 D7
PSWB7' chan 116 B7
PSWC6' chan 117 C6
PSWE6' chan 118 E6
PSWA6' chan 119 A6
PSWG5' chan 120 G5
PSWH6' chan 121 H6
PSWJ6' chan 122 J6
PSWF6' chan 123 F6
PSWG6' chan 124 G6
PSWH7' chan 125 H7
PSWF7' chan 126 F7
PSWJ7' chan 127 J7

Figure 14

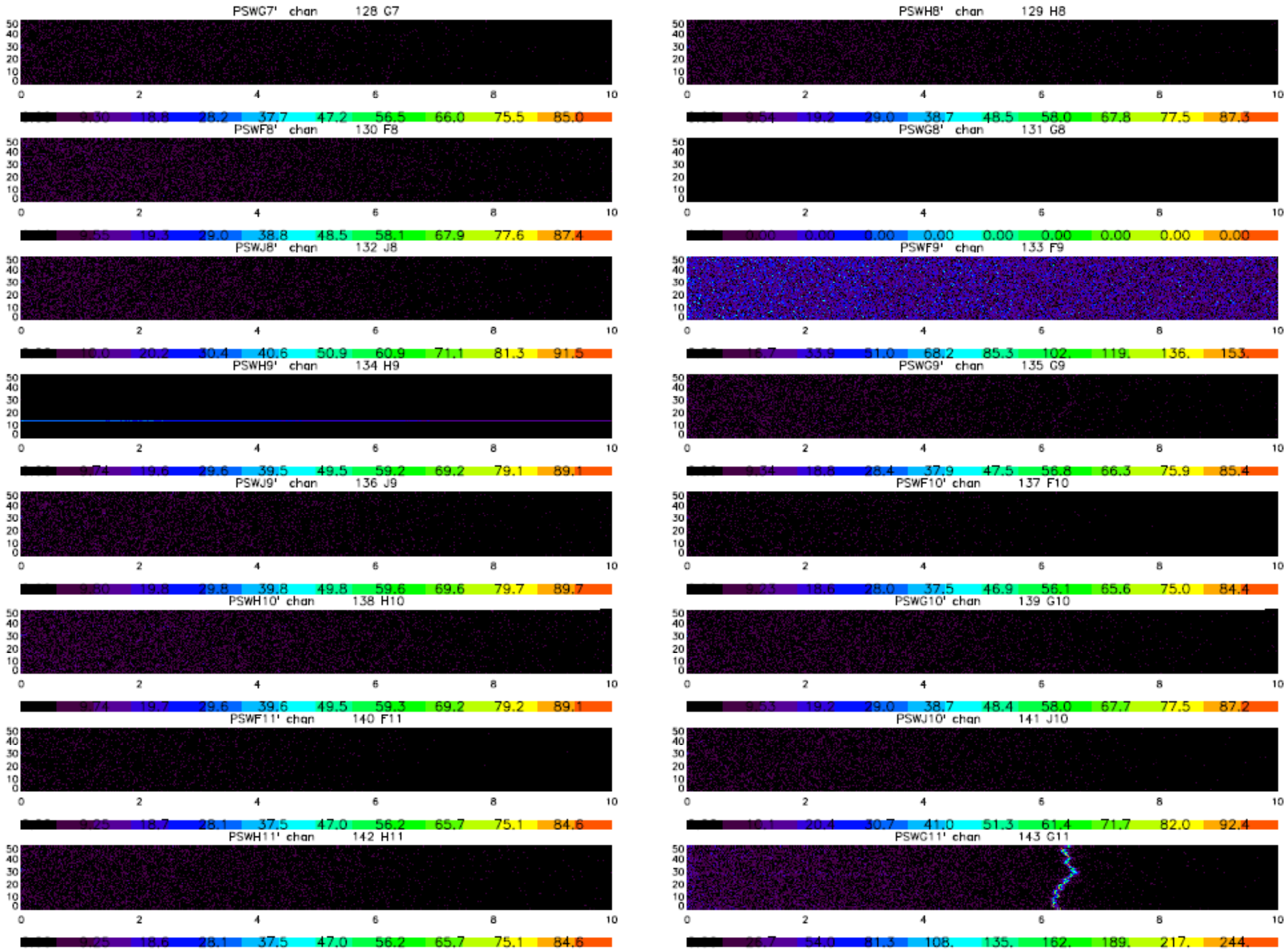
PSWG7' chan 128 G7
PSWH8' chan 129 H8
PSWF8' chan 130 F8
PSWG8' chan 131 G8
PSWJ8' chan 132 J8
PSWF9' chan 133 F9
PSWH9' chan 134 H9
PSWG9' chan 135 G9
PSWJ9' chan 136 J9
PSWF10' chan 137 F10
PSWH10' chan 138 H10
PSWG10' chan 139 G10
PSWF11' chan 140 F11
PSWJ10' chan 141 J10
PSWH11' chan 142 H11
PSWG11' chan 143 G11

Figure 15

6.1.4 PMW Spectrogrammes

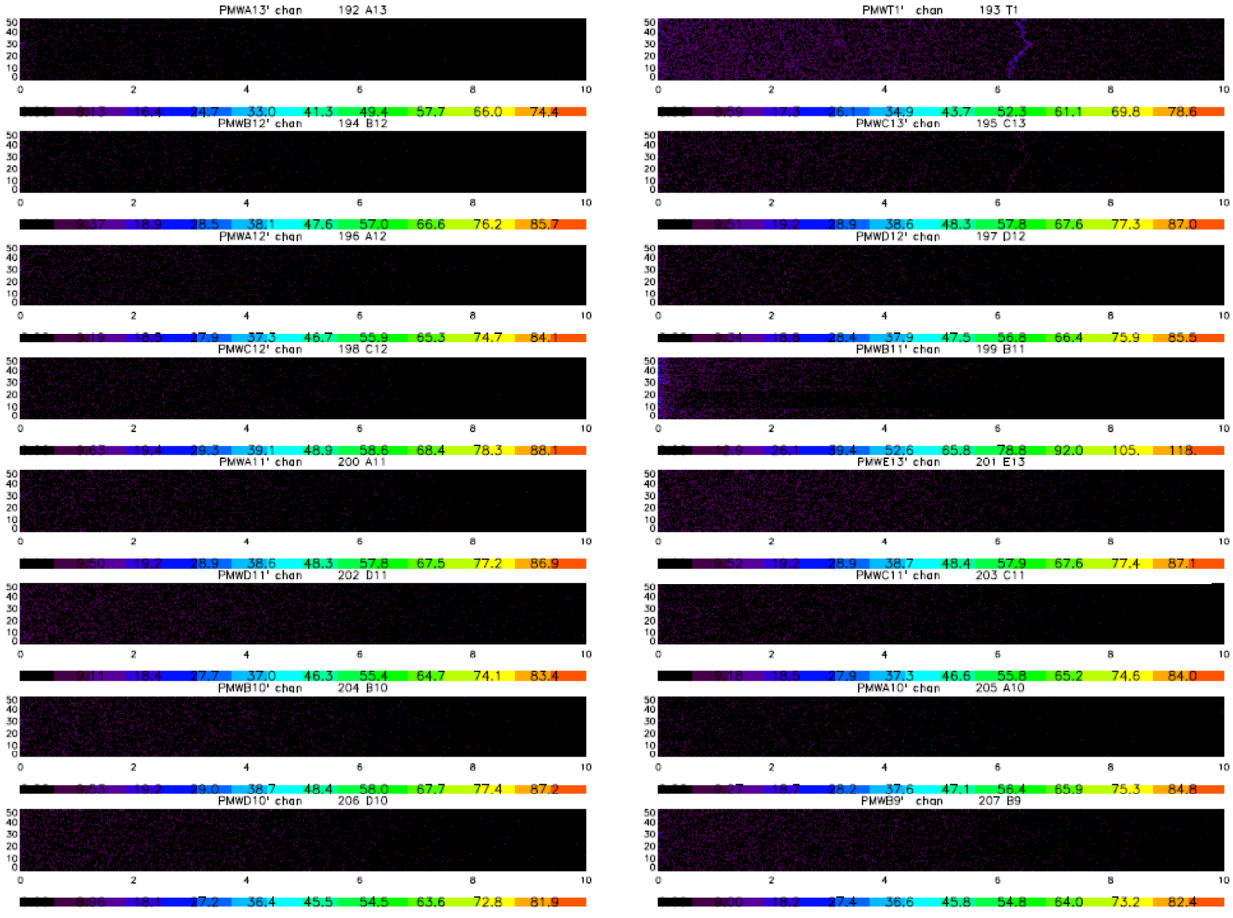

Figure 16

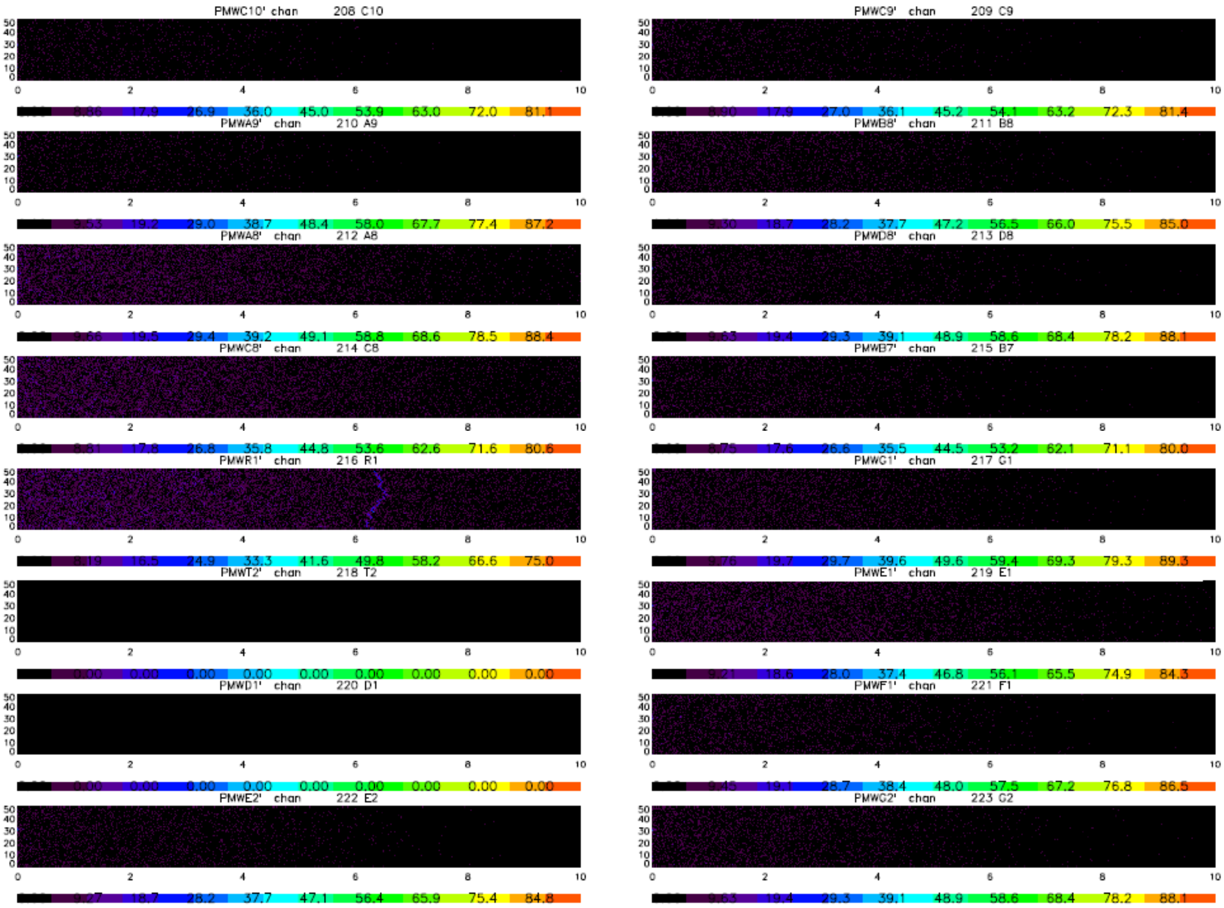

Figure 17

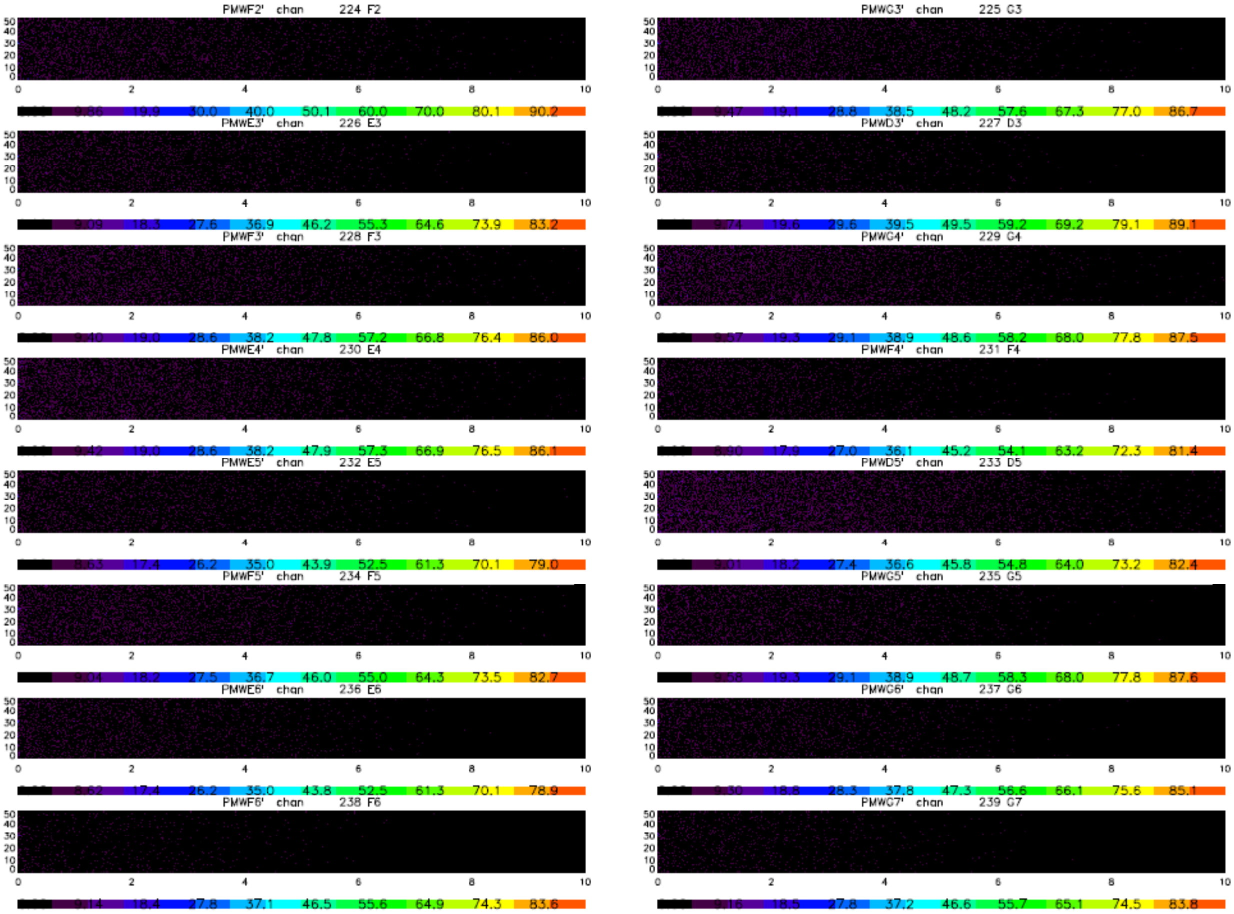
PMWF2' chan 224 F2
PMWG3' chan 225 G3
PMWE3' chan 226 E3
PMWD3' chan 227 D3
PMWF3' chan 228 F3
PMWG4' chan 229 G4
PMWE4' chan 230 E4
PMWF4' chan 231 F4
PMWE5' chan 232 E5
PMWD5' chan 233 D5
PMWF5' chan 234 F5
PMWG5' chan 235 G5
PMWE6' chan 236 E6
PMWG6' chan 237 G6
PMWF6' chan 238 F6
PMWG7' chan 239 G7

Figure 18

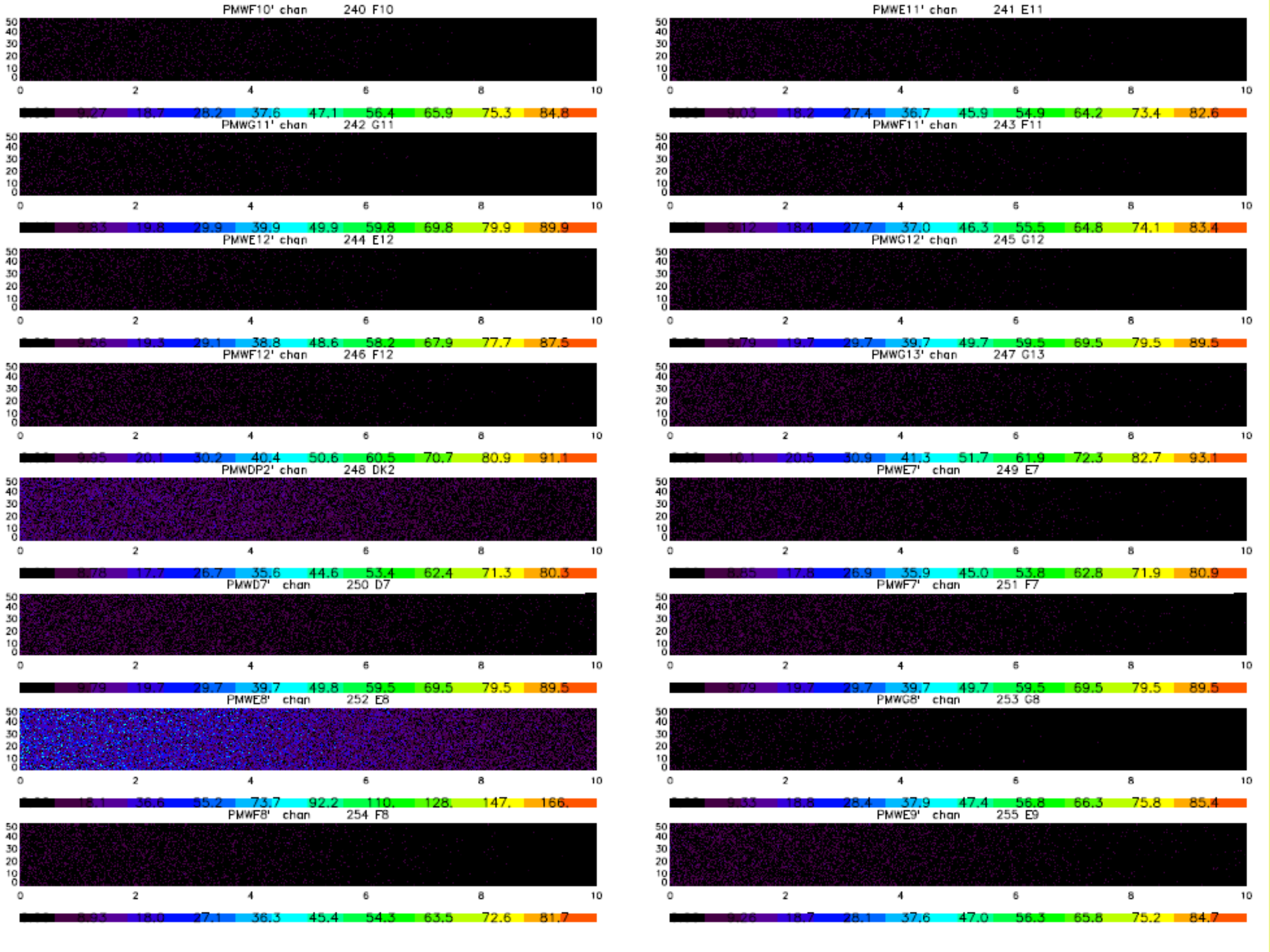
PMWF10' chan 240 F10
PMWE11' chan 241 E11
PMWG11' chan 242 G11
PMWF11' chan 243 F11
PMWE12' chan 244 E12
PMWG12' chan 245 G12
PMWF12' chan 246 F12
PMWG13' chan 247 G13
PMWDP2' chan 248 DK2
PMWE7' chan 249 E7
PMWD7' chan 250 D7
PMWF7' chan 251 F7
PMWE8' chan 252 E8
PMWG8' chan 253 G8
PMWF8' chan 254 F8
PMWE9' chan 255 E9

Figure 19

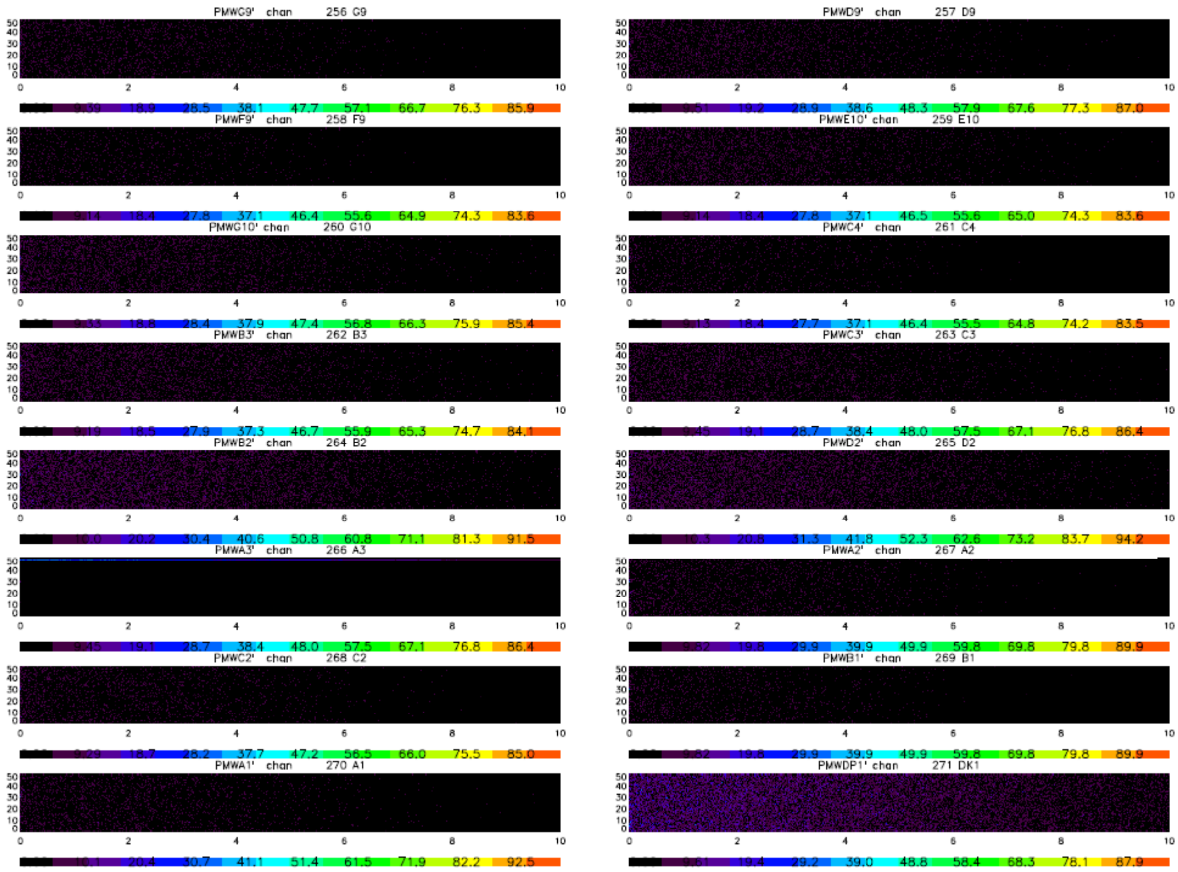
PMWG9' chan 256 G9
PMWD9' chan 257 D9
PMWF9' chan 258 F9
PMWE10' chan 259 E10
PMWG10' chan 260 G10
PMWC4' chan 261 C4
PMWB3' chan 262 B3
PMWC3' chan 263 C3
PMWB2' chan 264 B2
PMWD2' chan 265 D2
PMWA3' chan 266 A3
PMWA2' chan 267 A2
PMWC2' chan 268 C2
PMWB1' chan 269 B1
PMWA1' chan 270 A1
PMWDP1' chan 271 DK1

Figure 20

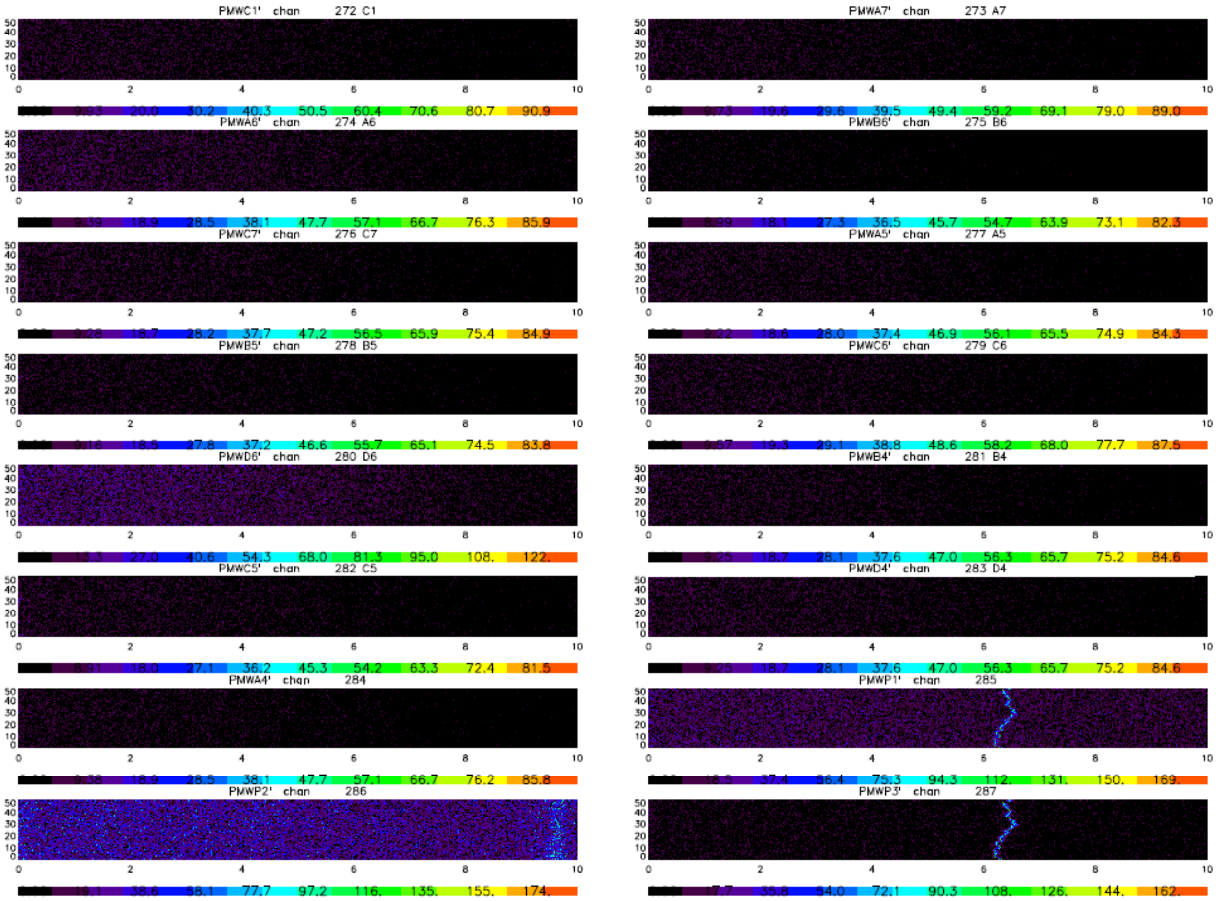

Figure 21

6.1.5 PLW Spectrogrammes

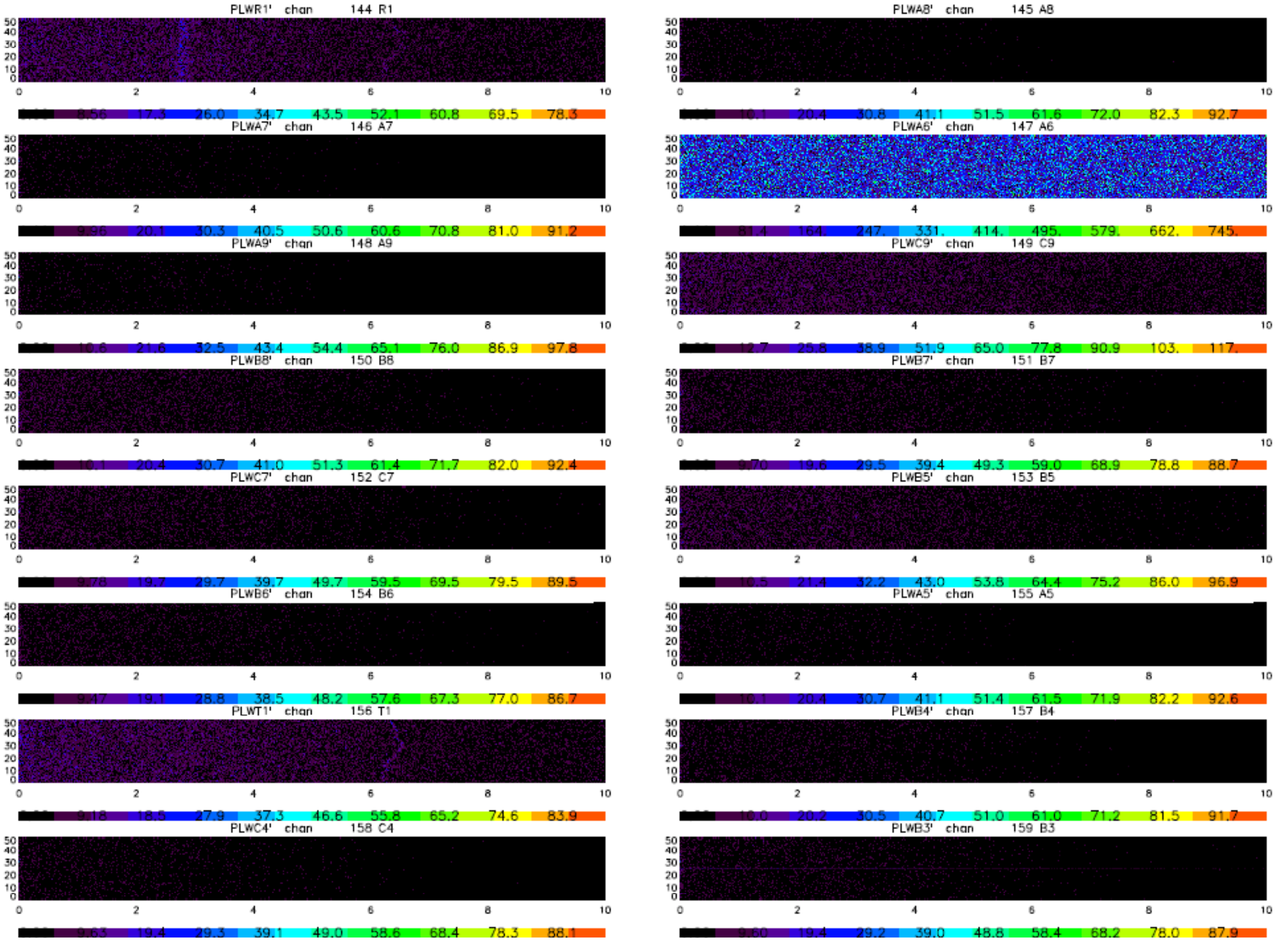

Figure 22

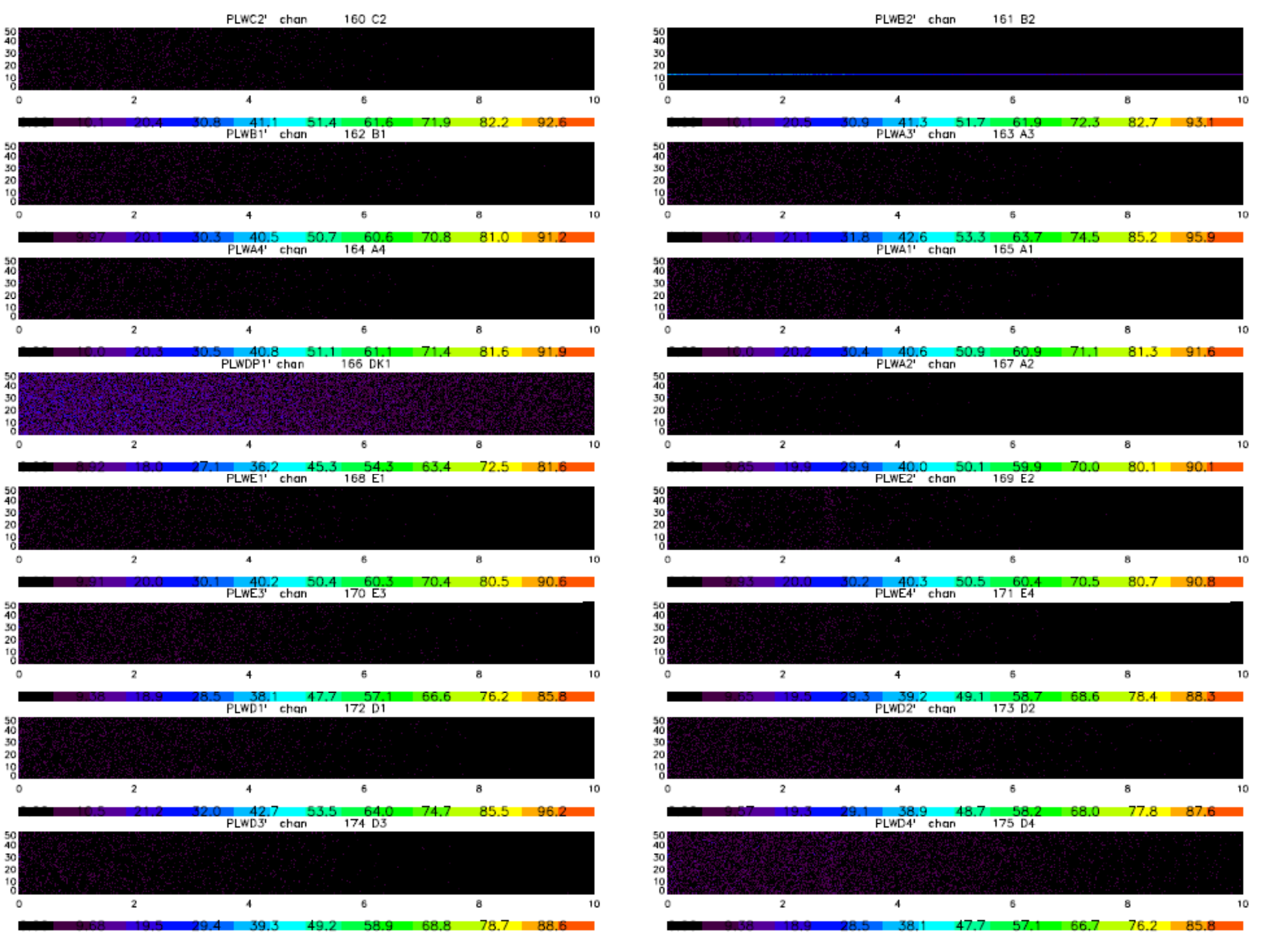
PLWC2' chan 160 C2
PLWB2' chan 161 B2
PLWB1' chan 162 B1
PLWA3' chan 163 A3
PLWA4' chan 164 A4
PLWA1' chan 165 A1
PLWDP1' chan 166 DK1
PLWA2' chan 167 A2
PLWE1' chan 168 E1
PLWE2' chan 169 E2
PLWE3' chan 170 E3
PLWE4' chan 171 E4
PLWD1' chan 172 D1
PLWD2' chan 173 D2
PLWD3' chan 174 D3
PLWD4' chan 175 D4

Figure 23

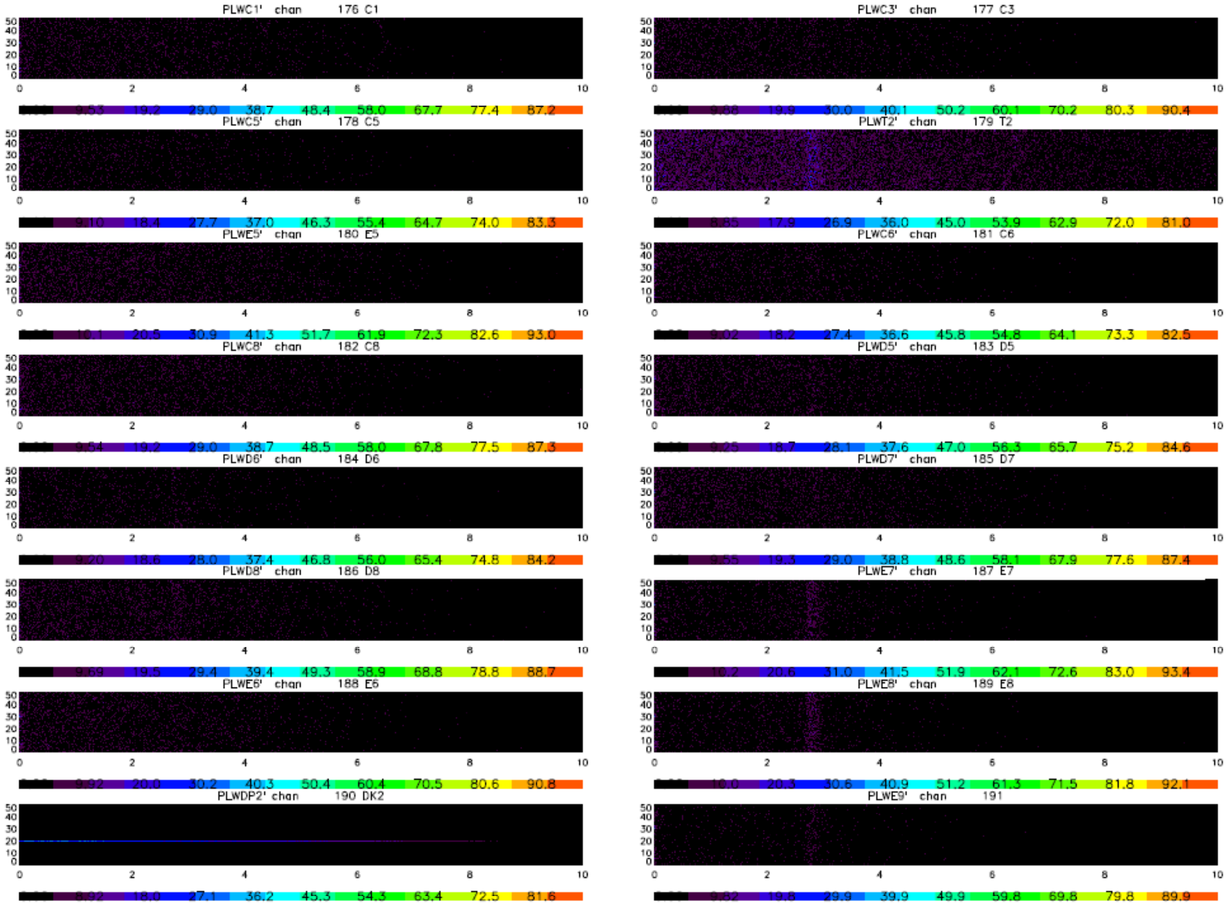

Figure 24

6.2 CS Differential Mode – Spectrometer (0xB00014C7)

6.2.1 Noise PSD (Averaged using N 10 second "chunks" of detector data)

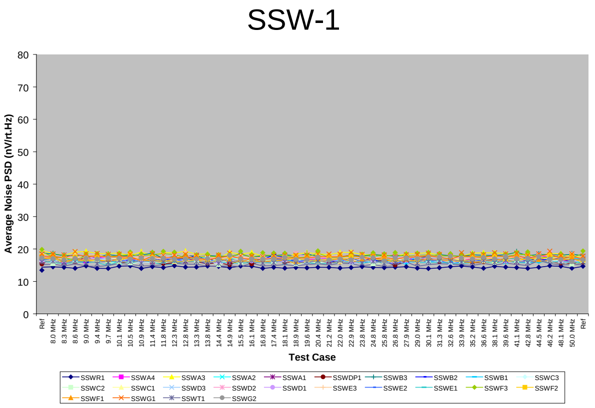

6.2.2 SSW and SLW Spectrogrammes

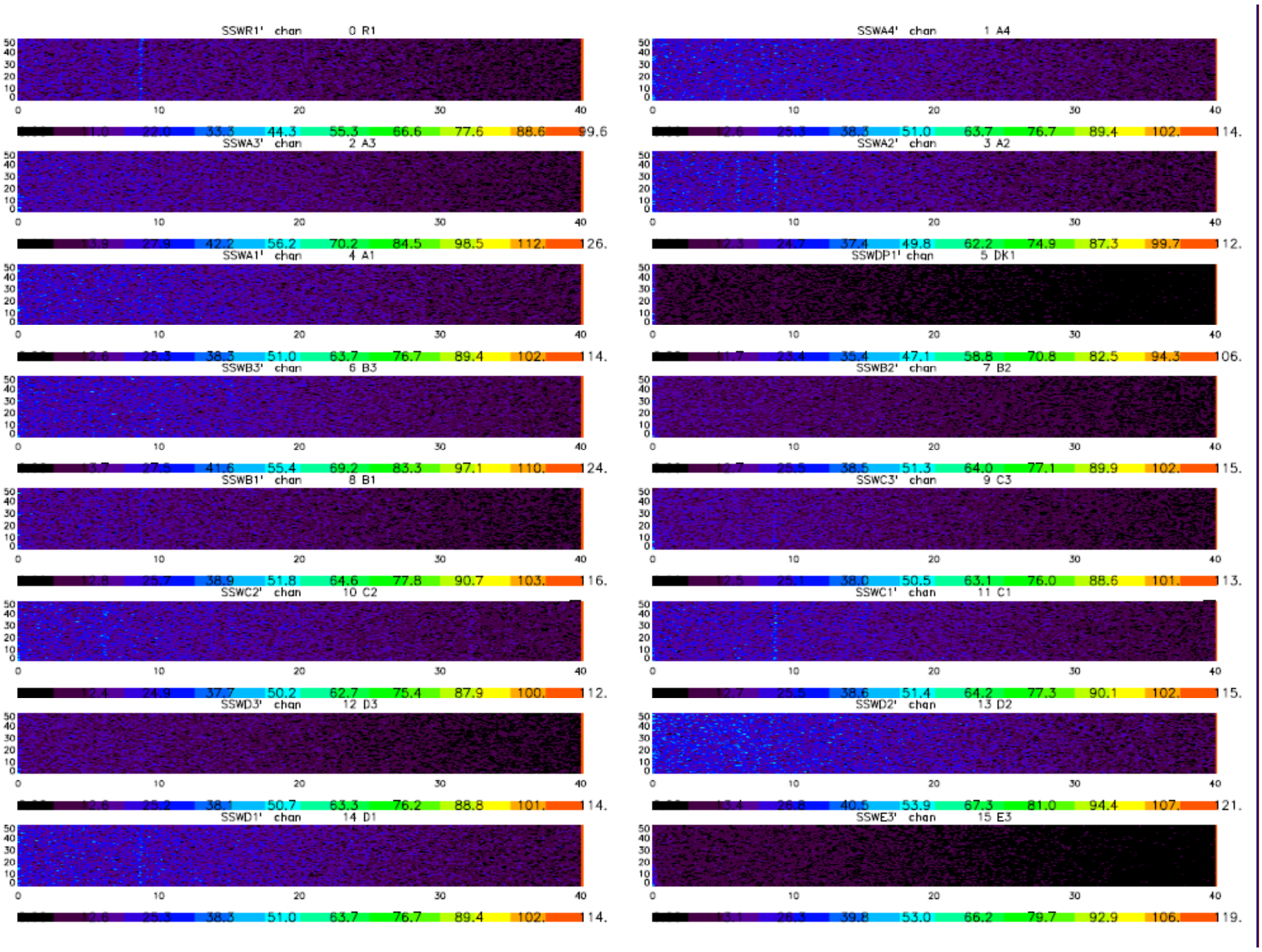

Figure 25

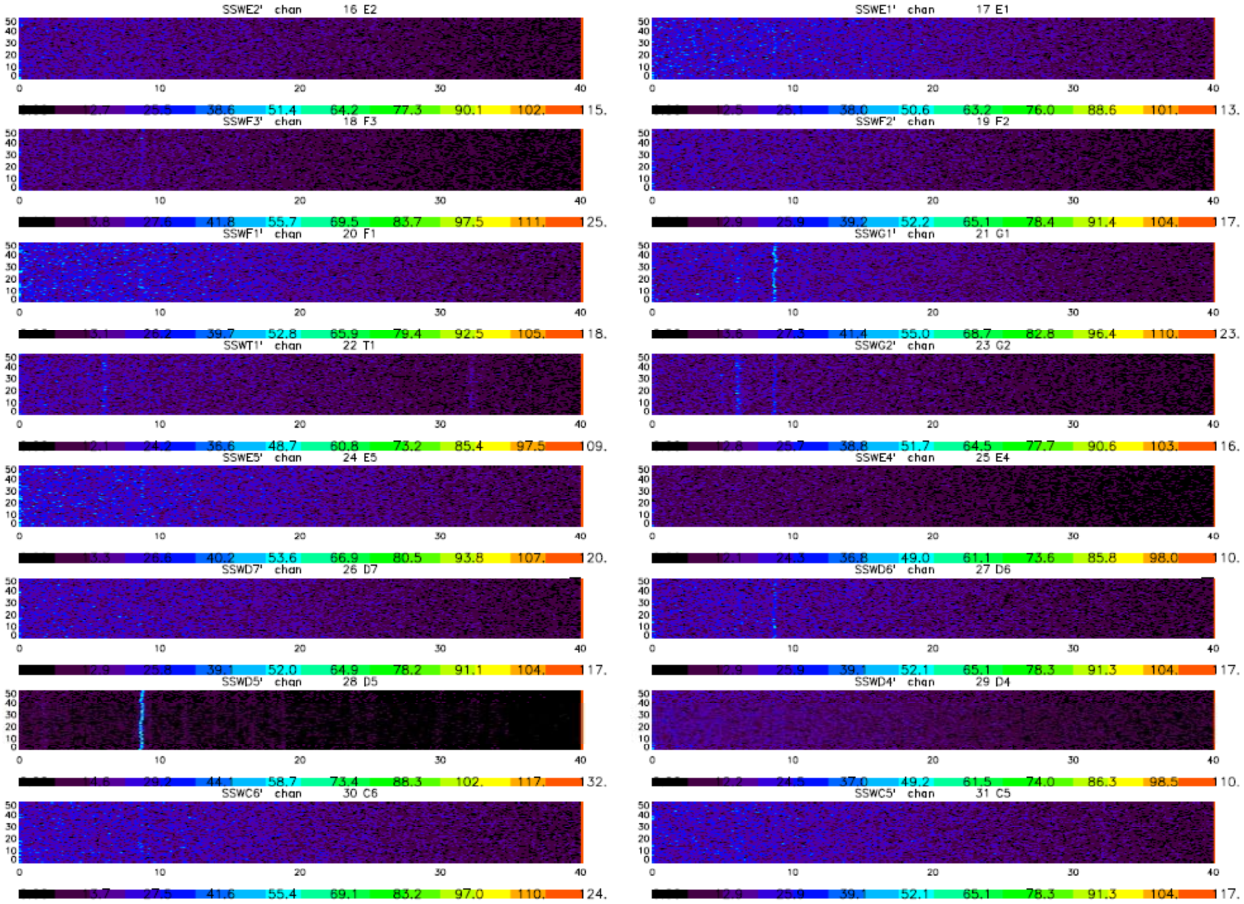

Figure 26

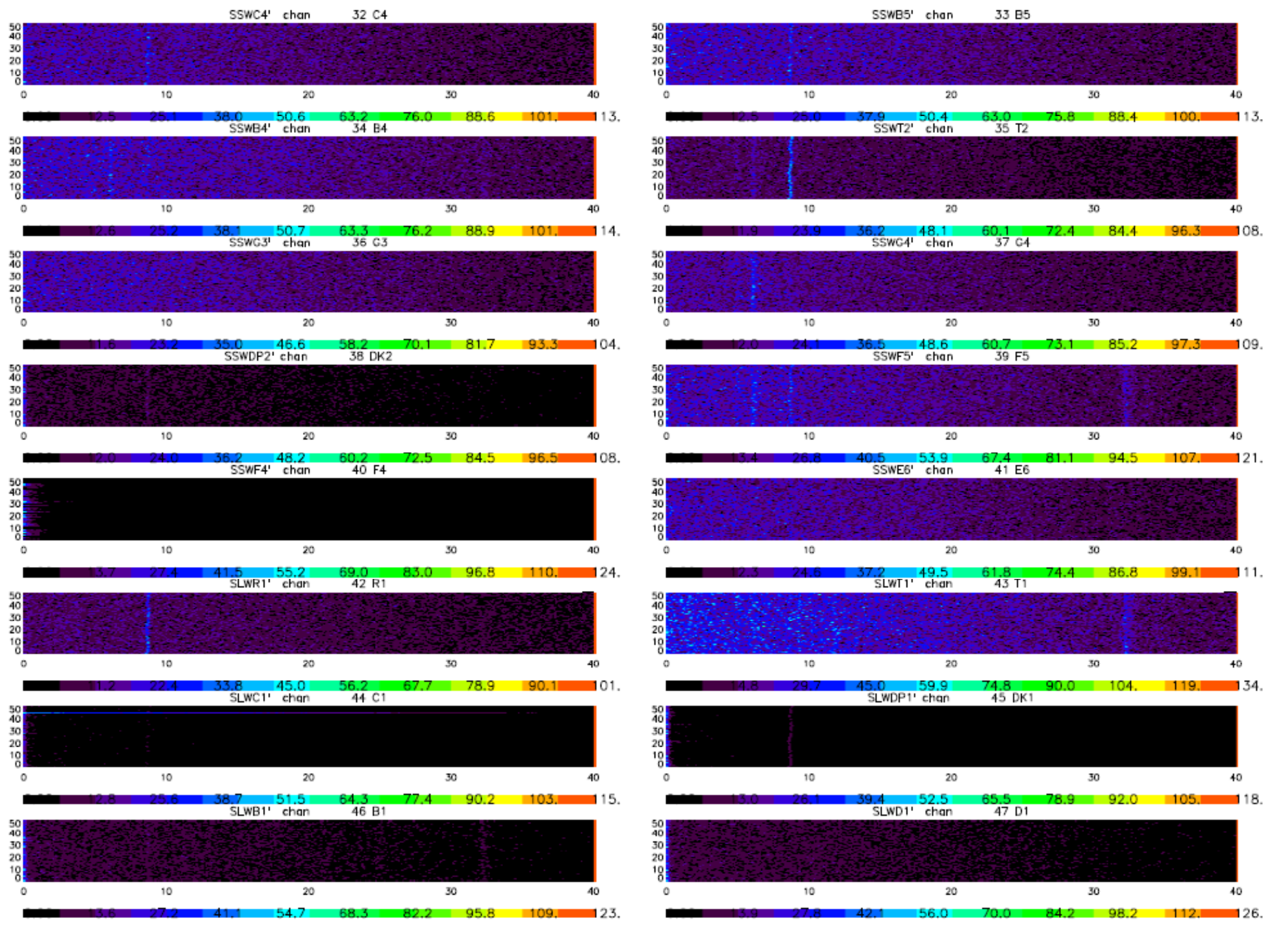
SSWC4' chan 32 C4
SSWB5' chan 33 B5
SSWB4' chan 34 B4
SSWT2' chan 35 T2
SSWG3' chan 36 G3
SSWG4' chan 37 G4
SSWDP2' chan 38 DK2
SSWF5' chan 39 F5
SSWF4' chan 40 F4
SSWE6' chan 41 E6
SLWR1' chan 42 R1
SLWT1' chan 43 T1
SLWC1' chan 44 C1
SLWDP1' chan 45 DK1
SLWB1' chan 46 B1
SLWD1' chan 47 D1

Figure 27

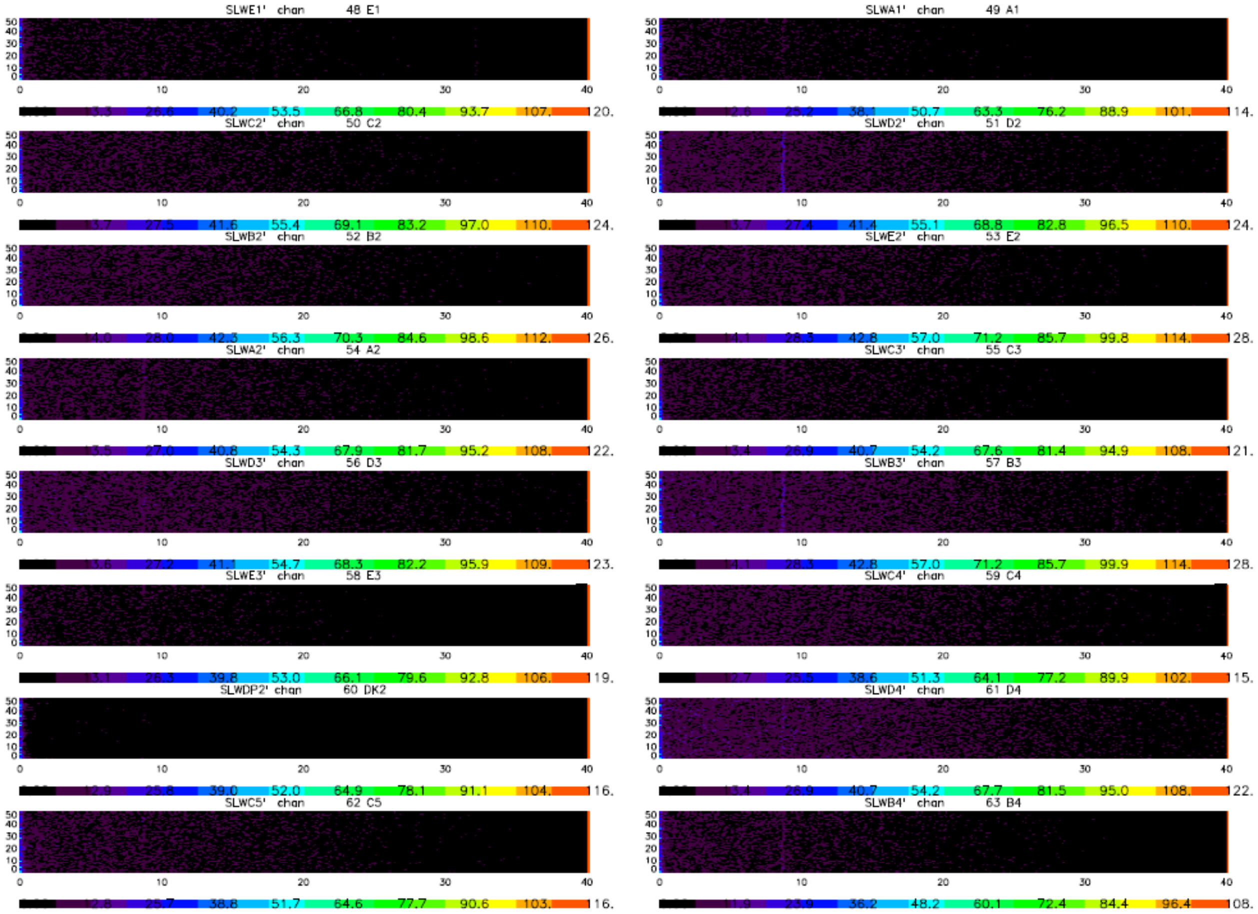

Figure 28

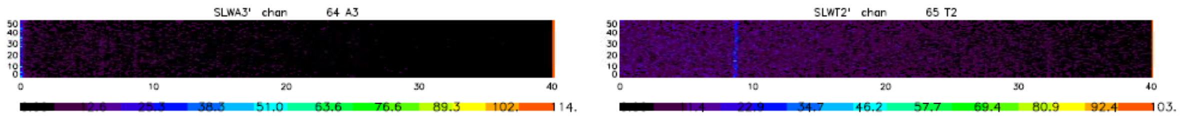

Figure 29

7. Appendix 2: CS Common Mode Detailed Results

7.1 CS Common Mode – Photometer (0xB00014D8)

7.1.1 Noise PSD (Averaged using N 10 second “chunks” of detector data)

PSW (A1-B2)

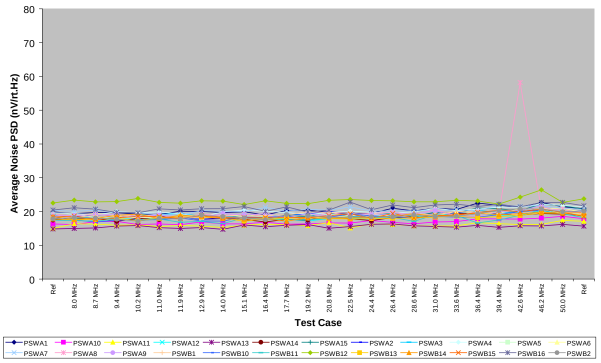

PSW A8 “spikes”

PMW (A1-B8)

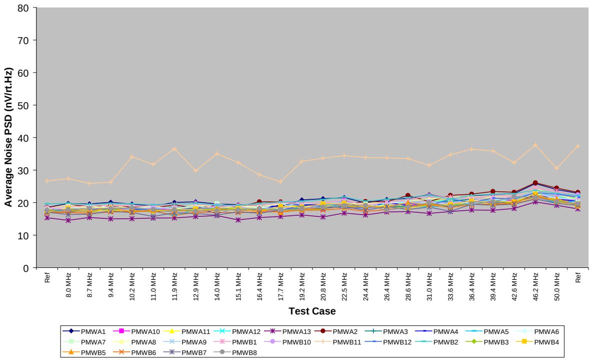

PMW-B11 shows excess noise @ ~ 30nV/√Hz

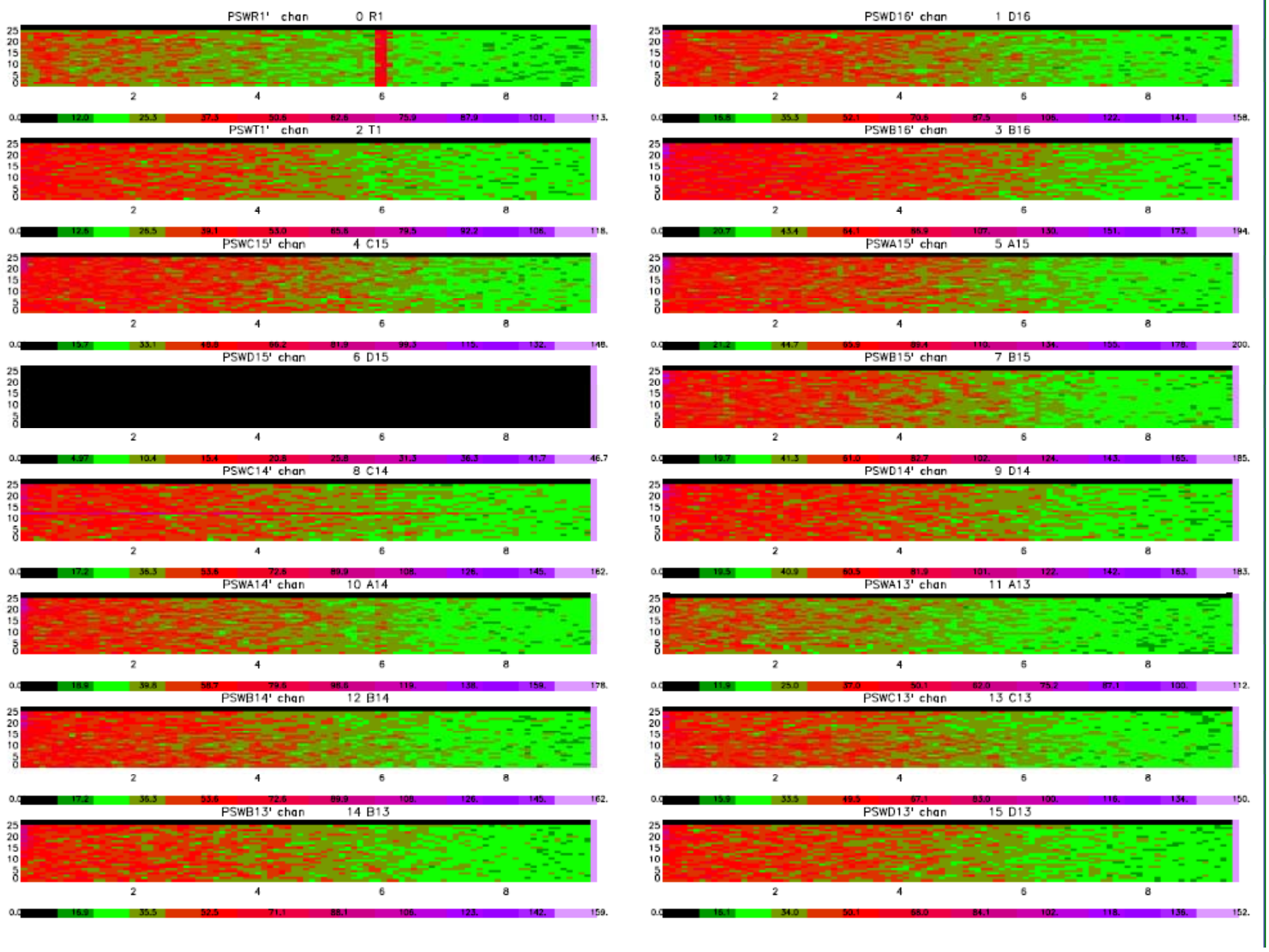
PSWR1' chan 0 R1
PSWD16' chan 1 D16
PSWT1' chan 2 T1
PSWB16' chan 3 B16
PSWC15' chan 4 C15
PSWA15' chan 5 A15
PSWD15' chan 6 D15
PSWB15' chan 7 B15
PSWC14' chan 8 C14
PSWD14' chan 9 D14
PSWA14' chan 10 A14
PSWA13' chan 11 A13
PSWB14' chan 12 B14
PSWC13' chan 13 C13
PSWB13' chan 14 B13
PSWD13' chan 15 D13

Figure 30

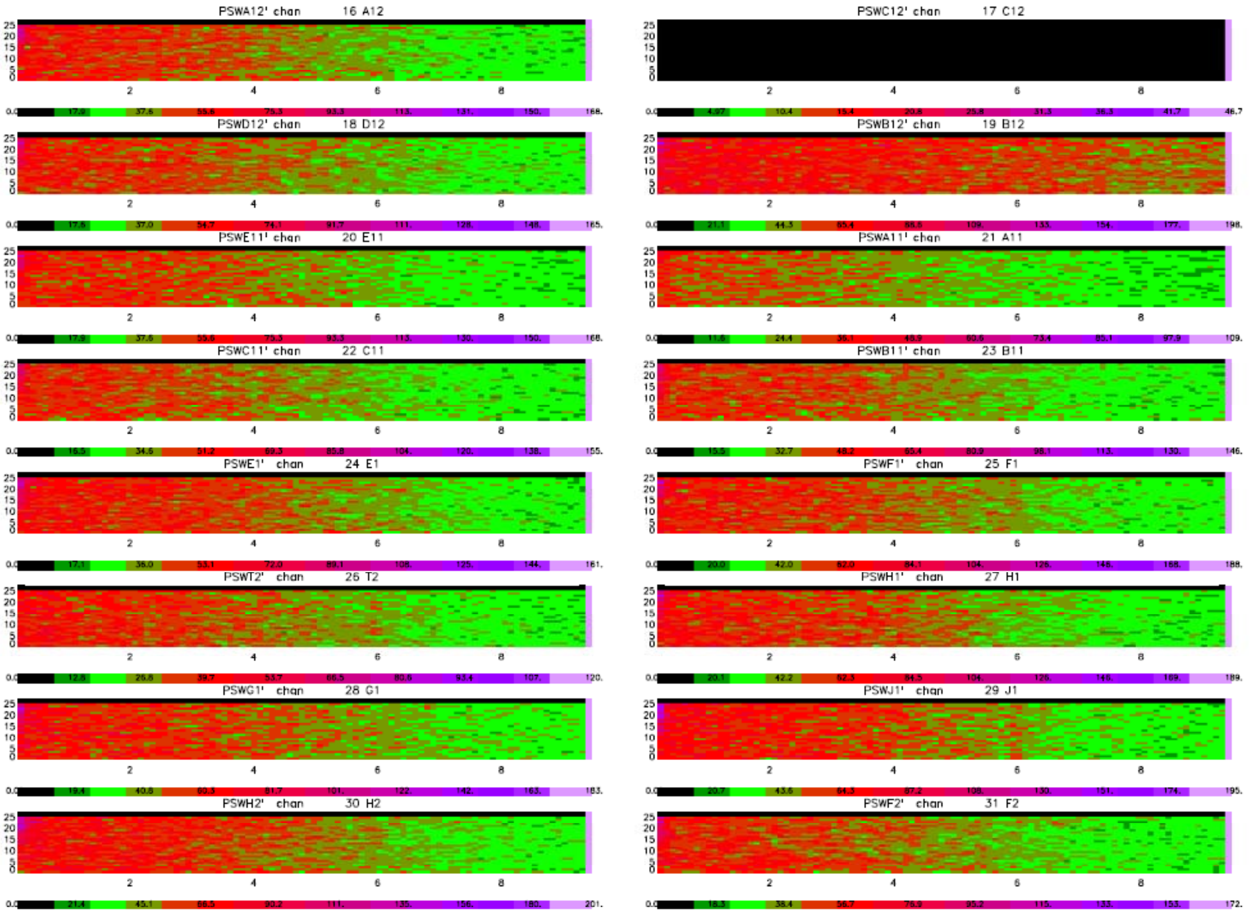
PSWA12' chan 16 A12
PSWC12' chan 17 C12
PSWD12' chan 18 D12
PSWB12' chan 19 B12
PSWE11' chan 20 E11
PSWA11' chan 21 A11
PSWC11' chan 22 C11
PSWB11' chan 23 B11
PSWE1' chan 24 E1
PSWF1' chan 25 F1
PSWT2' chan 26 T2
PSWH1' chan 27 H1
PSWG1' chan 28 G1
PSWJ1' chan 29 J1
PSWH2' chan 30 H2
PSWF2' chan 31 F2

Figure 31

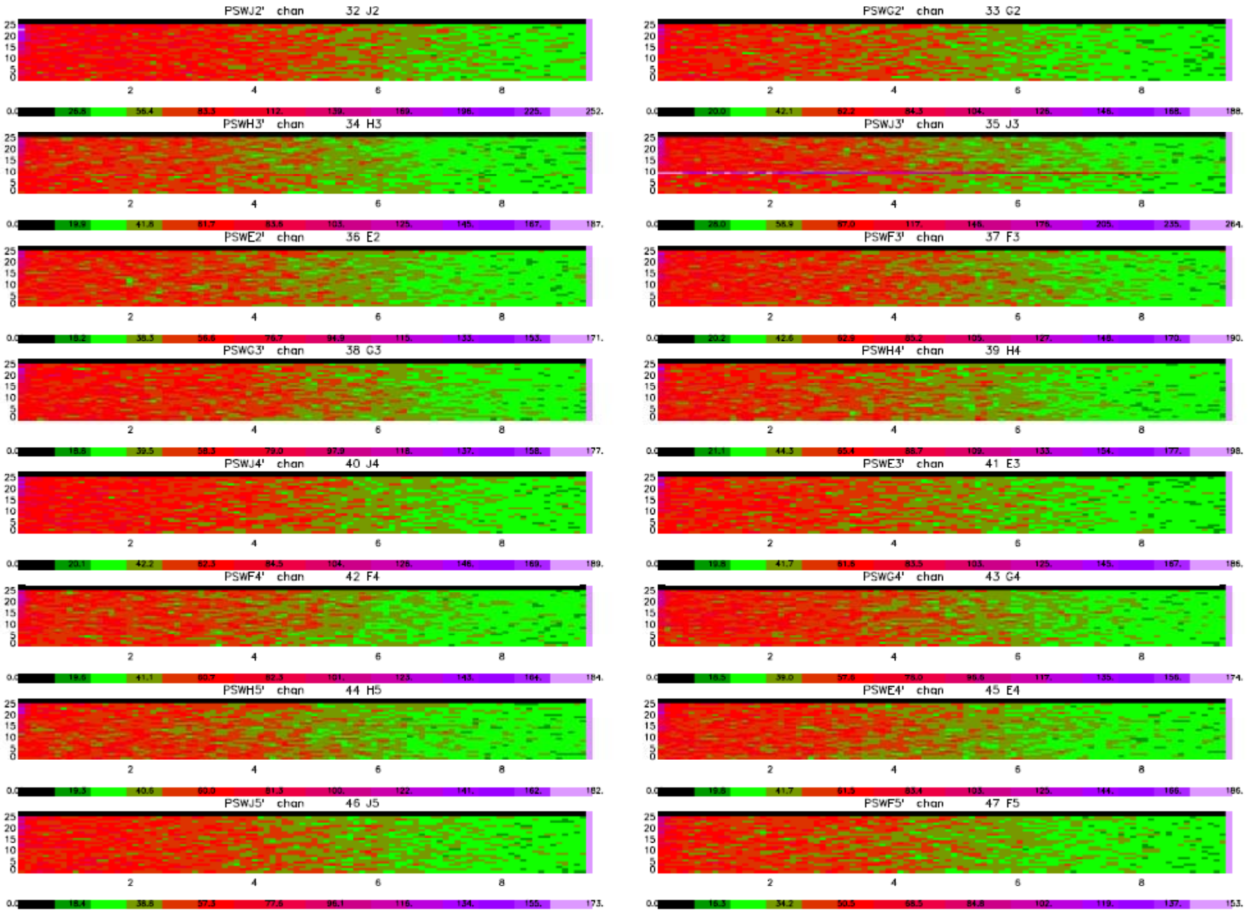

Figure 32

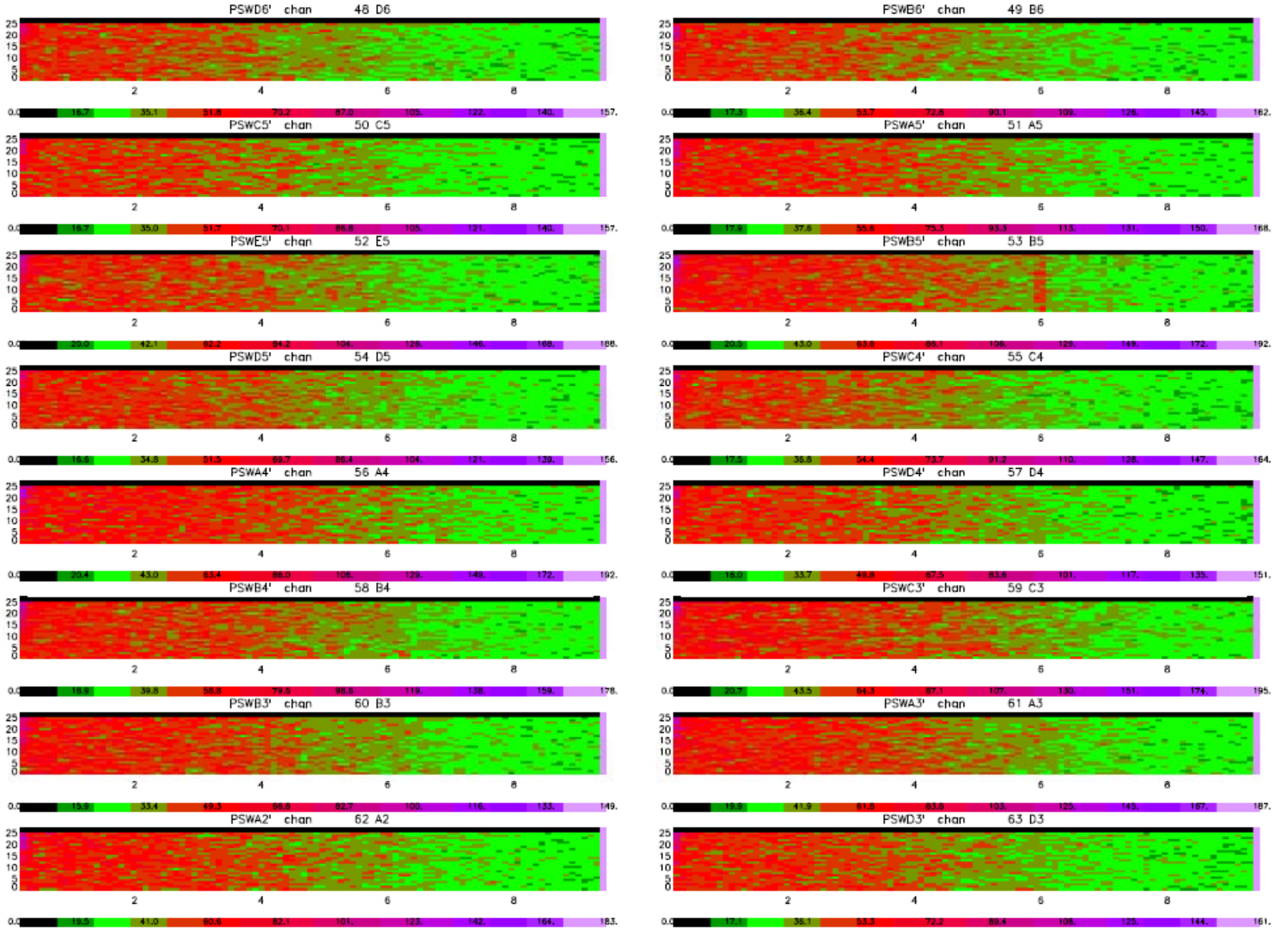
PSWD6' chan 48 D6
PSWB6' chan 49 B6
PSWC5' chan 50 C5
PSWA5' chan 51 A5
PSWE5' chan 52 E5
PSWB5' chan 53 B5
PSWD5' chan 54 D5
PSWC4' chan 55 C4
PSWA4' chan 56 A4
PSWD4' chan 57 D4
PSWB4' chan 58 B4
PSWC3' chan 59 C3
PSWB3' chan 60 B3
PSWA3' chan 61 A3
PSWA2' chan 62 A2
PSWD3' chan 63 D3

Figure 33

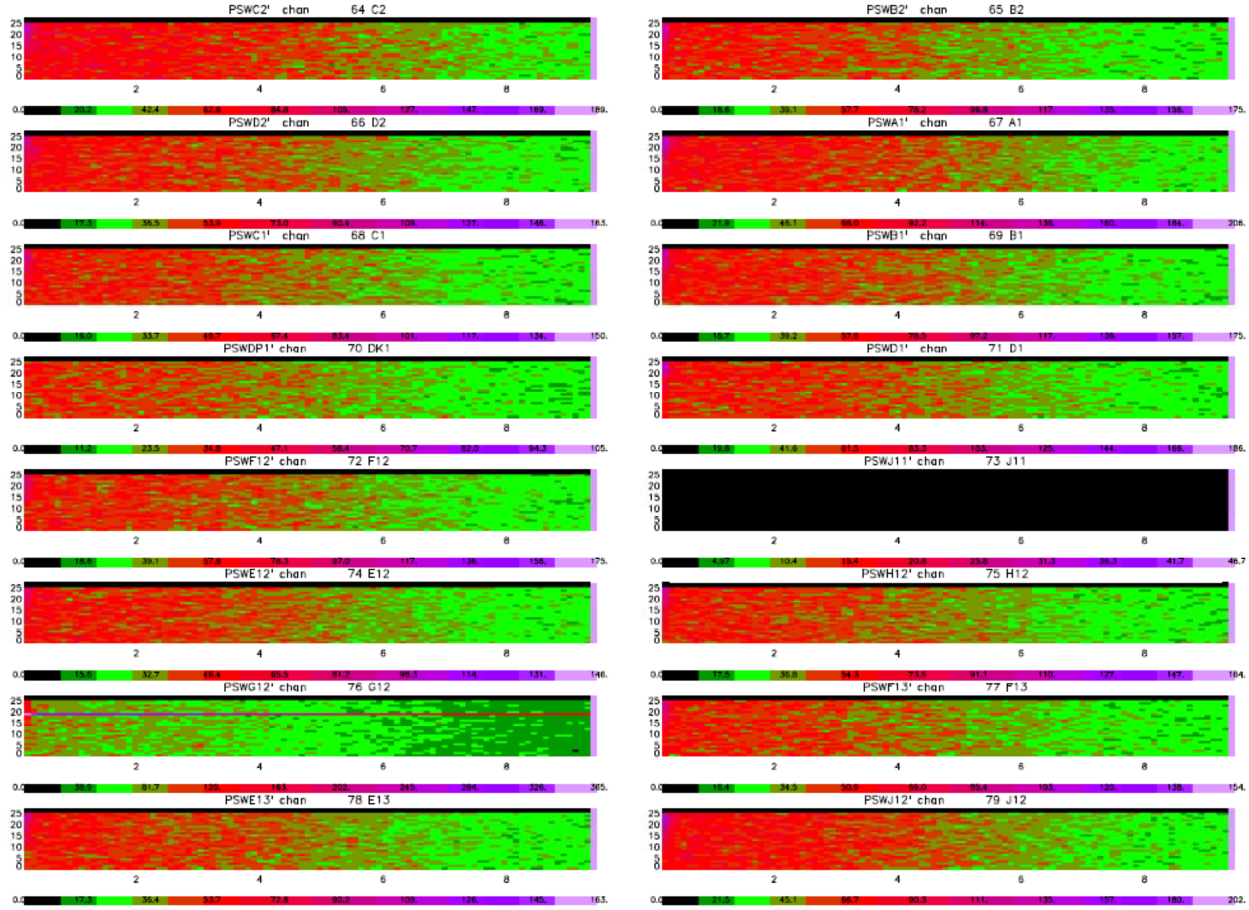
PSWC2' chan 64 C2
PSWB2' chan 65 B2
PSWD2' chan 66 D2
PSWA1' chan 67 A1
PSWC1' chan 68 C1
PSWB1' chan 69 B1
PSWDP1' chan 70 DK1
PSWD1' chan 71 D1
PSWF12' chan 72 F12
PSWJ11' chan 73 J11
PSWE12' chan 74 E12
PSWH12' chan 75 H12
PSWG12' chan 76 G12
PSWF13' chan 77 F13
PSWE13' chan 78 E13
PSWJ12' chan 79 J12

Figure 34

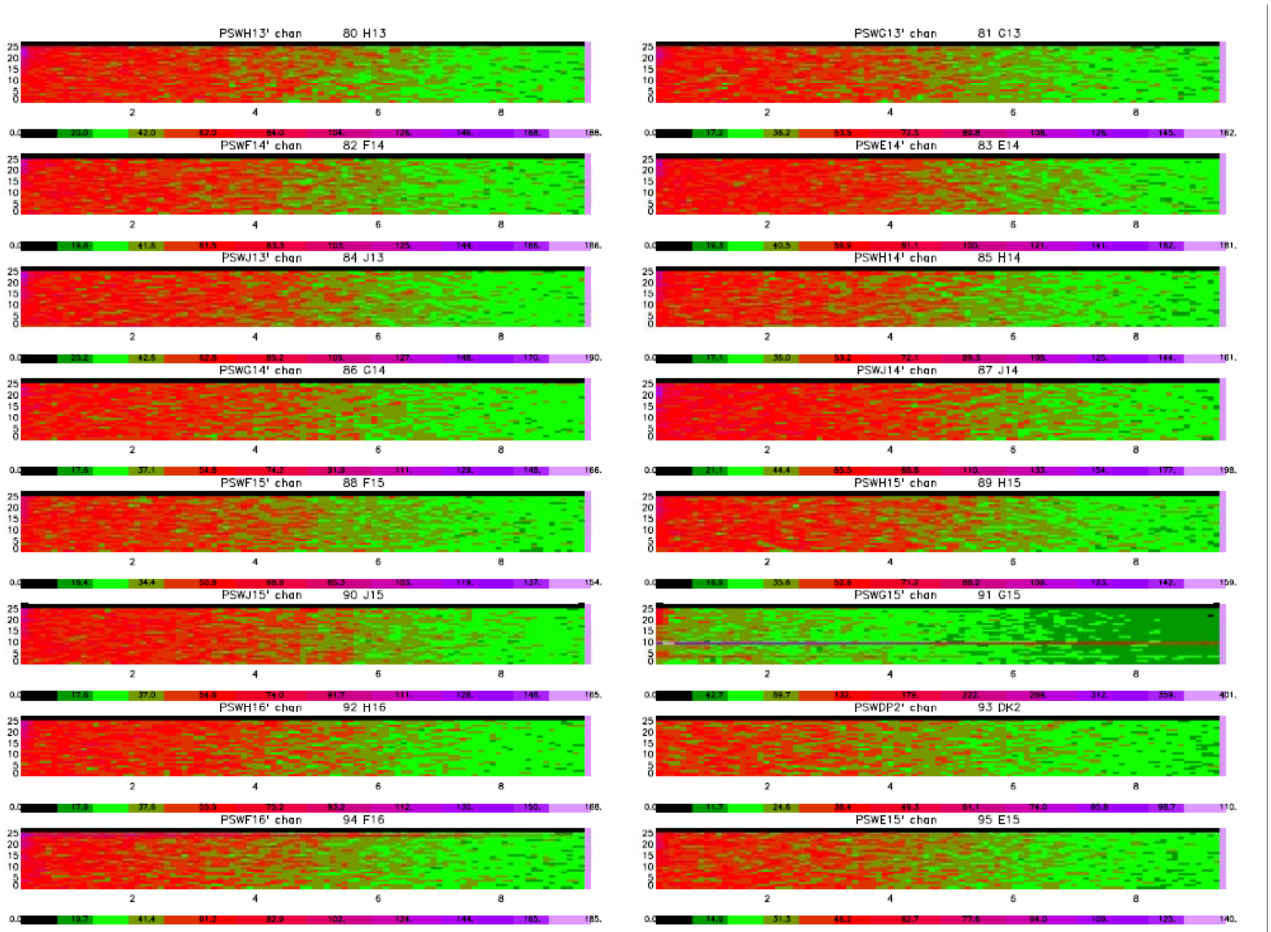
PSWH13' chan 80 H13
PSWG13' chan 81 G13
PSWF14' chan 82 F14
PSWE14' chan 83 E14
PSWJ13' chan 84 J13
PSWH14' chan 85 H14
PSWG14' chan 86 G14
PSWJ14' chan 87 J14
PSWF15' chan 88 F15
PSWH15' chan 89 H15
PSWJ15' chan 90 J15
PSWG15' chan 91 G15
PSWH16' chan 92 H16
PSWDP2' chan 93 DK2
PSWF16' chan 94 F16
PSWE15' chan 95 E15

Figure 35

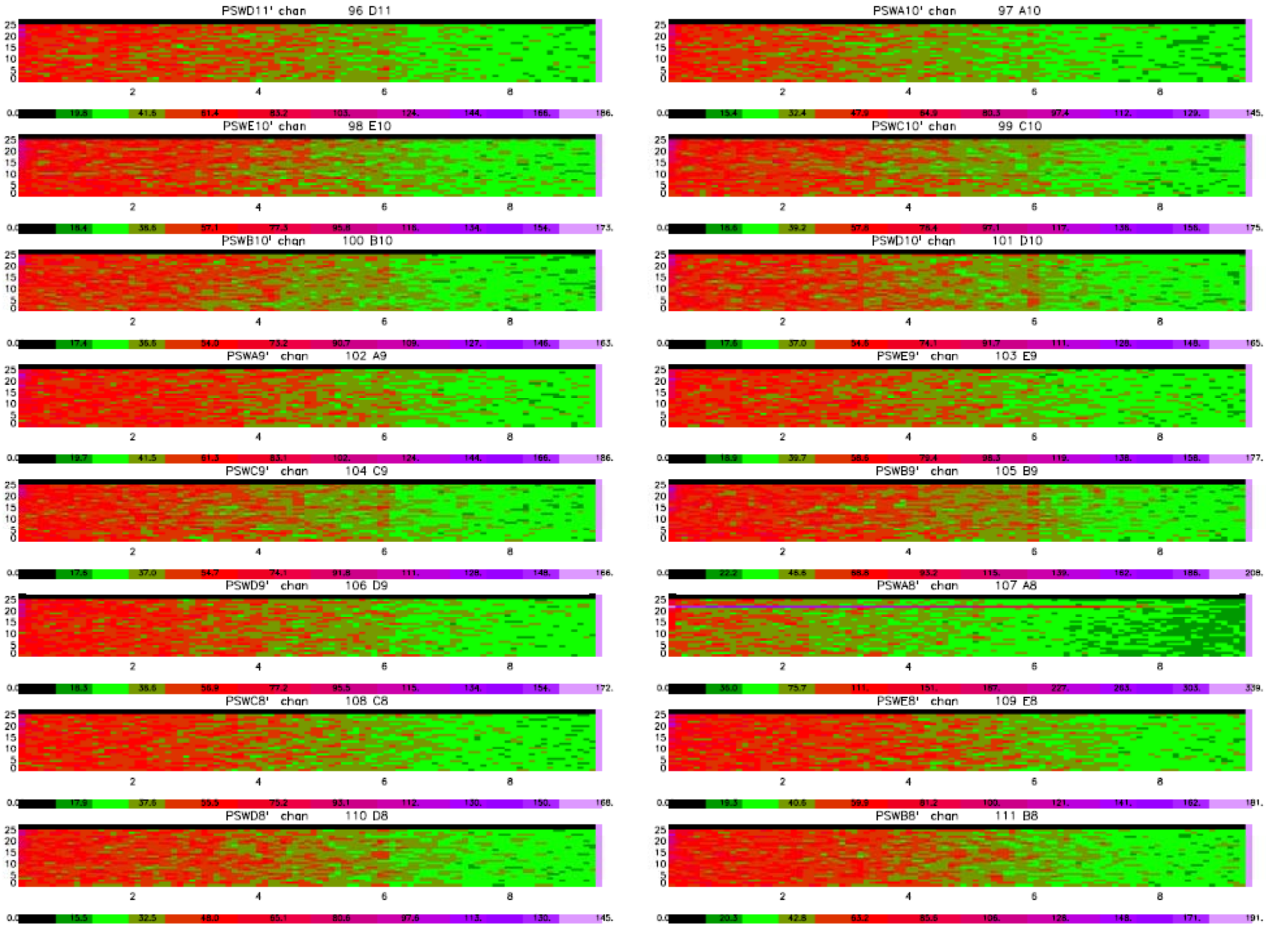

PSWD11' chan 96 D11
PSWA10' chan 97 A10
PSWE10' chan 98 E10
PSWC10' chan 99 C10
PSWB10' chan 100 B10
PSWD10' chan 101 D10
PSWA9' chan 102 A9
PSWE9' chan 103 E9
PSWC9' chan 104 C9
PSWB9' chan 105 B9
PSWD9' chan 106 D9
PSWA8' chan 107 A8
PSWC8' chan 108 C8
PSWE8' chan 109 E8
PSWD8' chan 110 D8
PSWB8' chan 111 B8

Figure 36

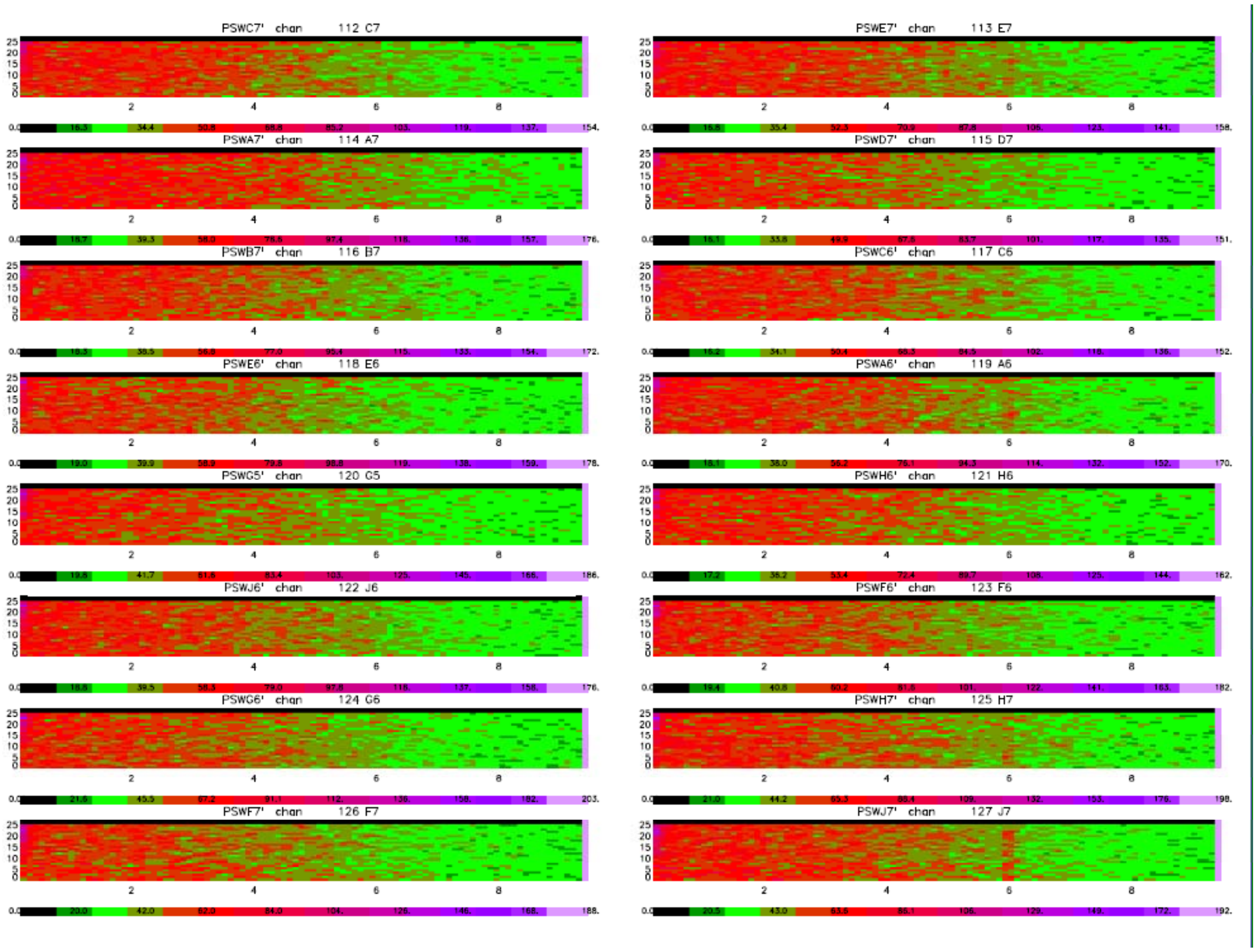
PSWC7' chan 112 C7
PSWE7' chan 113 E7
PSWA7' chan 114 A7
PSWD7' chan 115 D7
PSWB7' chan 116 B7
PSWC6' chan 117 C6
PSWE6' chan 118 E6
PSWA6' chan 119 A6
PSWG5' chan 120 G5
PSWH6' chan 121 H6
PSWJ6' chan 122 J6
PSWF6' chan 123 F6
PSWG6' chan 124 G6
PSWH7' chan 125 H7
PSWF7' chan 126 F7
PSWJ7' chan 127 J7

Figure 37

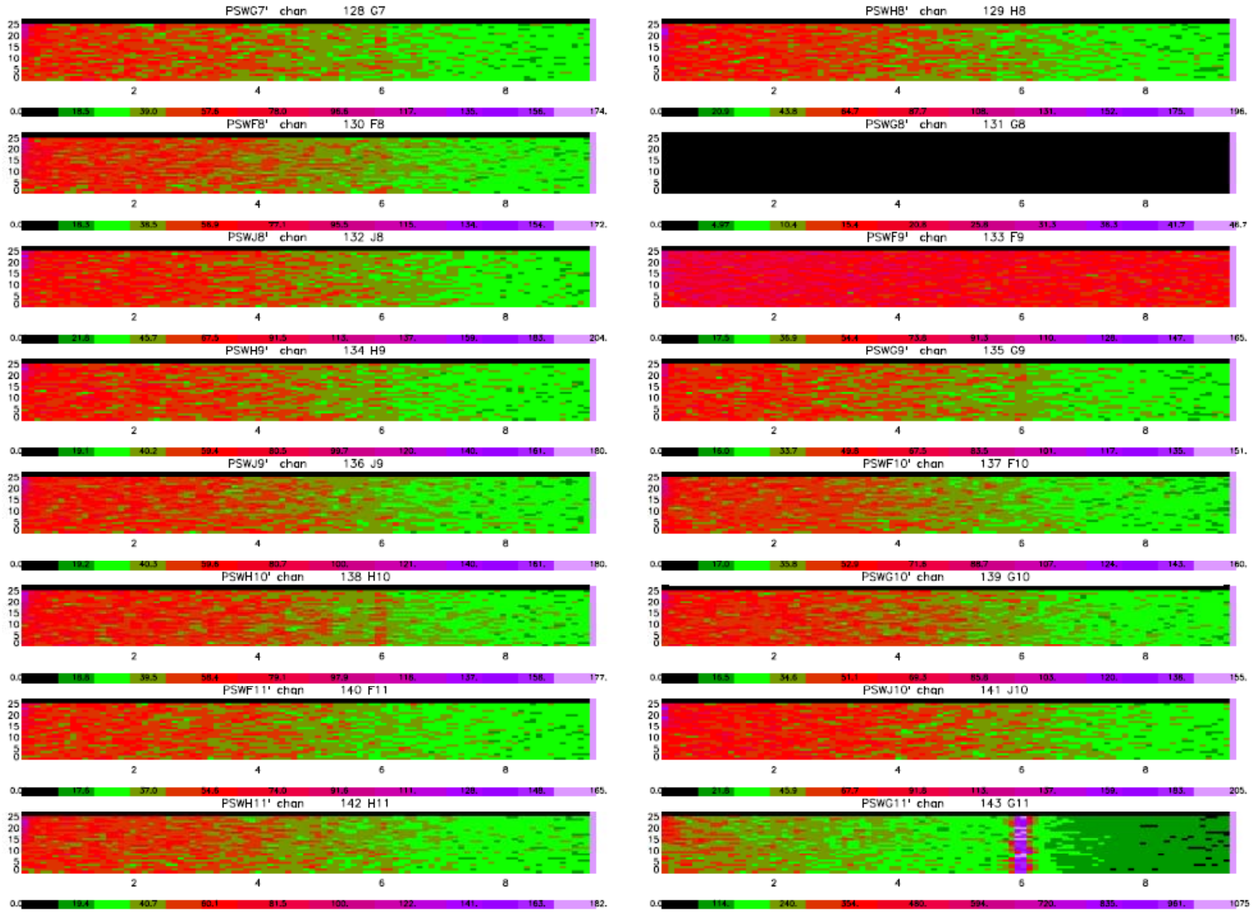
PSWG7' chan 128 G7
PSWH8' chan 129 H8
PSWF8' chan 130 F8
PSWG8' chan 131 G8
PSWJ8' chan 132 J8
PSWF9' chan 133 F9
PSWH9' chan 134 H9
PSWG9' chan 135 G9
PSWJ9' chan 136 J9
PSWF10' chan 137 F10
PSWH10' chan 138 H10
PSWG10' chan 139 G10
PSWF11' chan 140 F11
PSWJ10' chan 141 J10
PSWH11' chan 142 H11
PSWG11' chan 143 G11

Figure 38

7.1.3 PLW Spectrogrammes

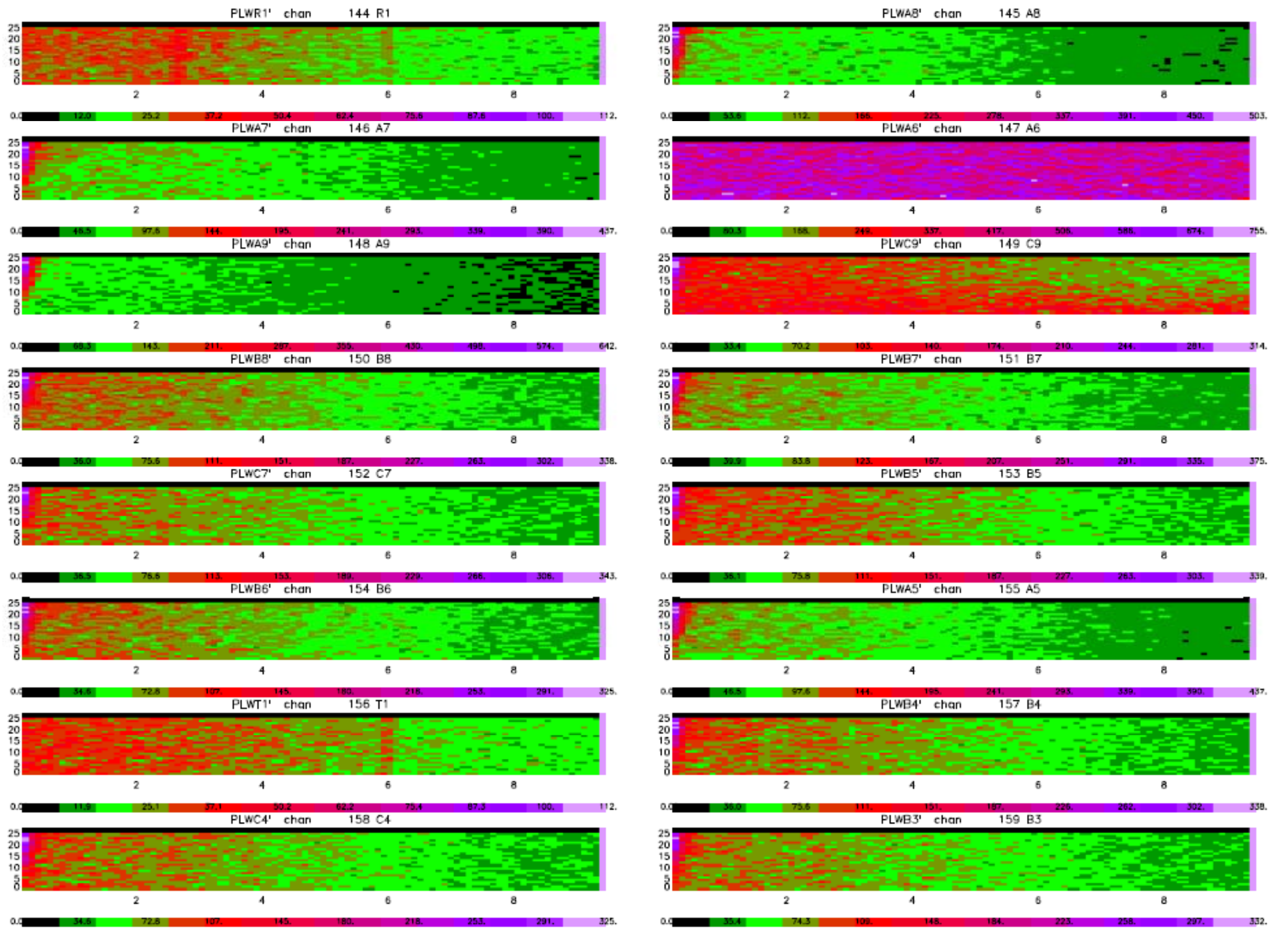

Figure 39

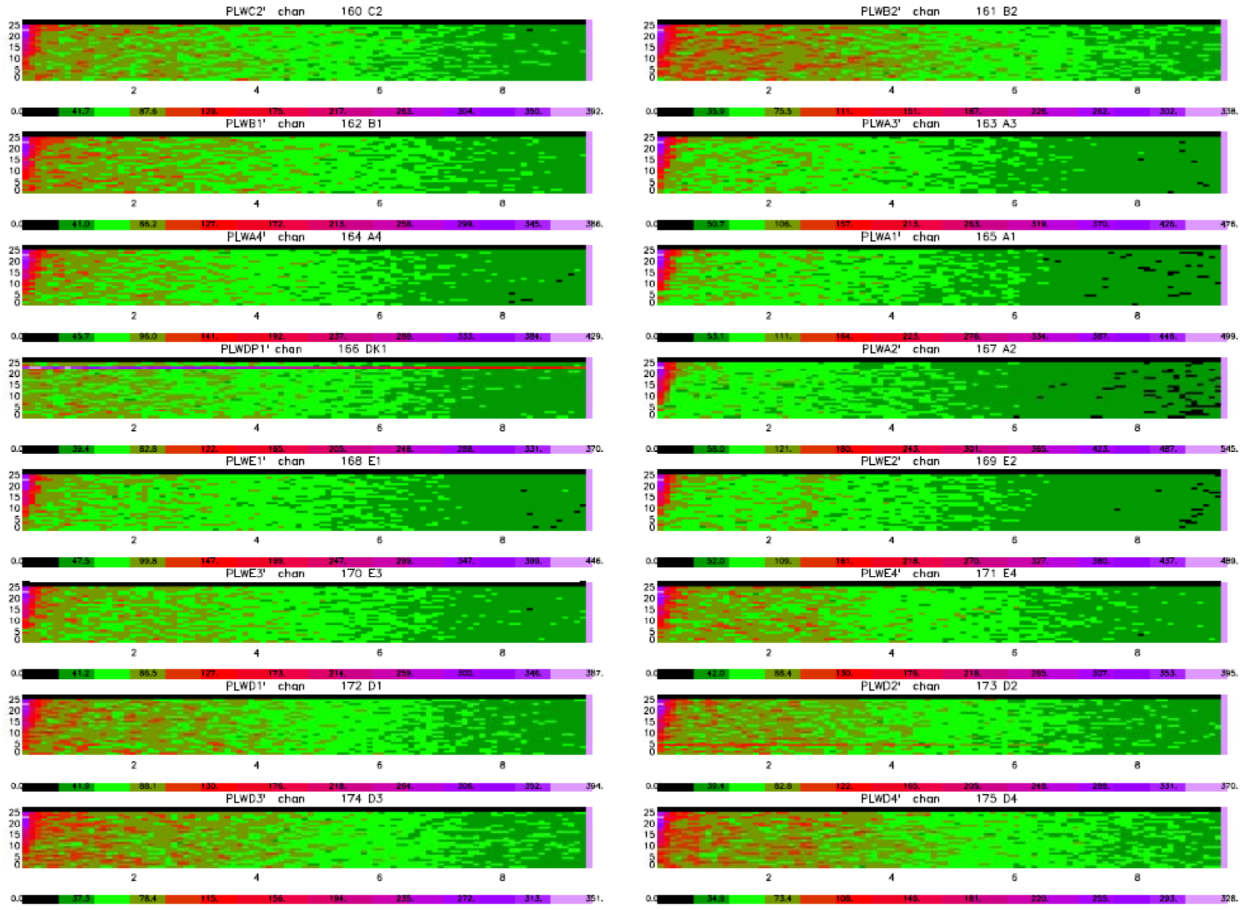

Figure 40

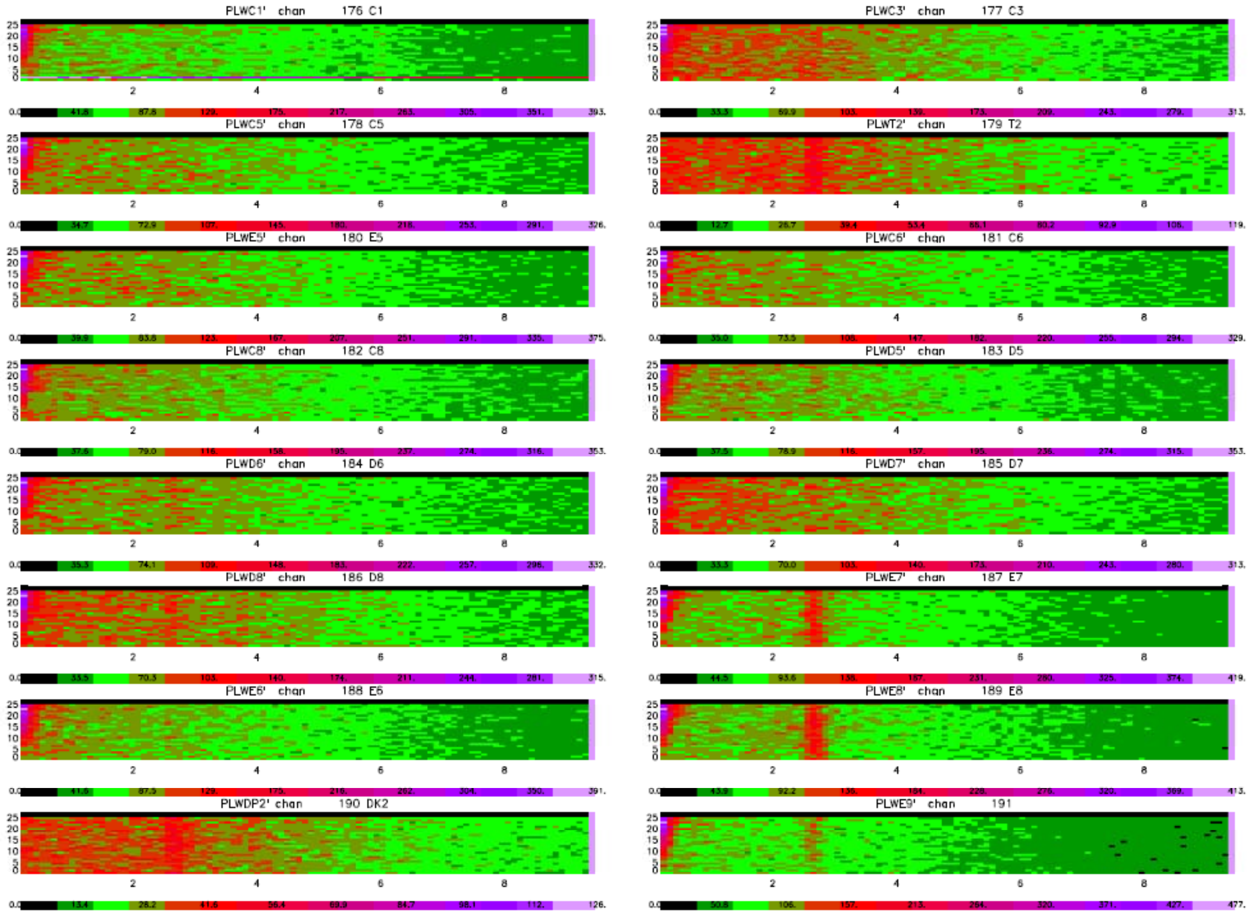
PLWC1' chan 176 C1
PLWC3' chan 177 C3
PLWC5' chan 178 C5
PLWT2' chan 179 T2
PLWE5' chan 180 E5
PLWC6' chan 181 C6
PLWC8' chan 182 C8
PLWD5' chan 183 D5
PLWD6' chan 184 D6
PLWD7' chan 185 D7
PLWD8' chan 186 D8
PLWE7' chan 187 E7
PLWE6' chan 188 E6
PLWE8' chan 189 E8
PLWDP2' chan 190 DK2
PLWE9' chan 191

Figure 41

7.1.4 PMW Spectrogrammes

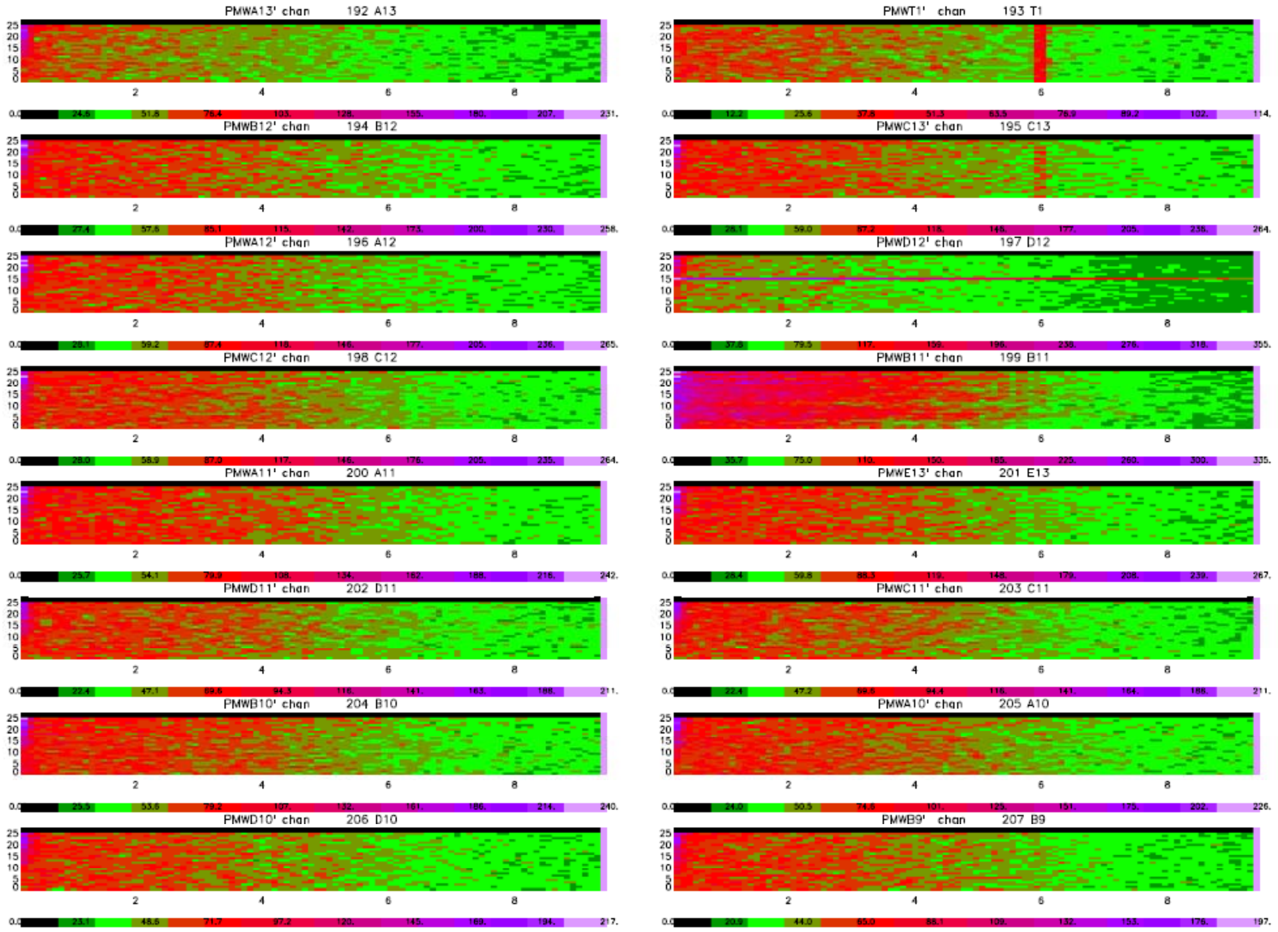

Figure 42

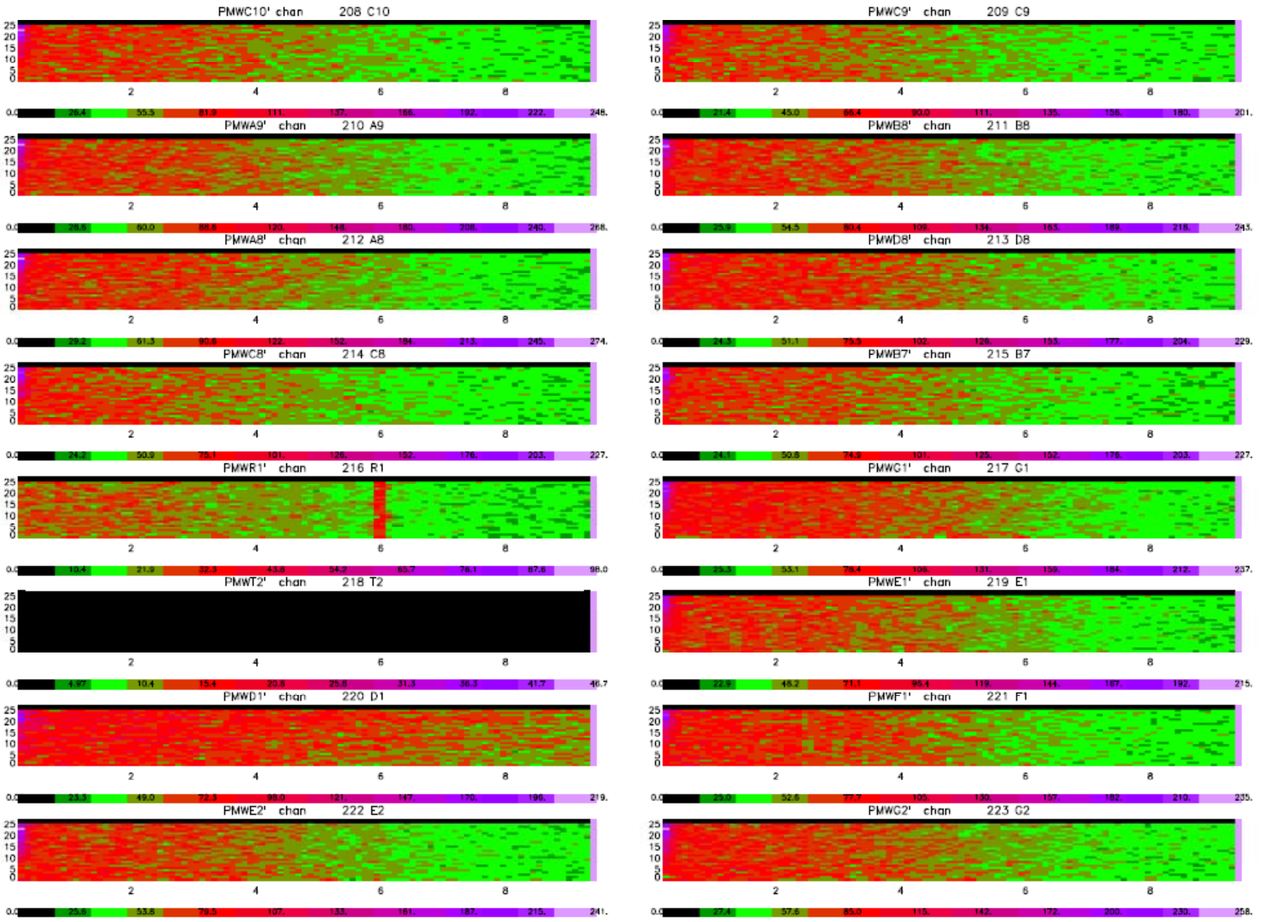
PMWC10' chan 208 C10
PMWC9' chan 209 C9
PMWA9' chan 210 A9
PMWB8' chan 211 B8
PMWA8' chan 212 A8
PMWD8' chan 213 D8
PMWC8' chan 214 C8
PMWB7' chan 215 B7
PMWR1' chan 216 R1
PMWG1' chan 217 G1
PMWT2' chan 218 T2
PMWE1' chan 219 E1
PMWD1' chan 220 D1
PMWF1' chan 221 F1
PMWE2' chan 222 E2
PMWG2' chan 223 G2

Figure 43

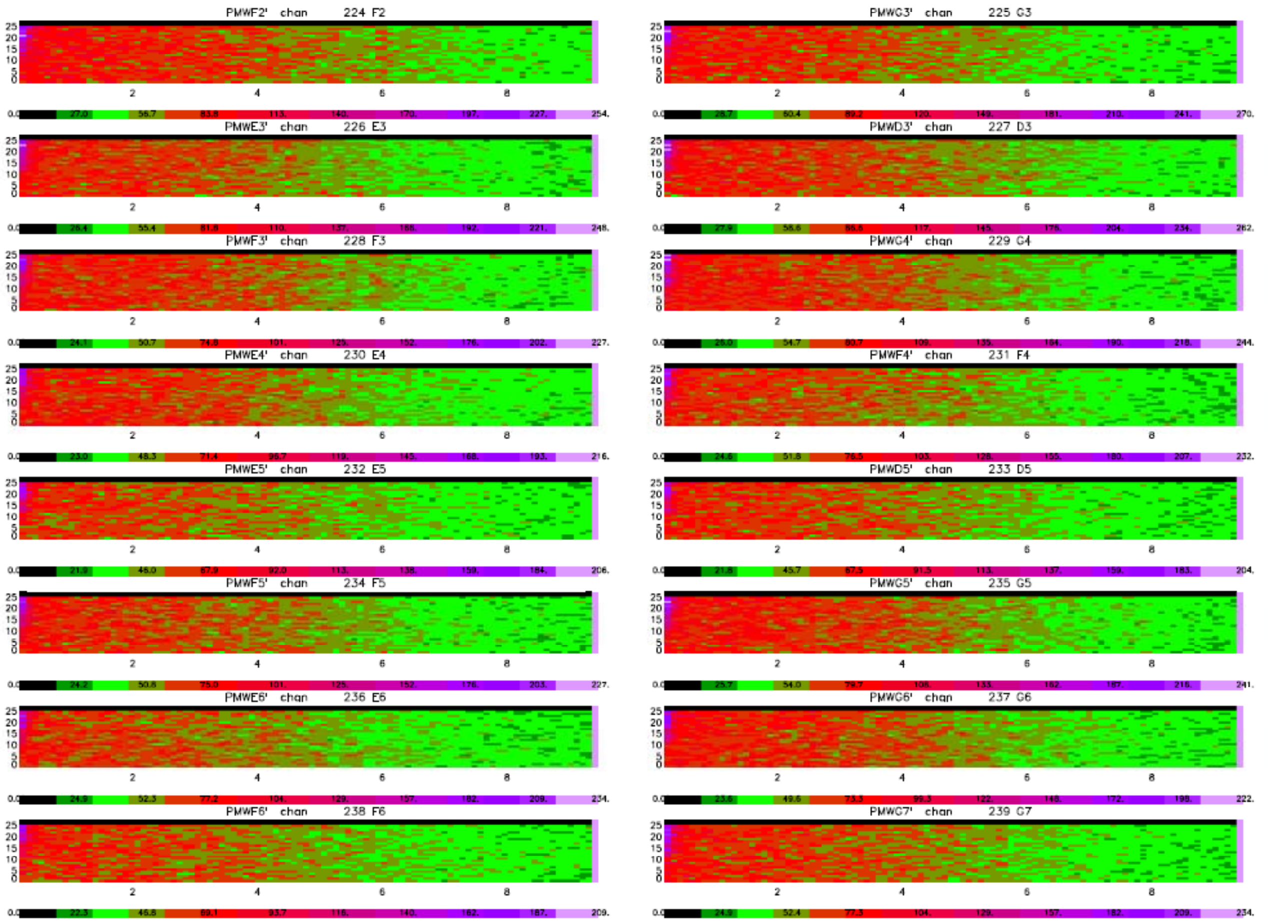
PMWF2' chan 224 F2
PMWG3' chan 225 G3
PMWE3' chan 226 E3
PMWD3' chan 227 D3
PMWF3' chan 228 F3
PMWG4' chan 229 G4
PMWE4' chan 230 E4
PMWF4' chan 231 F4
PMWE5' chan 232 E5
PMWD5' chan 233 D5
PMWF5' chan 234 F5
PMWG5' chan 235 G5
PMWE6' chan 236 E6
PMWG6' chan 237 G6
PMWF6' chan 238 F6
PMWG7' chan 239 G7

Figure 44

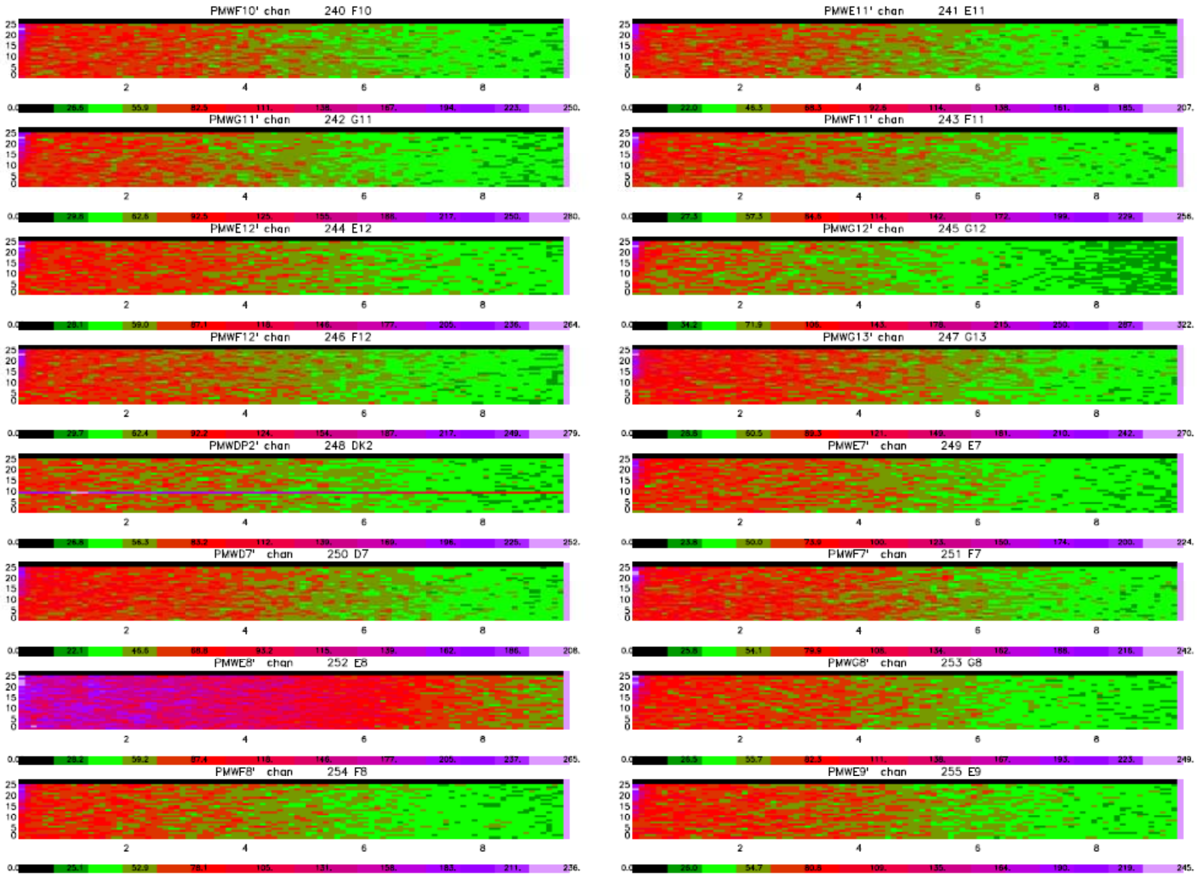
PMWF10' chan 240 F10
PMWE11' chan 241 E11
PMWG11' chan 242 G11
PMWF11' chan 243 F11
PMWE12' chan 244 E12
PMWG12' chan 245 G12
PMWF12' chan 246 F12
PMWG13' chan 247 G13
PMWDP2' chan 248 DK2
PMWE7' chan 249 E7
PMWD7' chan 250 D7
PMWF7' chan 251 F7
PMWE8' chan 252 E8
PMWG8' chan 253 G8
PMWF8' chan 254 F8
PMWE9' chan 255 E9

Figure 45

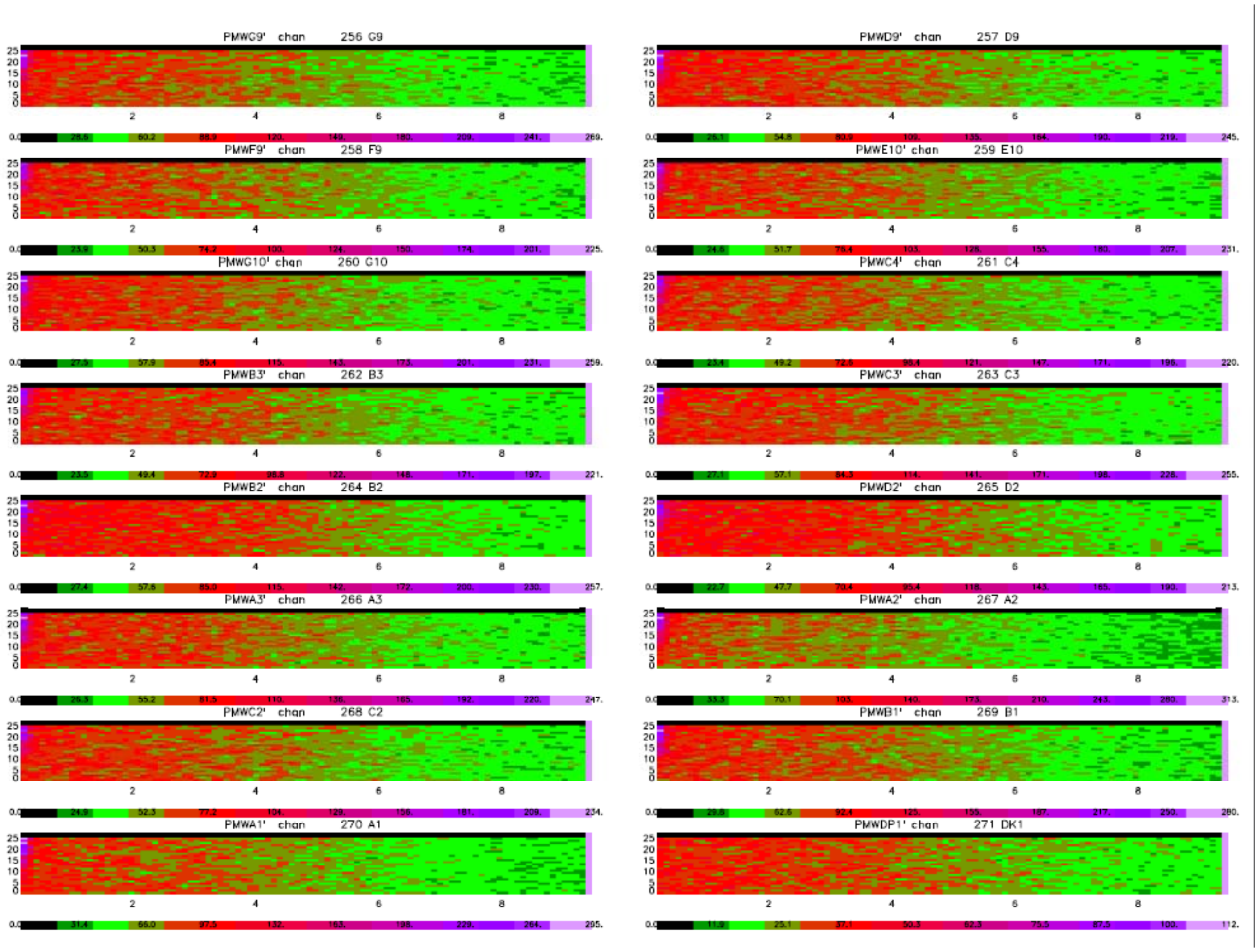
PMWG9' chan 256 G9
PMWD9' chan 257 D9
PMWF9' chan 258 F9
PMWE10' chan 259 E10
PMWG10' chan 260 G10
PMWC4' chan 261 C4
PMWB3' chan 262 B3
PMWC3' chan 263 C3
PMWB2' chan 264 B2
PMWD2' chan 265 D2
PMWA3' chan 266 A3
PMWA2' chan 267 A2
PMWC2' chan 268 C2
PMWB1' chan 269 B1
PMWA1' chan 270 A1
PMWDP1' chan 271 DK1

Figure 46

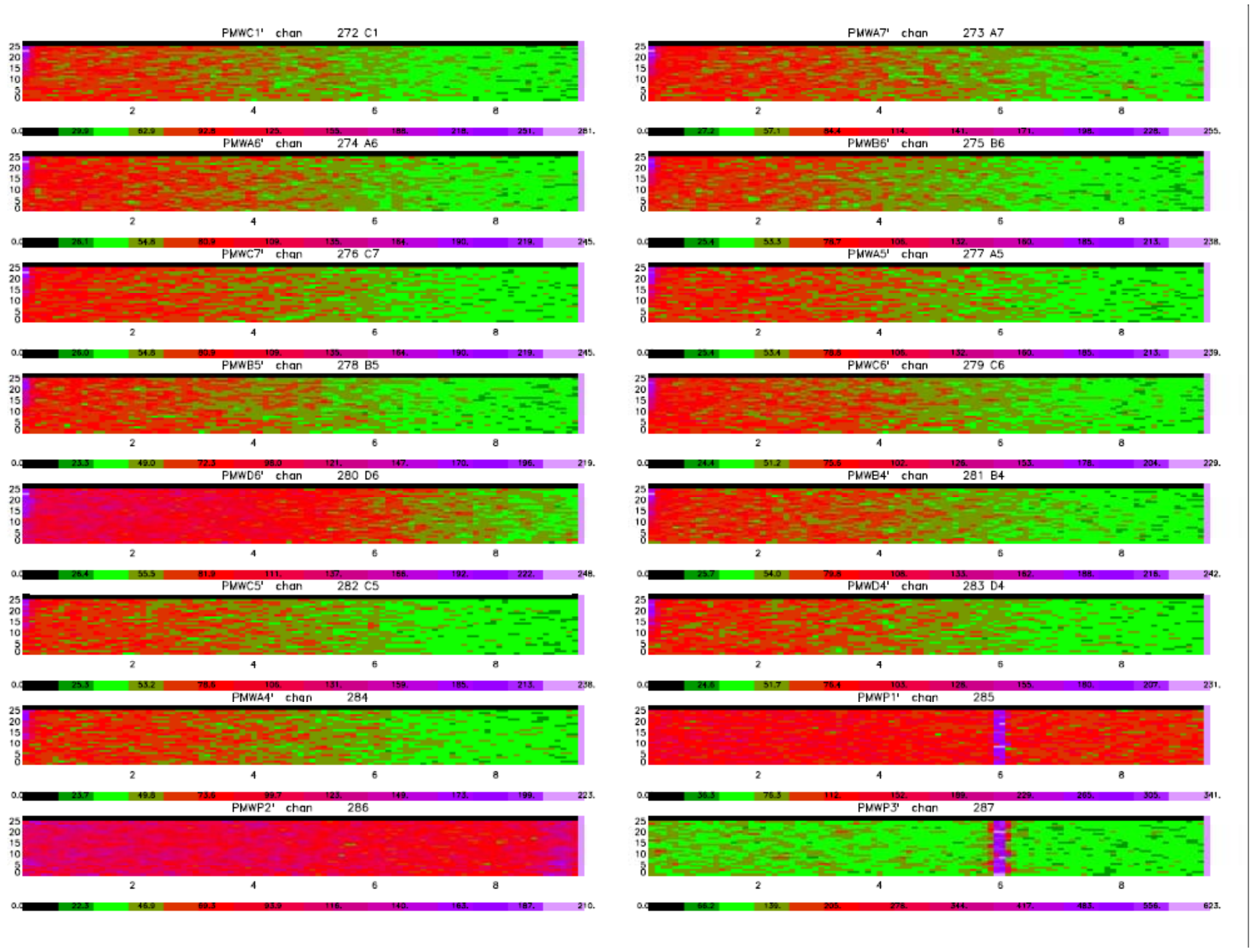

Figure 47

7.2 CS Common Mode – Spectrometer (0xB00014E1)

7.2.1 Noise PSD (using 10 seconds blocks of detector data)

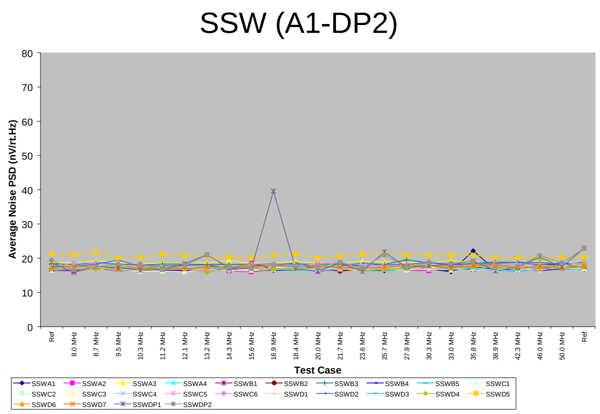

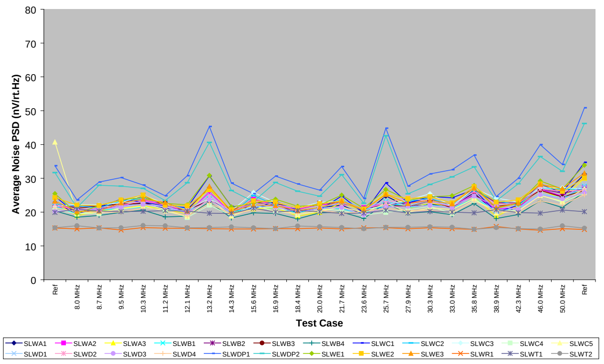

SLW-DP1 and DP2 show highest excess noise
SLW-R1, T1 and T2 have low noise and show no apparent Frequency dependency

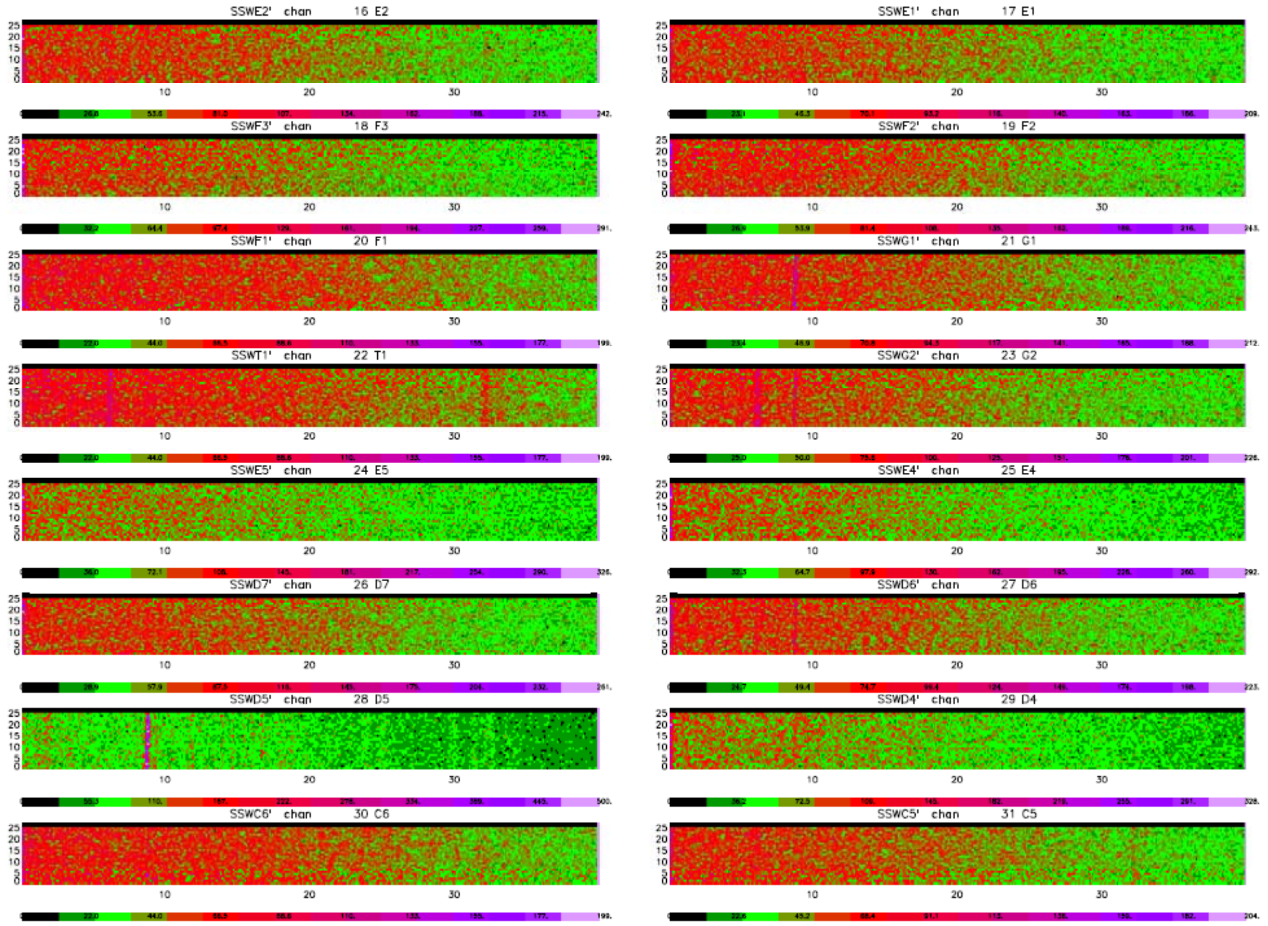
SSWE2' chan 16 E2
SSWE1' chan 17 E1
SSWF3' chan 18 F3
SSWF2' chan 19 F2
SSWF1' chan 20 F1
SSWG1' chan 21 G1
SSWT1' chan 22 T1
SSWG2' chan 23 G2
SSWE5' chan 24 E5
SSWE4' chan 25 E4
SSWD7' chan 26 D7
SSWD6' chan 27 D6
SSWD5' chan 28 D5
SSWD4' chan 29 D4
SSWC6' chan 30 C6
SSWC5' chan 31 C5

Figure 49

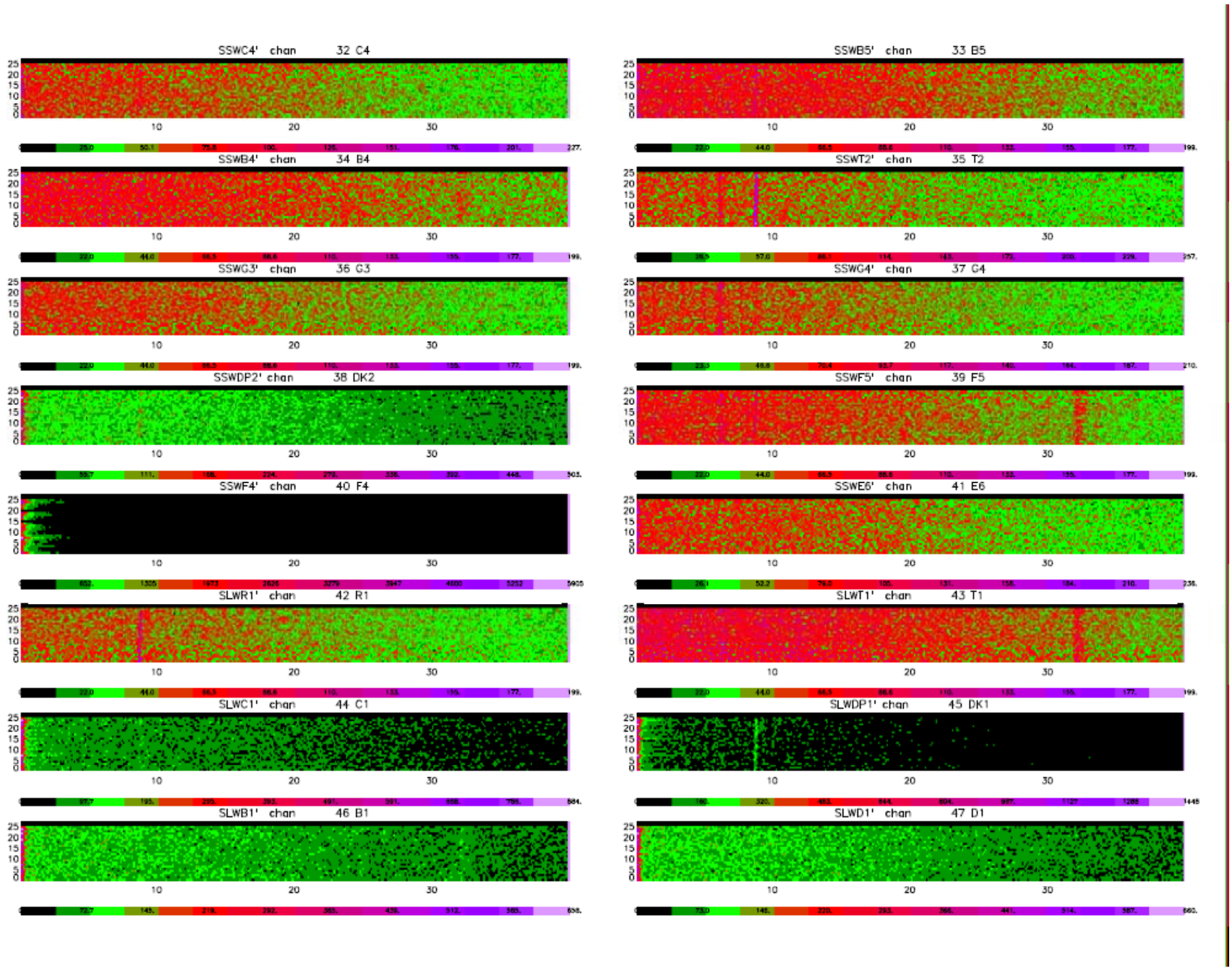

Figure 50

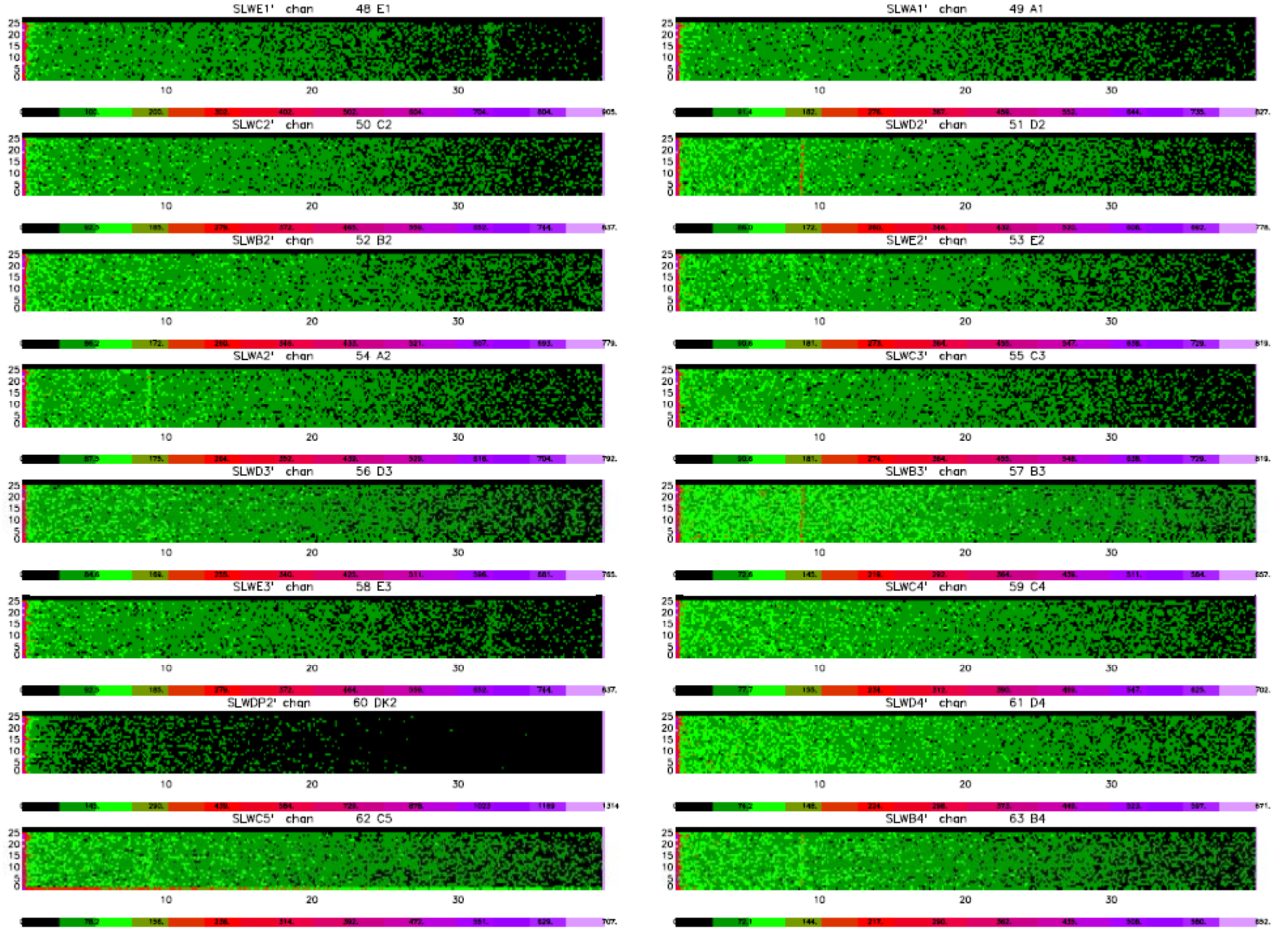

Figure 51

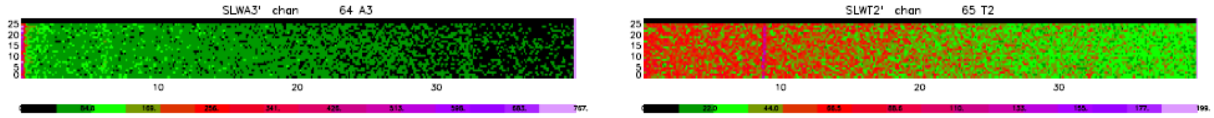

Figure 52

8. Appendix 3: Radiated Susceptibility Detailed Results

8.1 RS – Photometer: V-Polarization (0xB00014EB Step 1)

PSW (A1-B2)

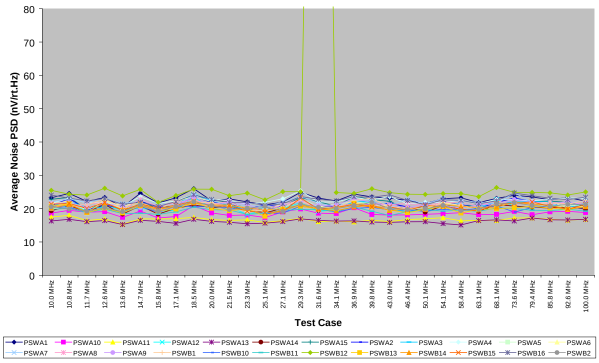

PSW B12 “spikes”

PMW (A1-B8)

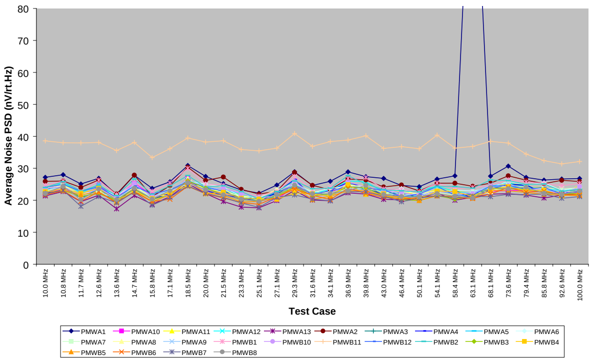

PMW-B11 shows excess noise @ ~ 35nV/√Hz
PMW-A1 “spikes”

8.1.1 PSW Spectrogrammes

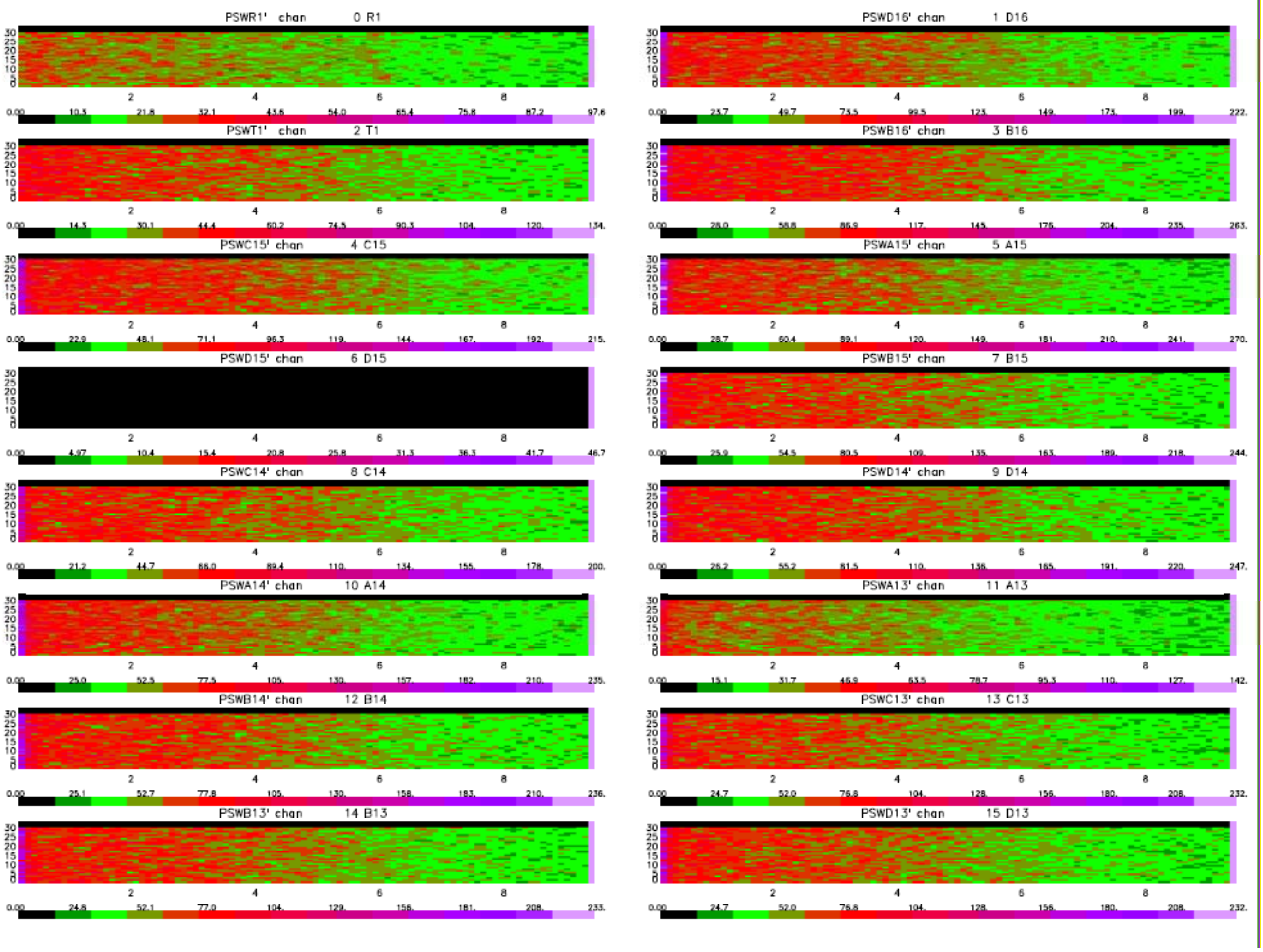

Figure 53

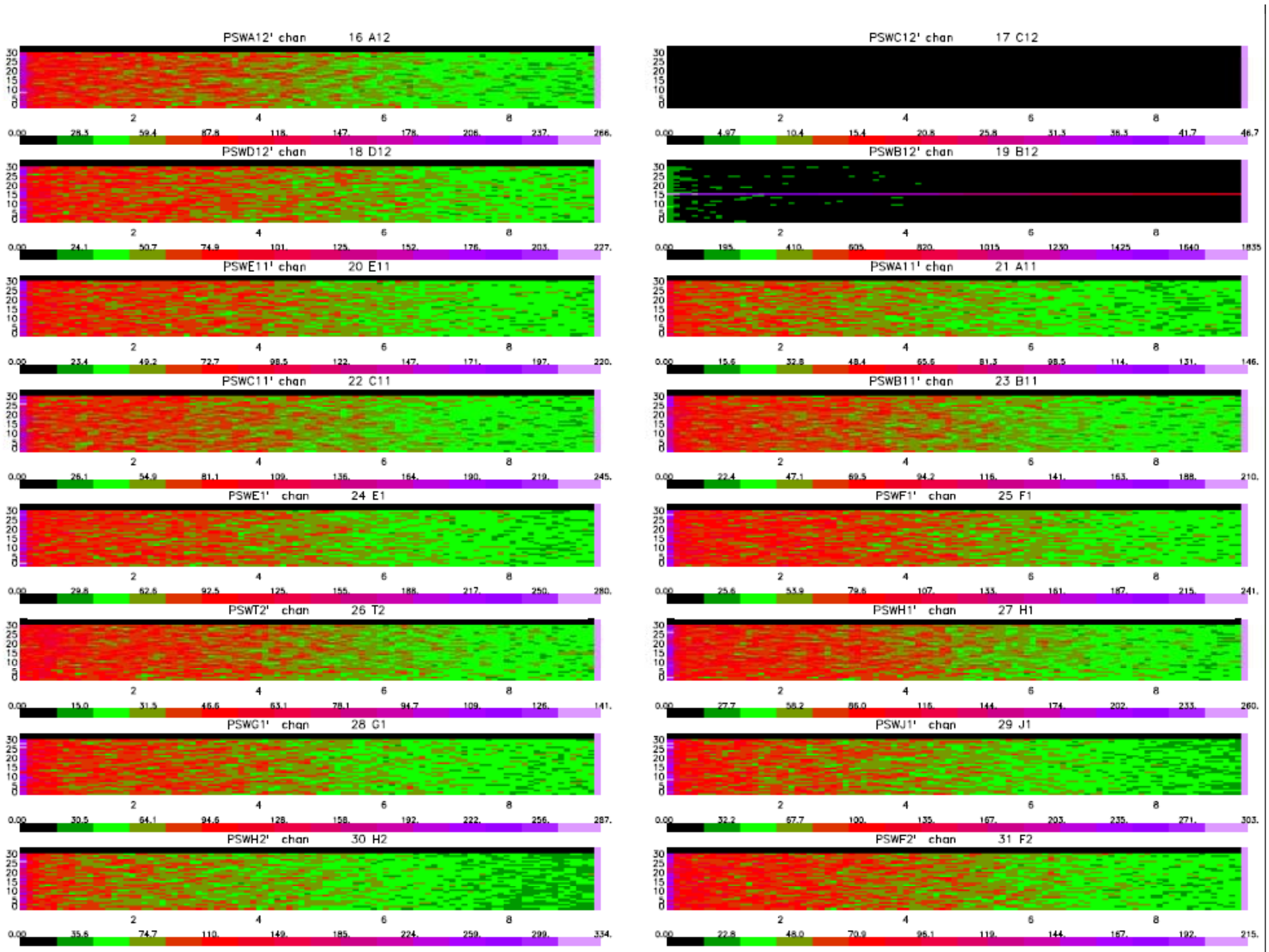

Figure 54

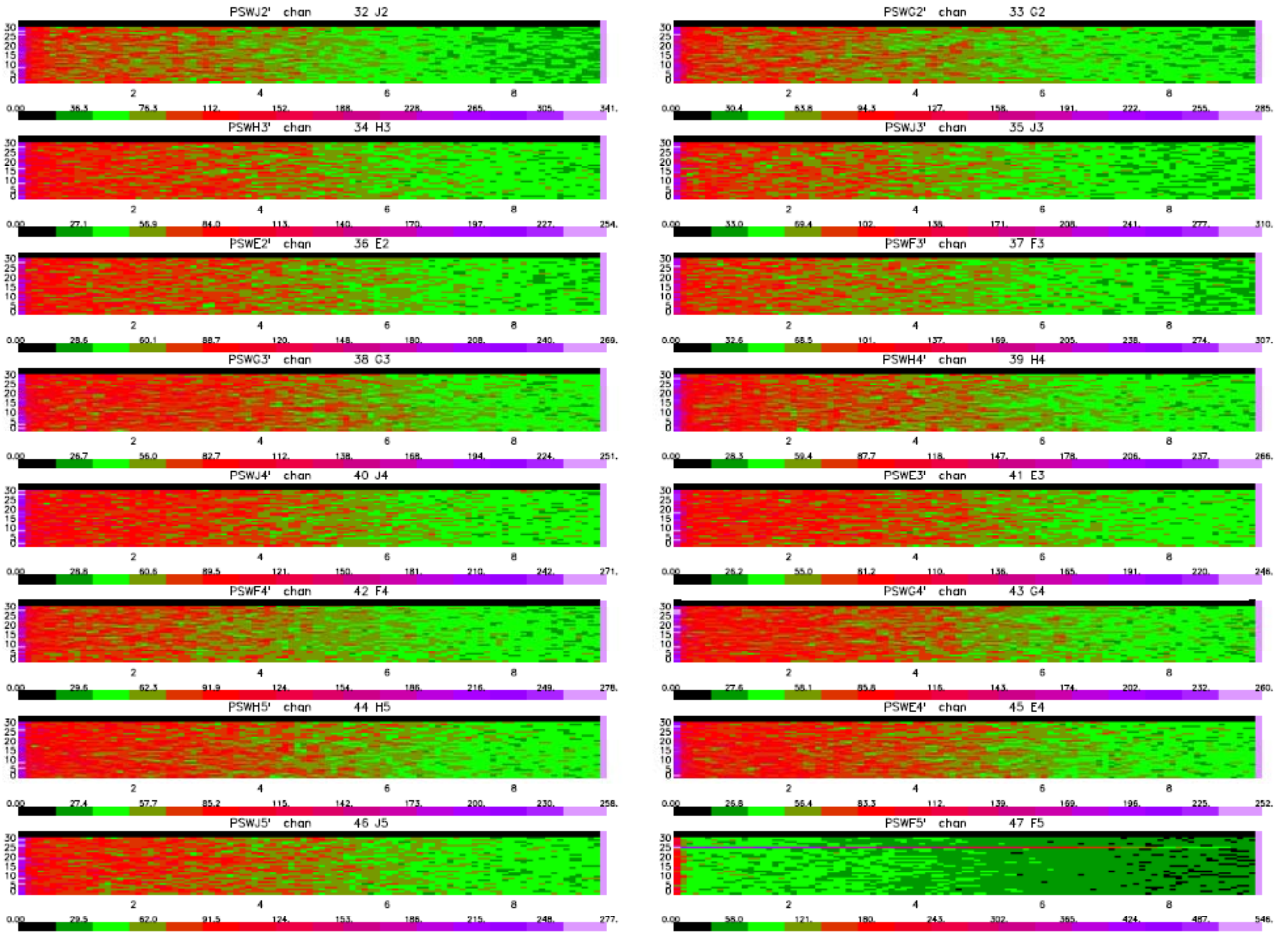
PSWJ2' chan 32 J2
PSWG2' chan 33 G2
PSWH3' chan 34 H3
PSWJ3' chan 35 J3
PSWE2' chan 36 E2
PSWF3' chan 37 F3
PSWG3' chan 38 G3
PSWH4' chan 39 H4
PSWJ4' chan 40 J4
PSWE3' chan 41 E3
PSWF4' chan 42 F4
PSWG4' chan 43 G4
PSWH5' chan 44 H5
PSWE4' chan 45 E4
PSWJ5' chan 46 J5
PSWF5' chan 47 F5

Figure 55

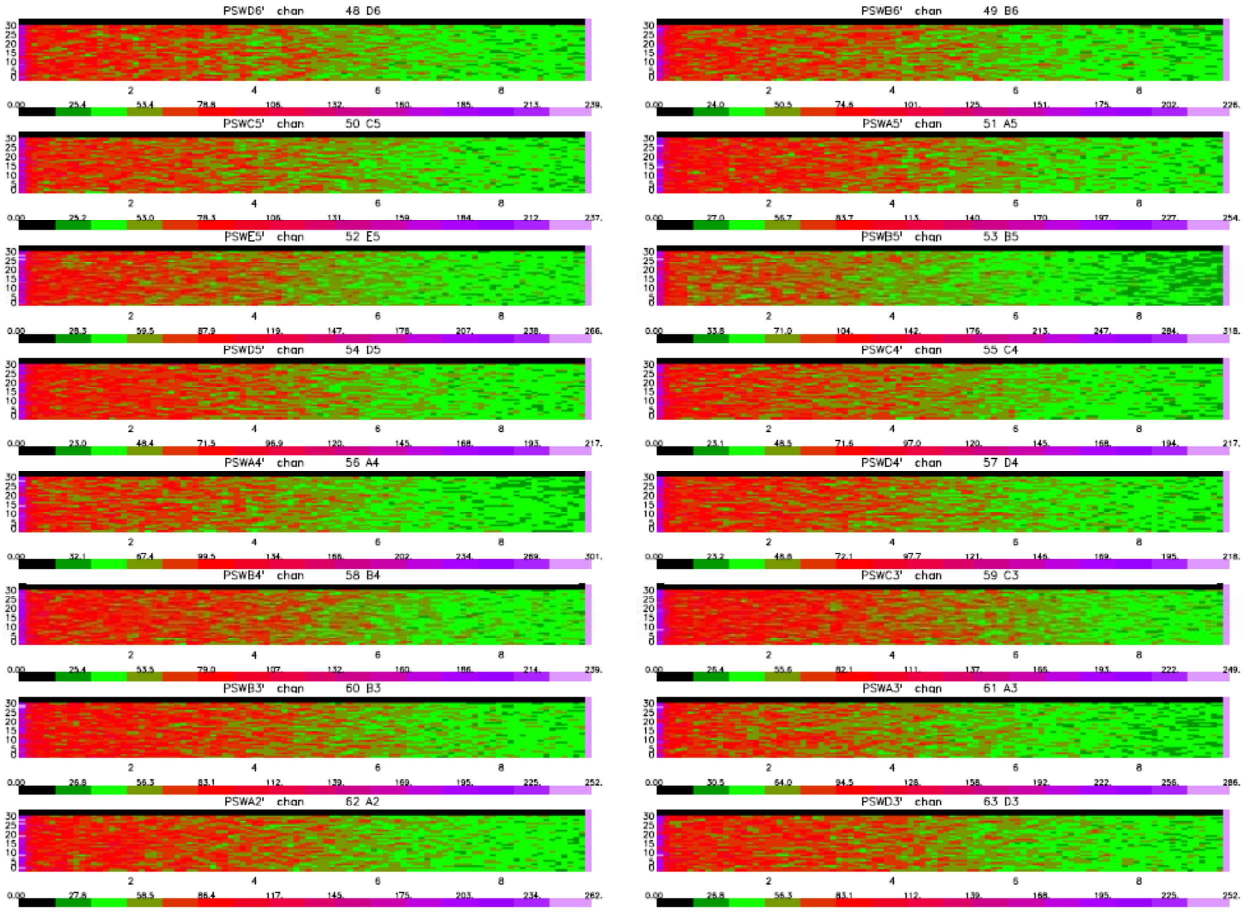
PSWD6' chan 48 D6
PSWB6' chan 49 B6
PSWC5' chan 50 C5
PSWA5' chan 51 A5
PSWE5' chan 52 E5
PSWB5' chan 53 B5
PSWD5' chan 54 D5
PSWC4' chan 55 C4
PSWA4' chan 56 A4
PSWD4' chan 57 D4
PSWB4' chan 58 B4
PSWC3' chan 59 C3
PSWB3' chan 60 B3
PSWA3' chan 61 A3
PSWA2' chan 62 A2
PSWD3' chan 63 D3

Figure 56

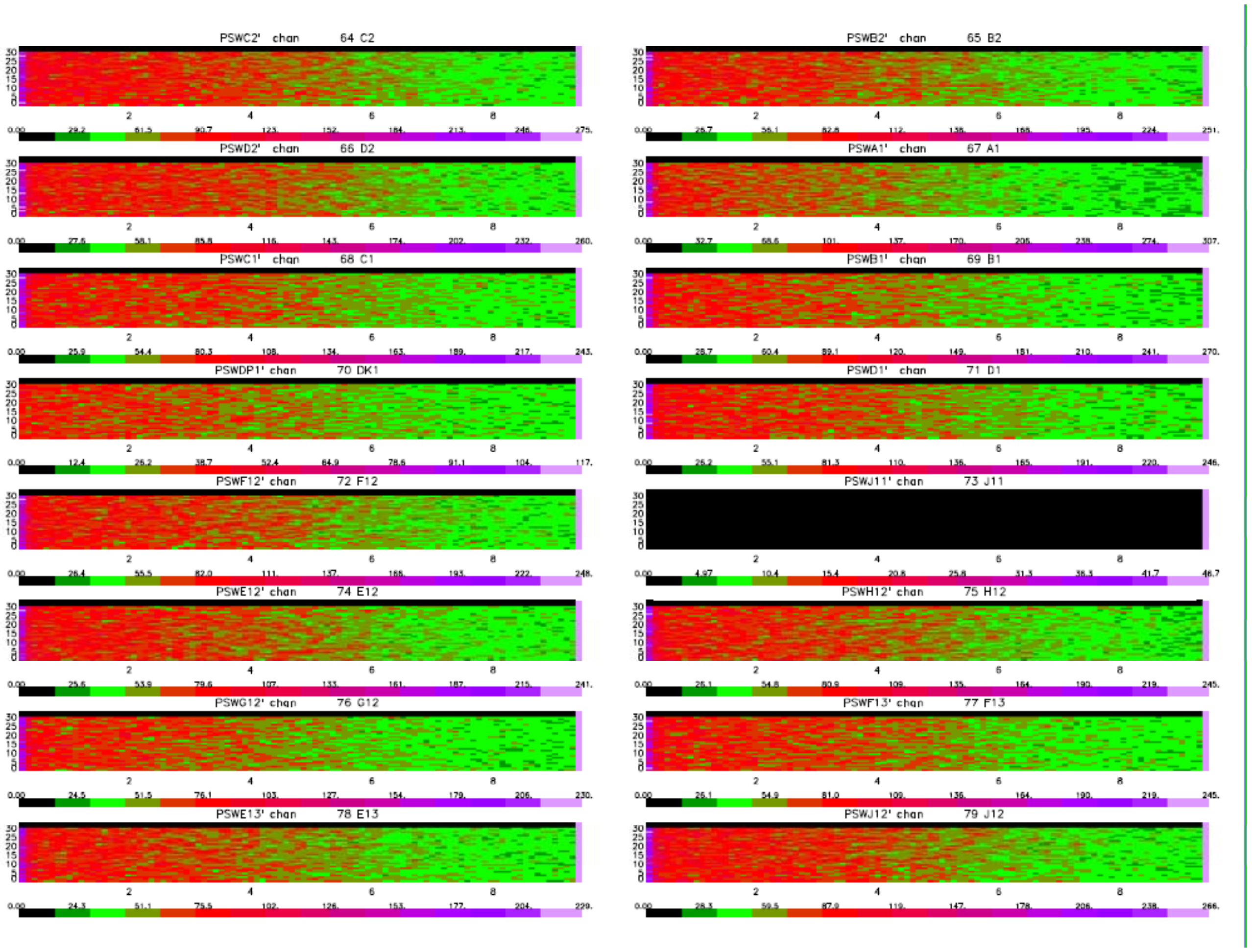
PSWC2' chan 64 C2
PSWB2' chan 65 B2
PSWD2' chan 66 D2
PSWA1' chan 67 A1
PSWC1' chan 68 C1
PSWB1' chan 69 B1
PSWDP1' chan 70 DK1
PSWD1' chan 71 D1
PSWF12' chan 72 F12
PSWJ11' chan 73 J11
PSWE12' chan 74 E12
PSWH12' chan 75 H12
PSWG12' chan 76 G12
PSWF13' chan 77 F13
PSWE13' chan 78 E13
PSWJ12' chan 79 J12

Figure 57

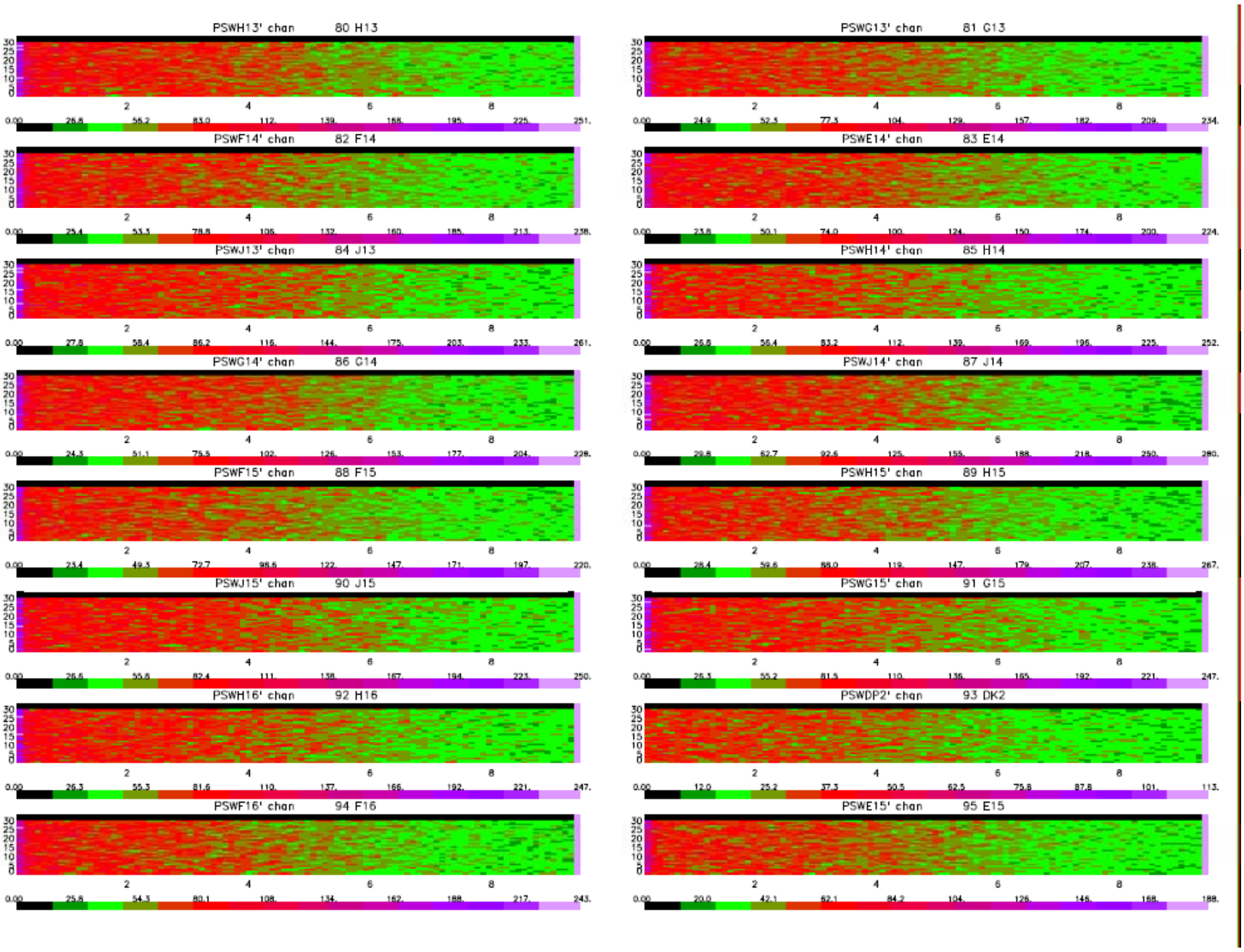

Figure 58

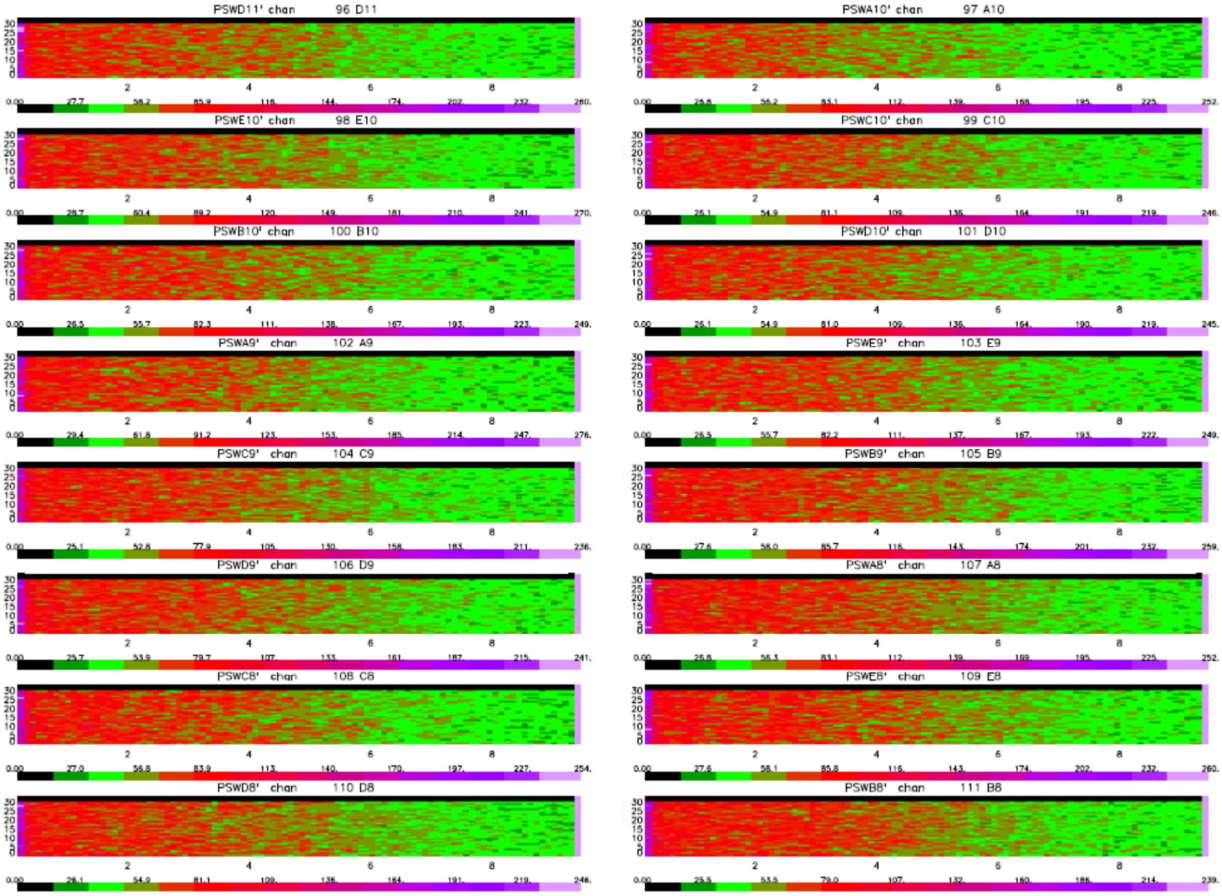

PSWD11' chan 96 D11
PSWA10' chan 97 A10
PSWE10' chan 98 E10
PSWC10' chan 99 C10
PSWB10' chan 100 B10
PSWD10' chan 101 D10
PSWA9' chan 102 A9
PSWE9' chan 103 E9
PSWC9' chan 104 C9
PSWB9' chan 105 B9
PSWD9' chan 106 D9
PSWA8' chan 107 A8
PSWC8' chan 108 C8
PSWE8' chan 109 E8
PSWD8' chan 110 D8
PSWB8' chan 111 B8

Figure 59

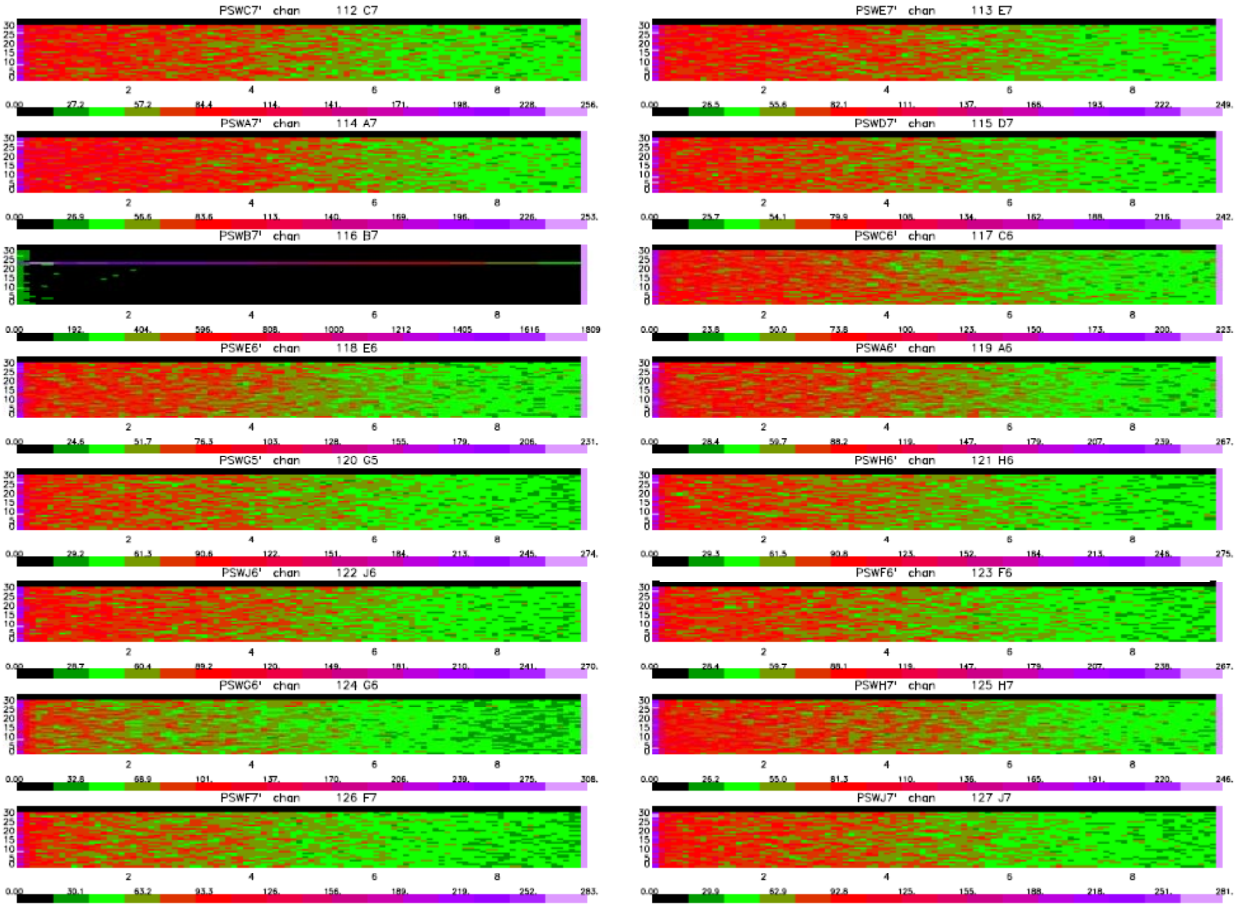
PSWC7' chan 112 C7
PSWE7' chan 113 E7
PSWA7' chan 114 A7
PSWD7' chan 115 D7
PSWB7' chan 116 B7
PSWC6' chan 117 C6
PSWE6' chan 118 E6
PSWA6' chan 119 A6
PSWG5' chan 120 G5
PSWH6' chan 121 H6
PSWJ6' chan 122 J6
PSWF6' chan 123 F6
PSWG6' chan 124 G6
PSWH7' chan 125 H7
PSWF7' chan 126 F7
PSWJ7' chan 127 J7

Figure 60

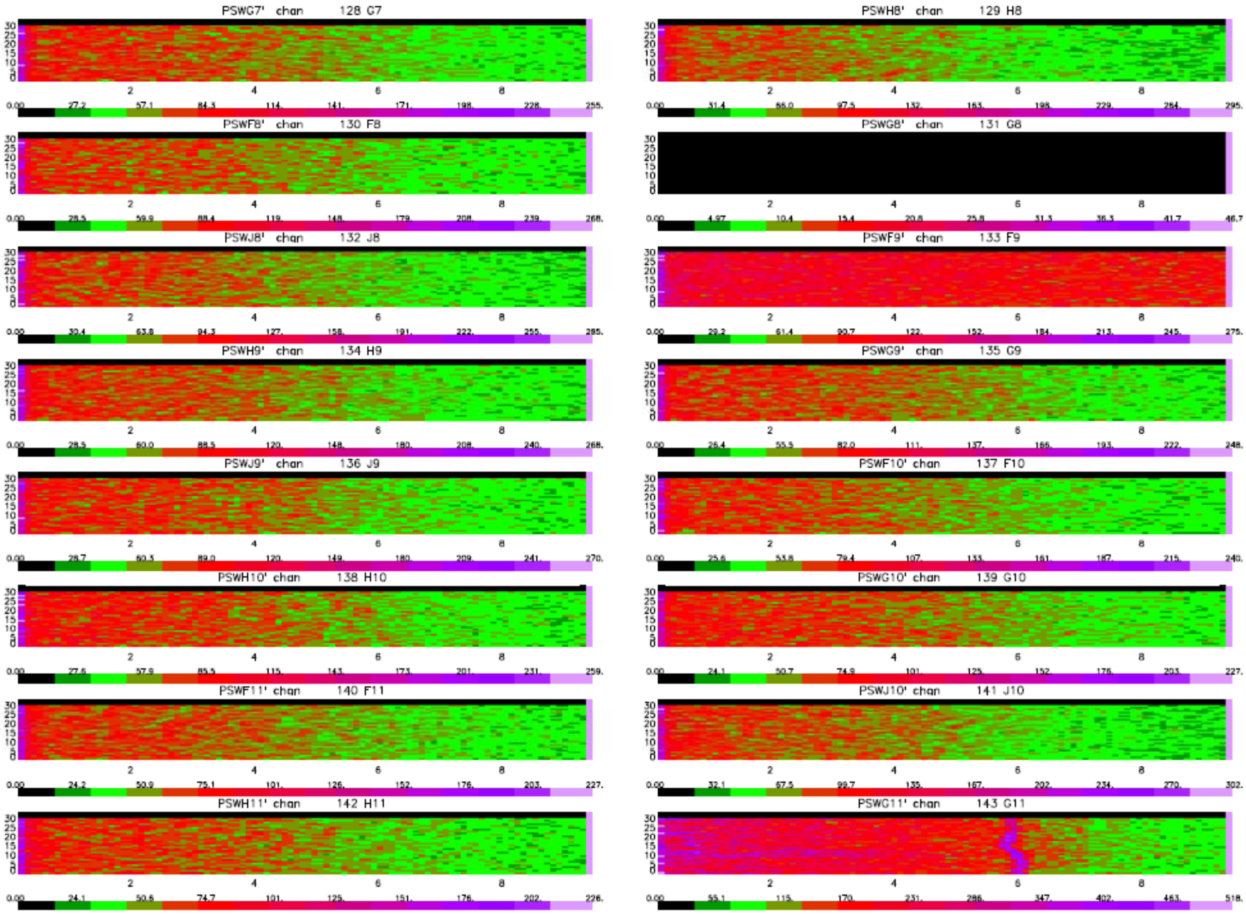
PSWG7' chan 128 G7
PSWH8' chan 129 H8
PSWF8' chan 130 F8
PSWG8' chan 131 G8
PSWJ8' chan 132 J8
PSWF9' chan 133 F9
PSWH9' chan 134 H9
PSWG9' chan 135 G9
PSWJ9' chan 136 J9
PSWF10' chan 137 F10
PSWH10' chan 138 H10
PSWG10' chan 139 G10
PSWF11' chan 140 F11
PSWJ10' chan 141 J10
PSWH11' chan 142 H11
PSWG11' chan 143 G11

Figure 61

8.1.2 PLW Spectrogrammes

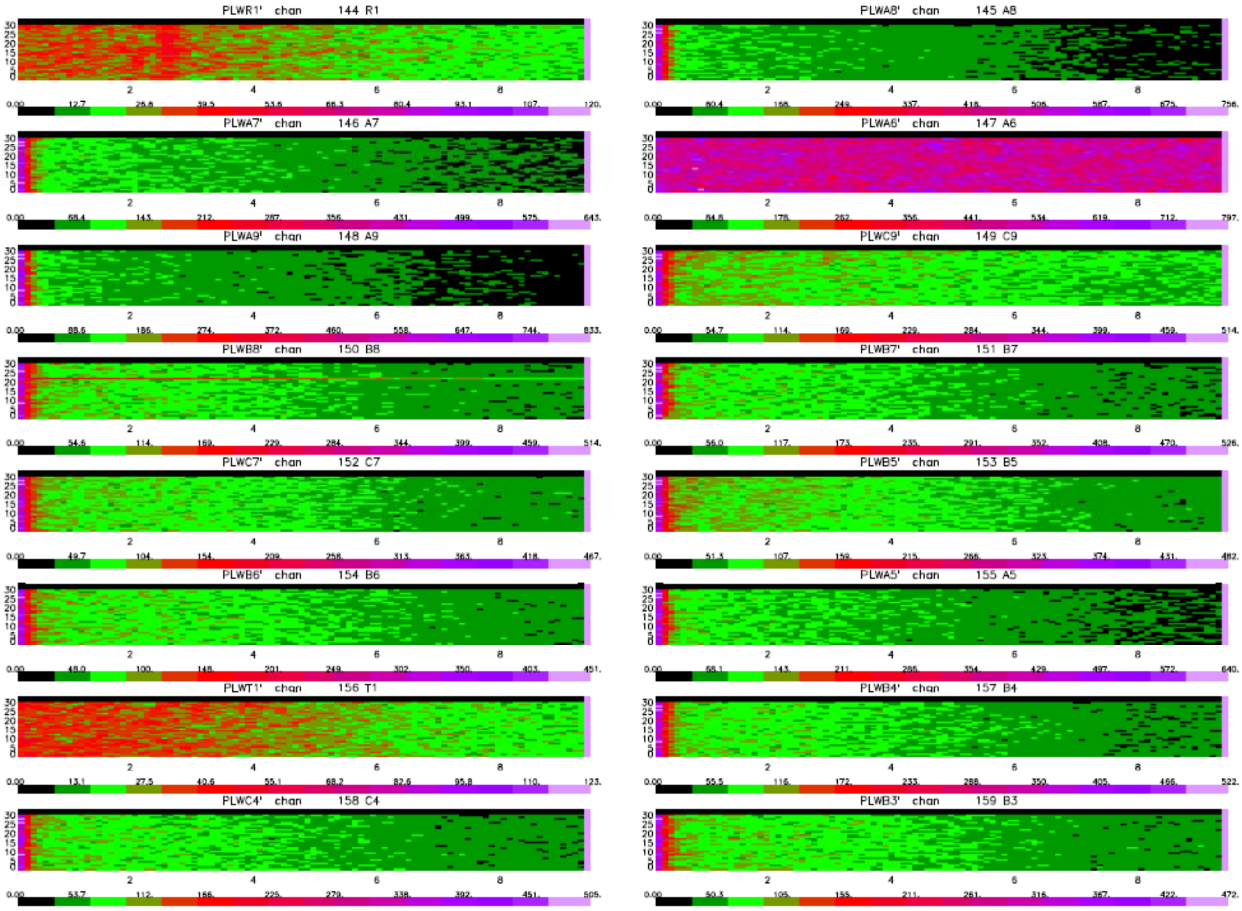

Figure 62

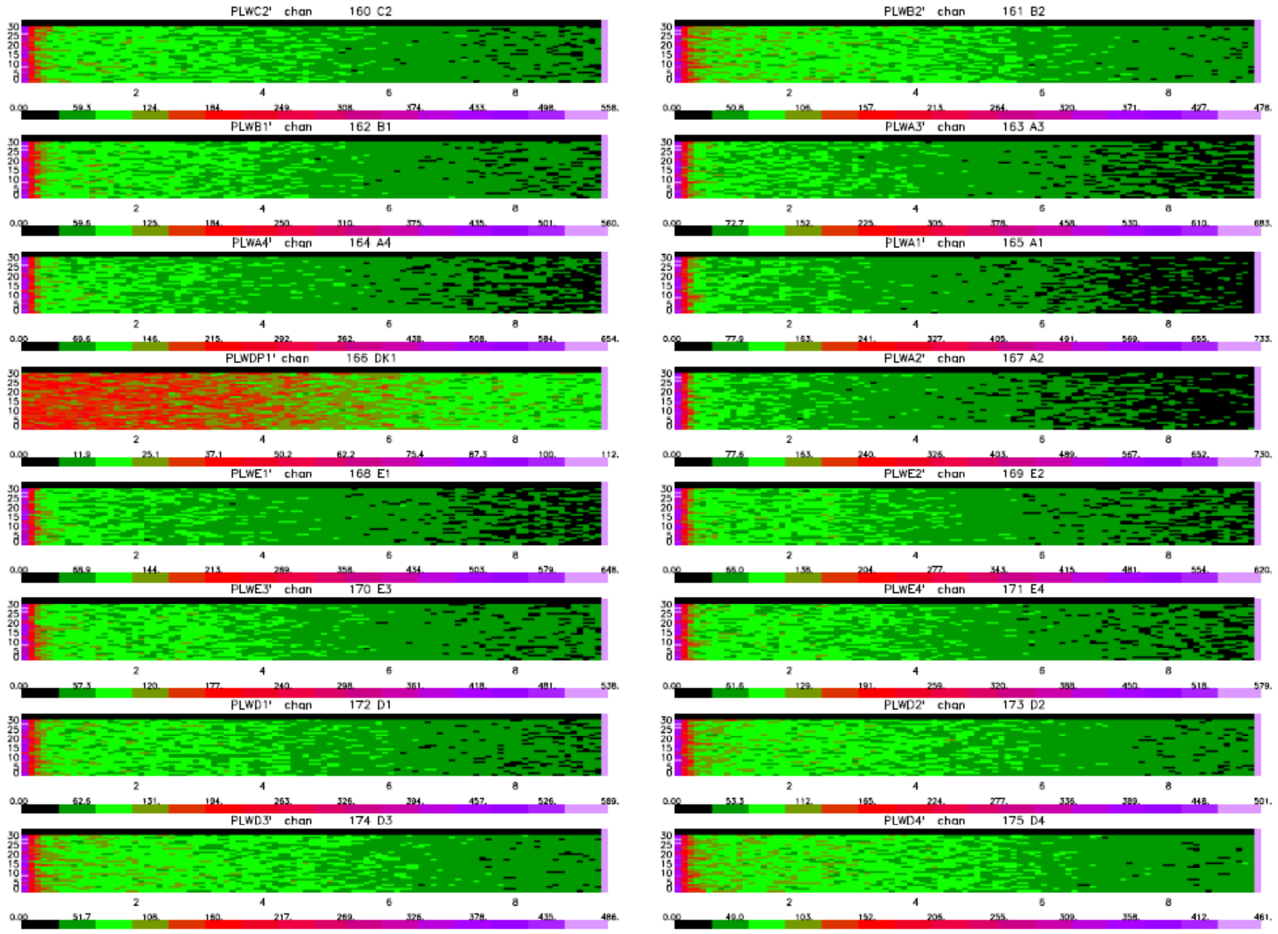
PLWC2' chan 160 C2
PLWB2' chan 161 B2
PLWB1' chan 162 B1
PLWA3' chan 163 A3
PLWA4' chan 164 A4
PLWA1' chan 165 A1
PLWDP1' chan 166 DK1
PLWA2' chan 167 A2
PLWE1' chan 168 E1
PLWE2' chan 169 E2
PLWE3' chan 170 E3
PLWE4' chan 171 E4
PLWD1' chan 172 D1
PLWD2' chan 173 D2
PLWD3' chan 174 D3
PLWD4' chan 175 D4

Figure 63

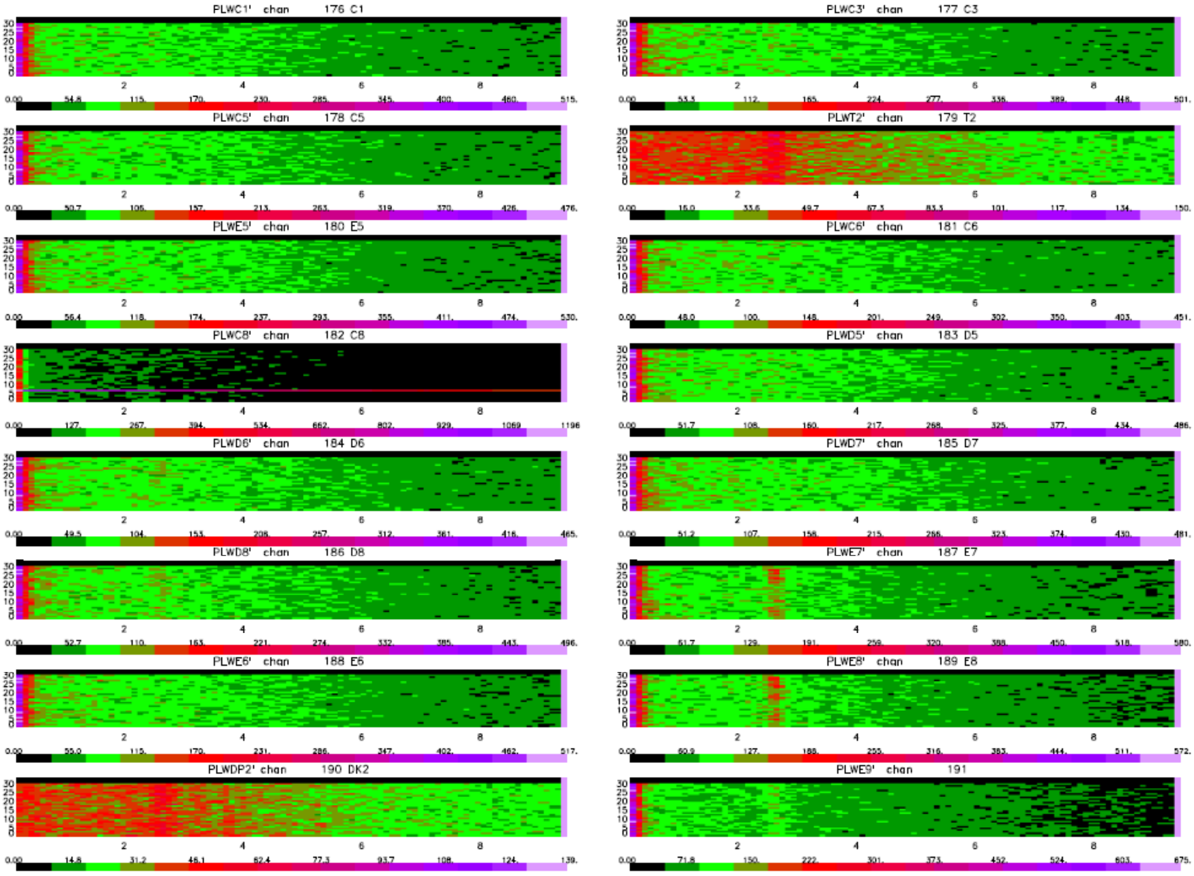
PLWC1' chan 176 C1
PLWC3' chan 177 C3
PLWC5' chan 178 C5
PLWT2' chan 179 T2
PLWE5' chan 180 E5
PLWC6' chan 181 C6
PLWC8' chan 182 C8
PLWD5' chan 183 D5
PLWD6' chan 184 D6
PLWD7' chan 185 D7
PLWD8' chan 186 D8
PLWE7' chan 187 E7
PLWE6' chan 188 E6
PLWE8' chan 189 E8
PLWDP2' chan 190 DK2
PLWE9' chan 191

Figure 64

8.1.3 PMW Spectrogrammes

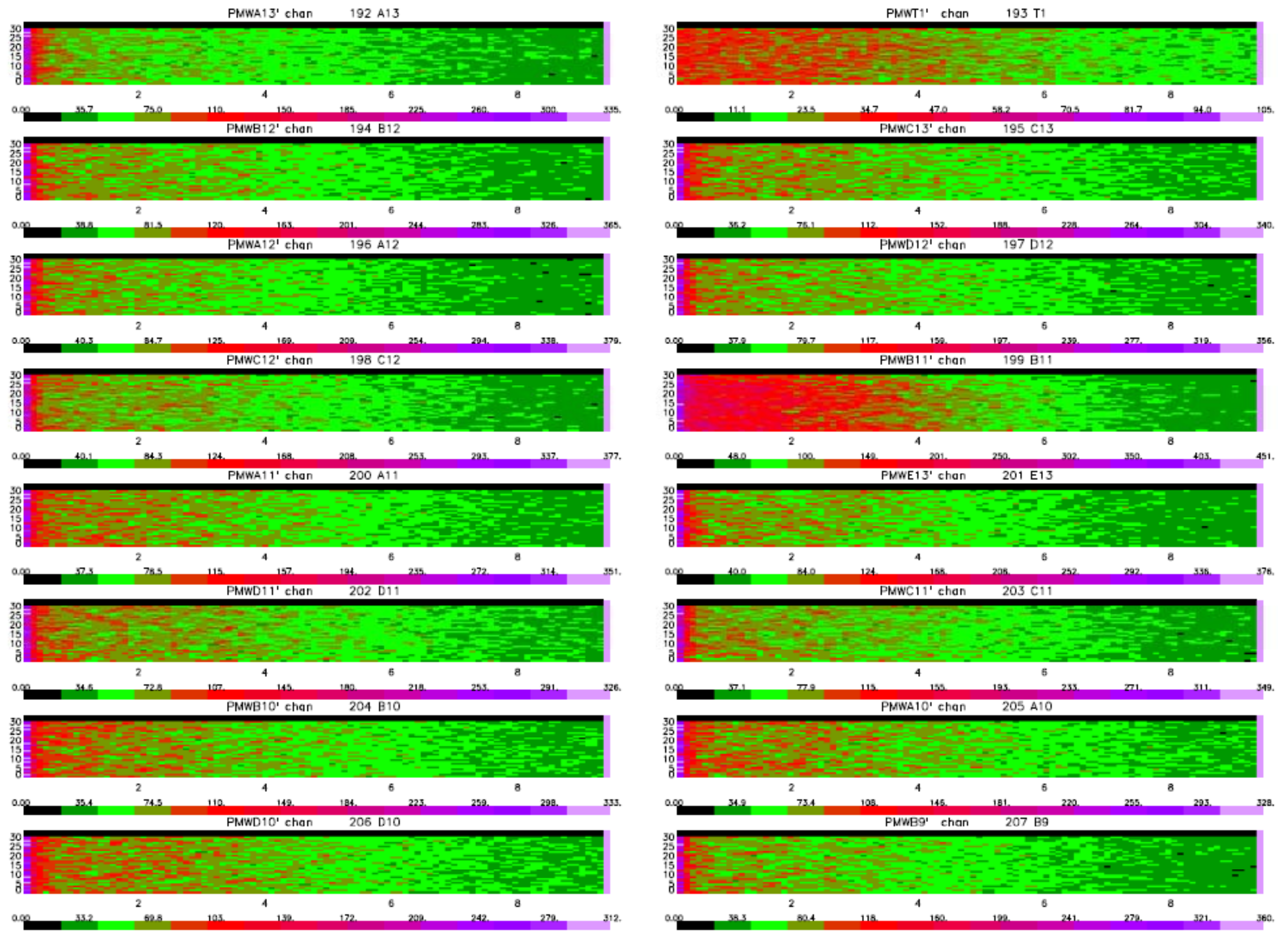

Figure 65

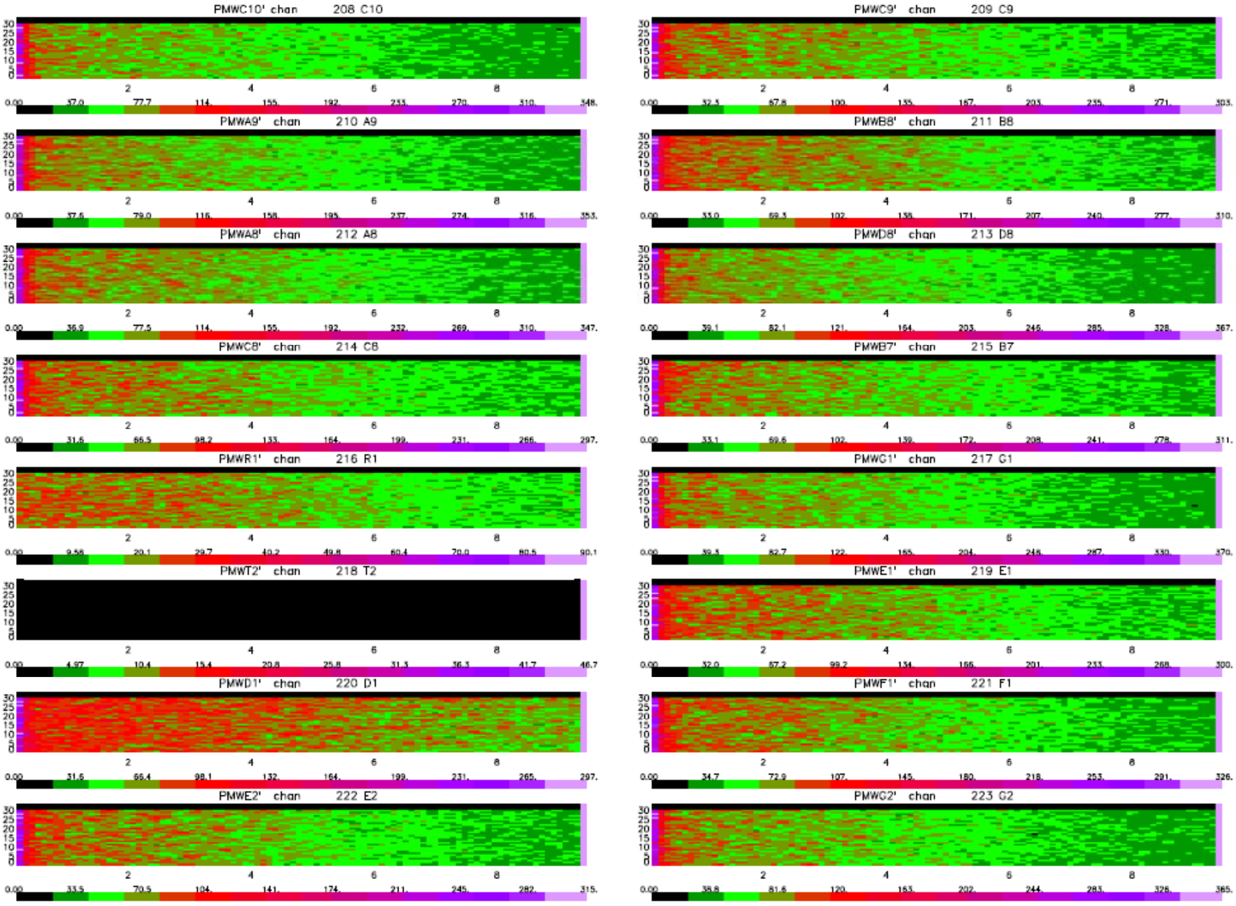

Figure 66

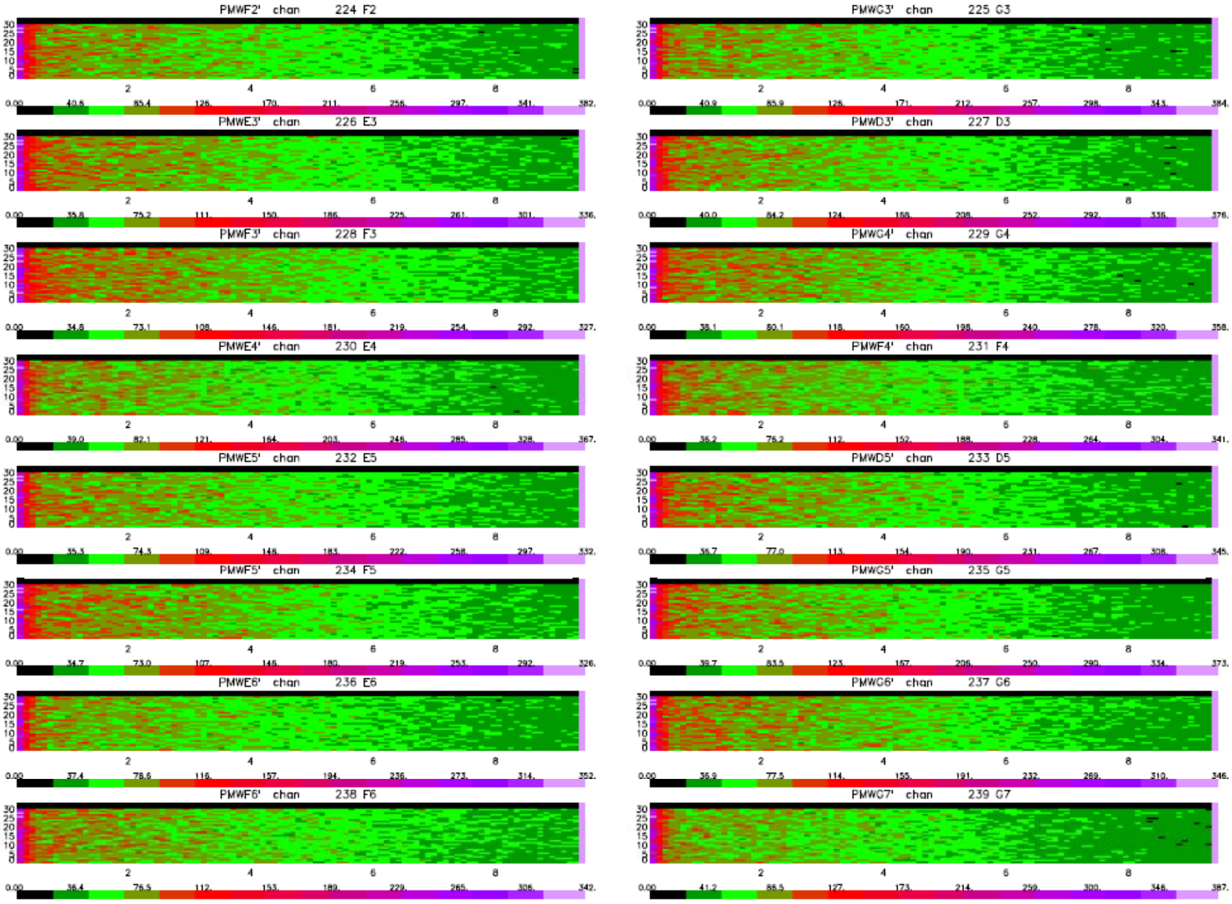

Figure 67

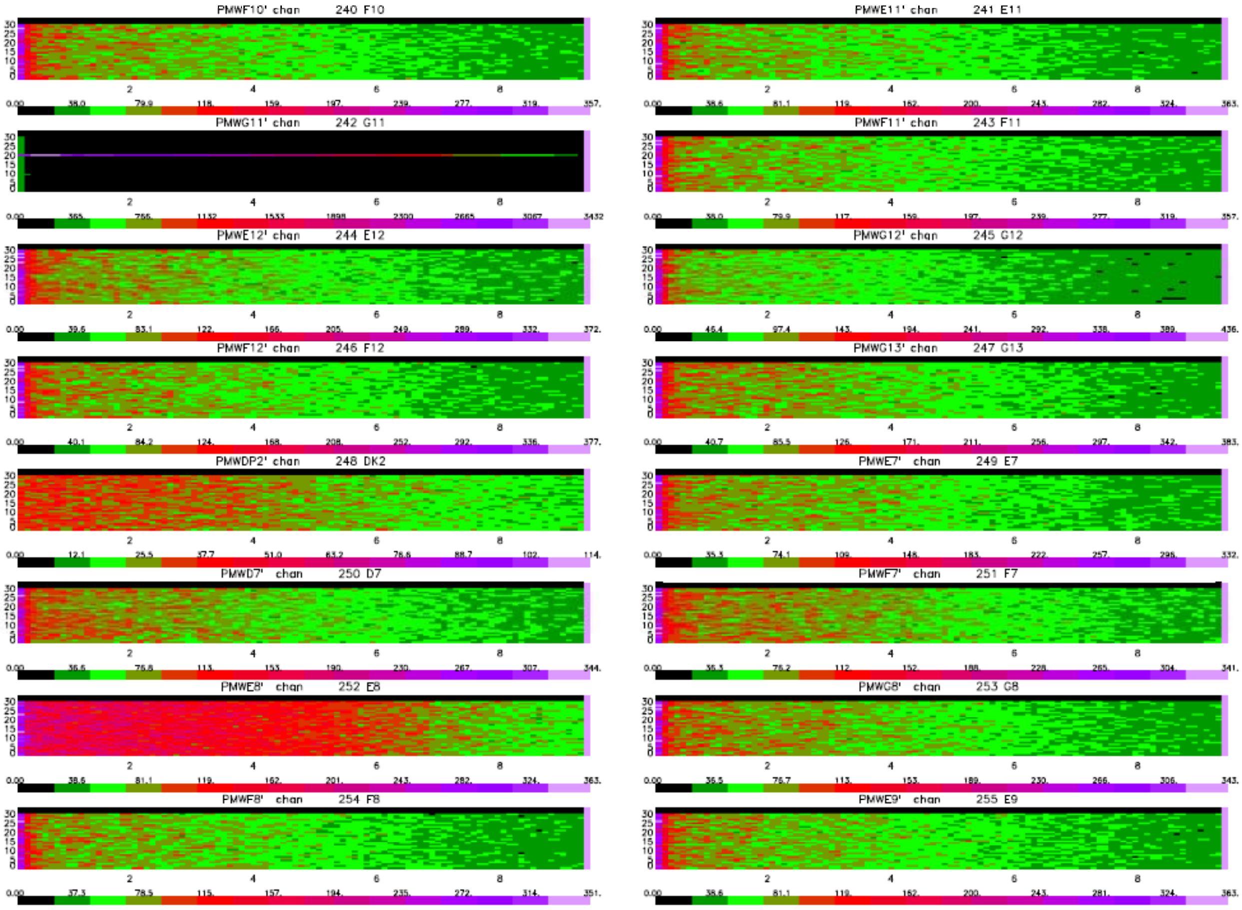

Figure 68

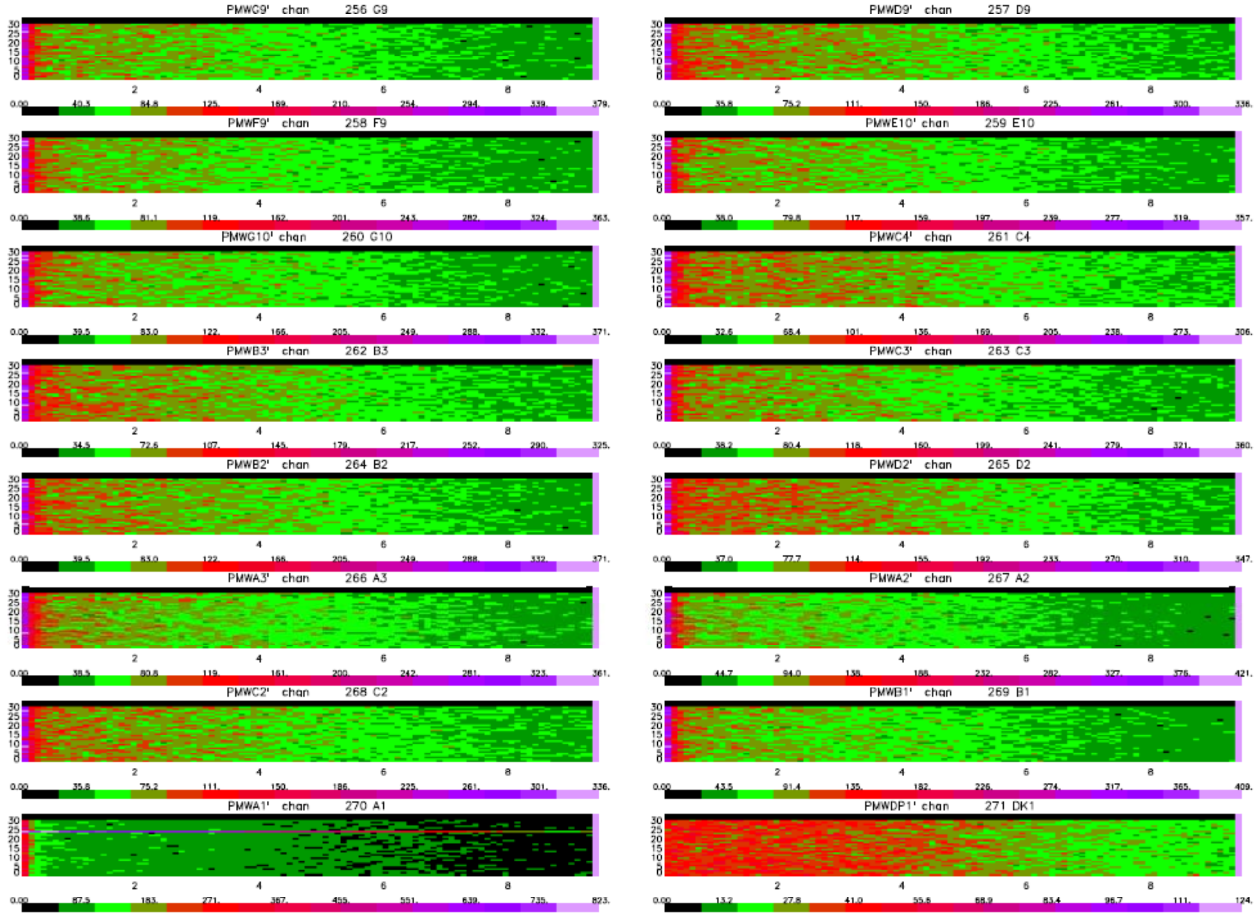
PMWG9' chan 256 G9
PMWD9' chan 257 D9
PMWF9' chan 258 F9
PMWE10' chan 259 E10
PMWG10' chan 260 G10
PMWC4' chan 261 C4
PMWB3' chan 262 B3
PMWC3' chan 263 C3
PMWB2' chan 264 B2
PMWD2' chan 265 D2
PMWA3' chan 266 A3
PMWA2' chan 267 A2
PMWC2' chan 268 C2
PMWB1' chan 269 B1
PMWA1' chan 270 A1
PMWDP1' chan 271 DK1

Figure 69

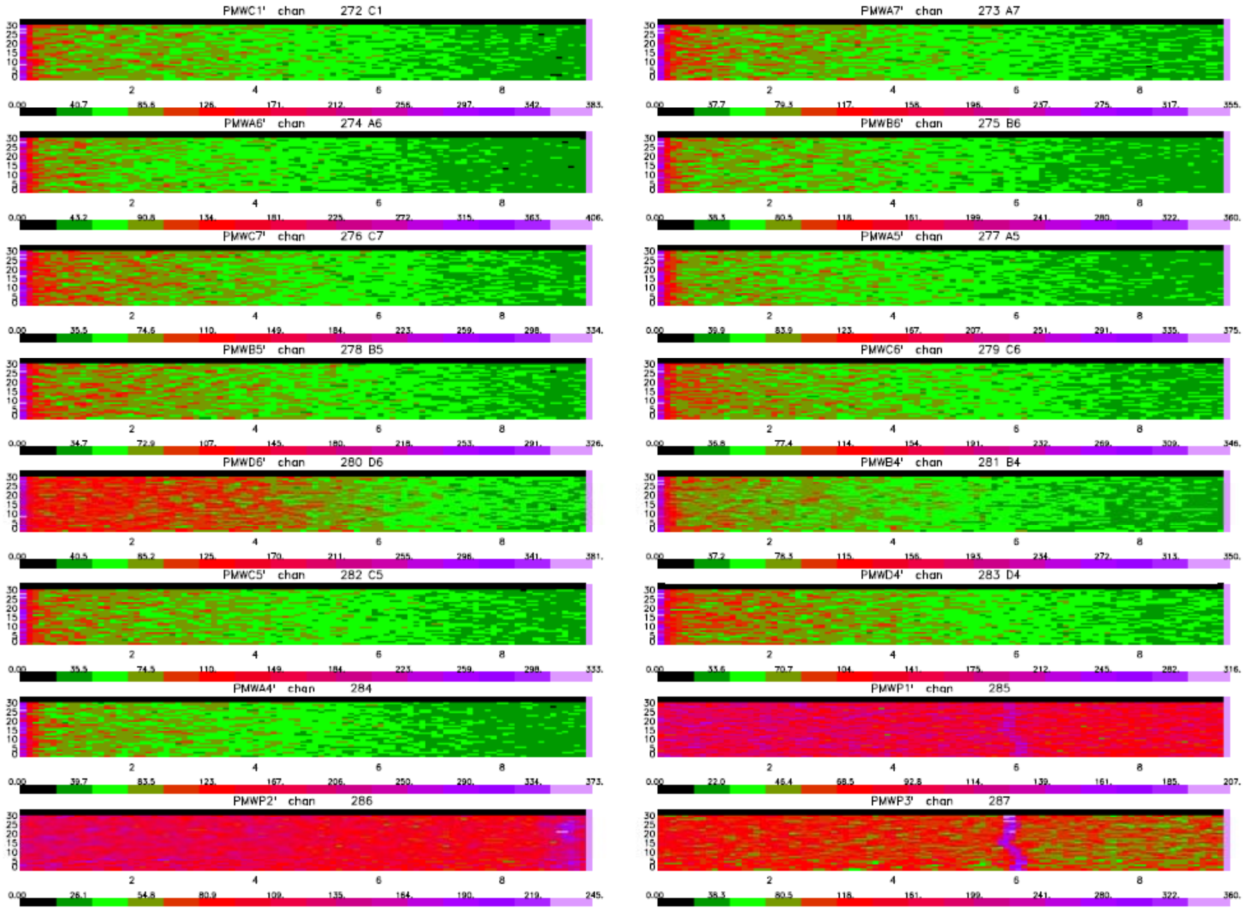

Figure 70

8.2 RS – Photometer: H-Polarization (0xB00014EB Step 2)

PSW (A1-B2)

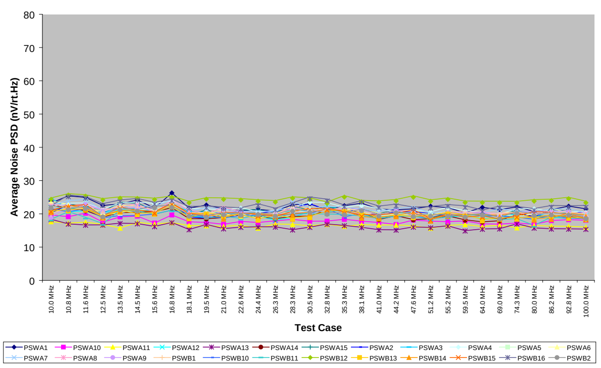

PSW (D11-E2)

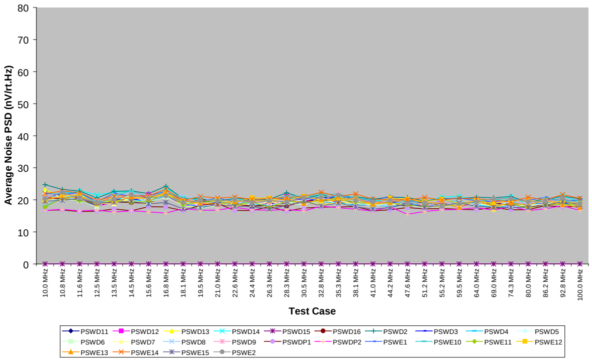

PSW DP1 and DP2 have flat noise traces

PMW (D8-F4)

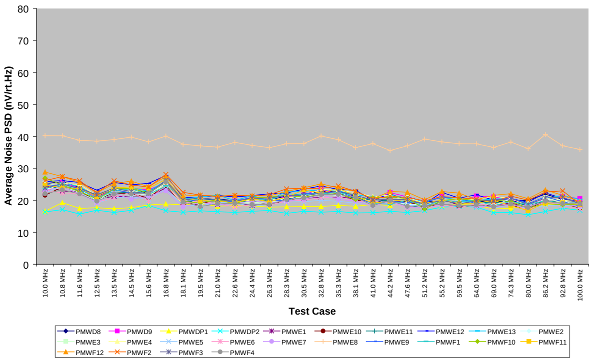

PMW-E8 shows excess noise @ ~ 37nV/√Hz
PMW DP1 and DP2 have flat noise traces

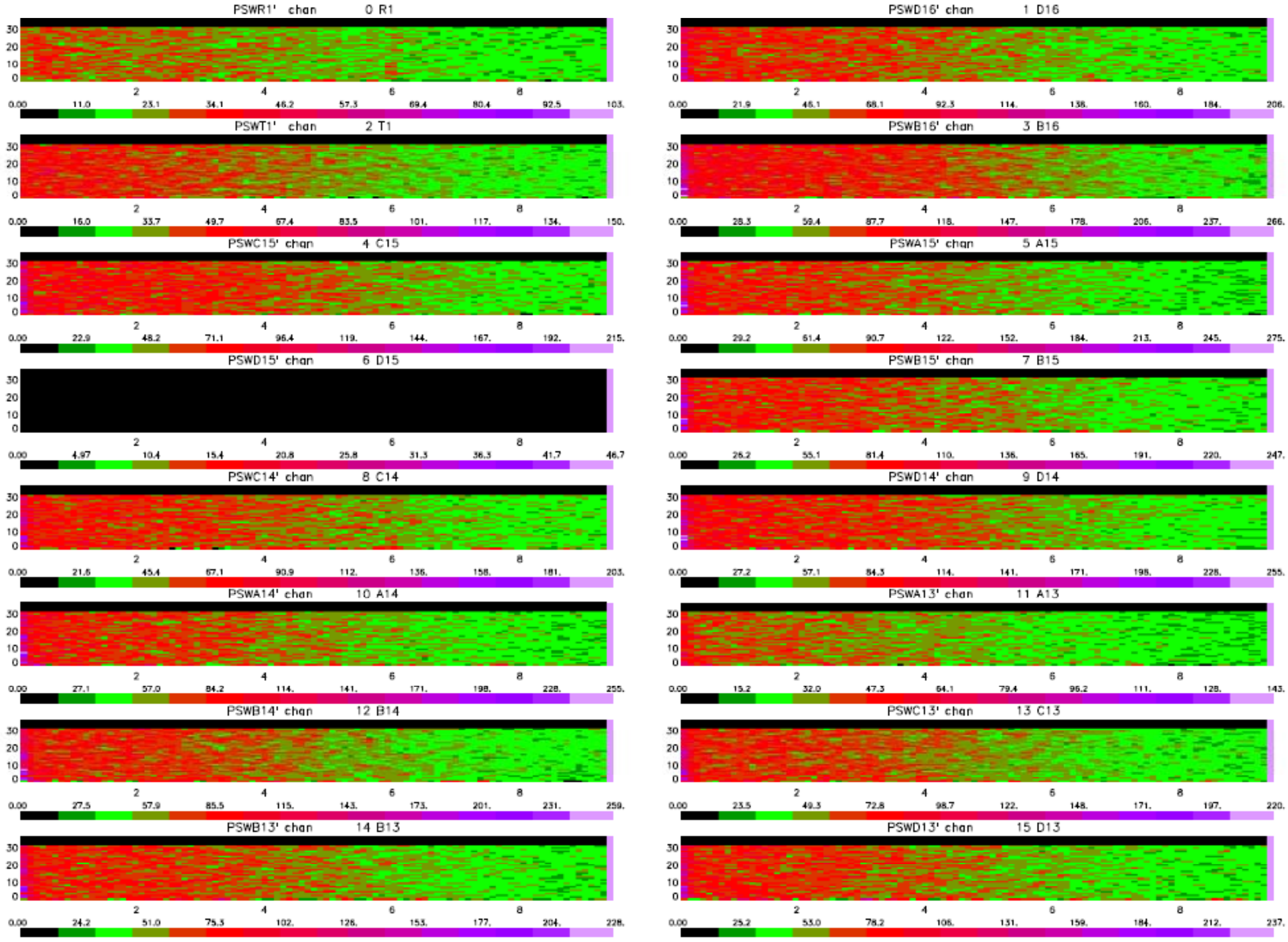

Figure 71

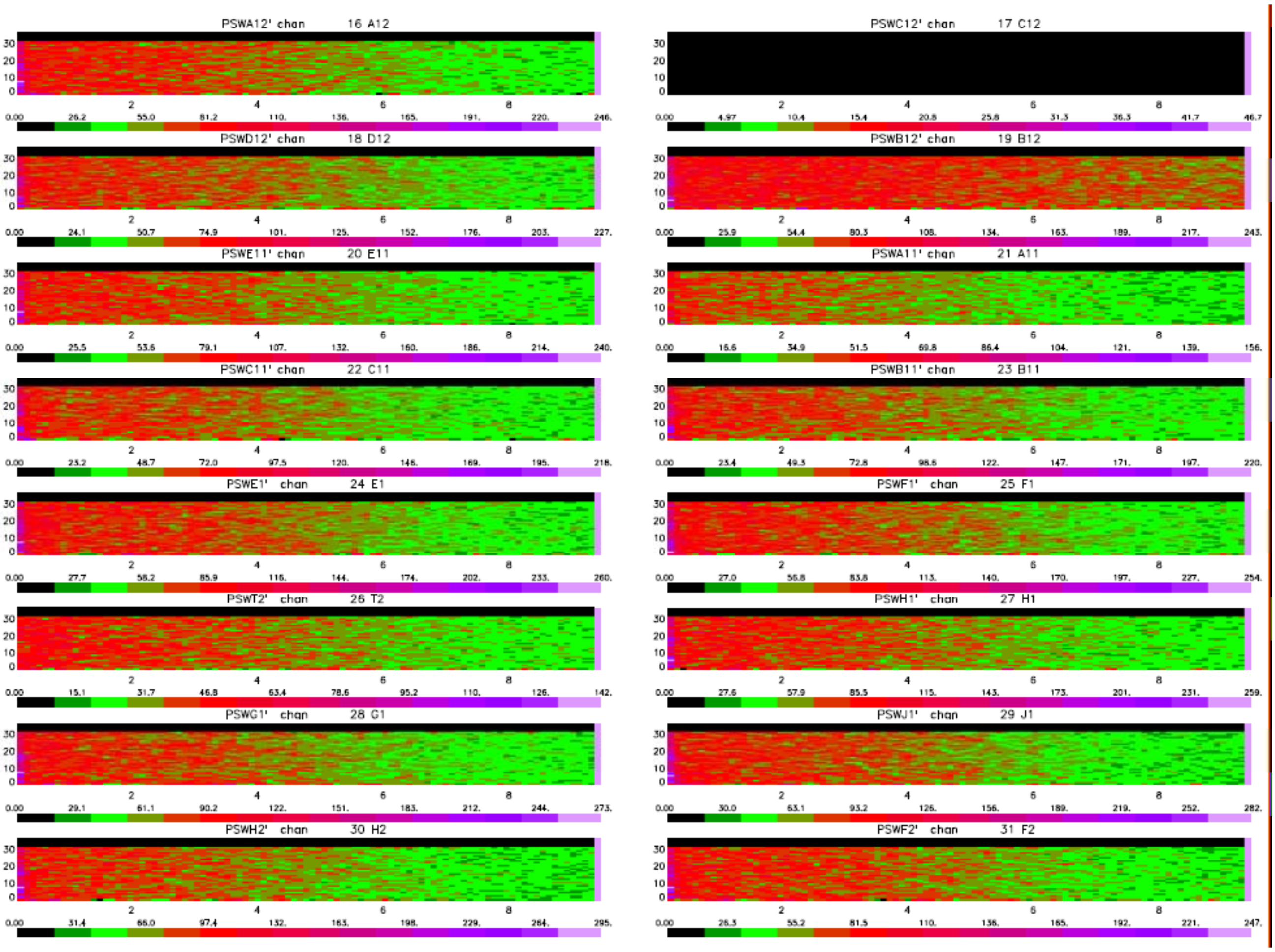
PSWA12' chan 16 A12
PSWC12' chan 17 C12
PSWD12' chan 18 D12
PSWB12' chan 19 B12
PSWE11' chan 20 E11
PSWA11' chan 21 A11
PSWC11' chan 22 C11
PSWB11' chan 23 B11
PSWE1' chan 24 E1
PSWF1' chan 25 F1
PSWT2' chan 26 T2
PSWH1' chan 27 H1
PSWG1' chan 28 G1
PSWJ1' chan 29 J1
PSWH2' chan 30 H2
PSWF2' chan 31 F2

Figure 72

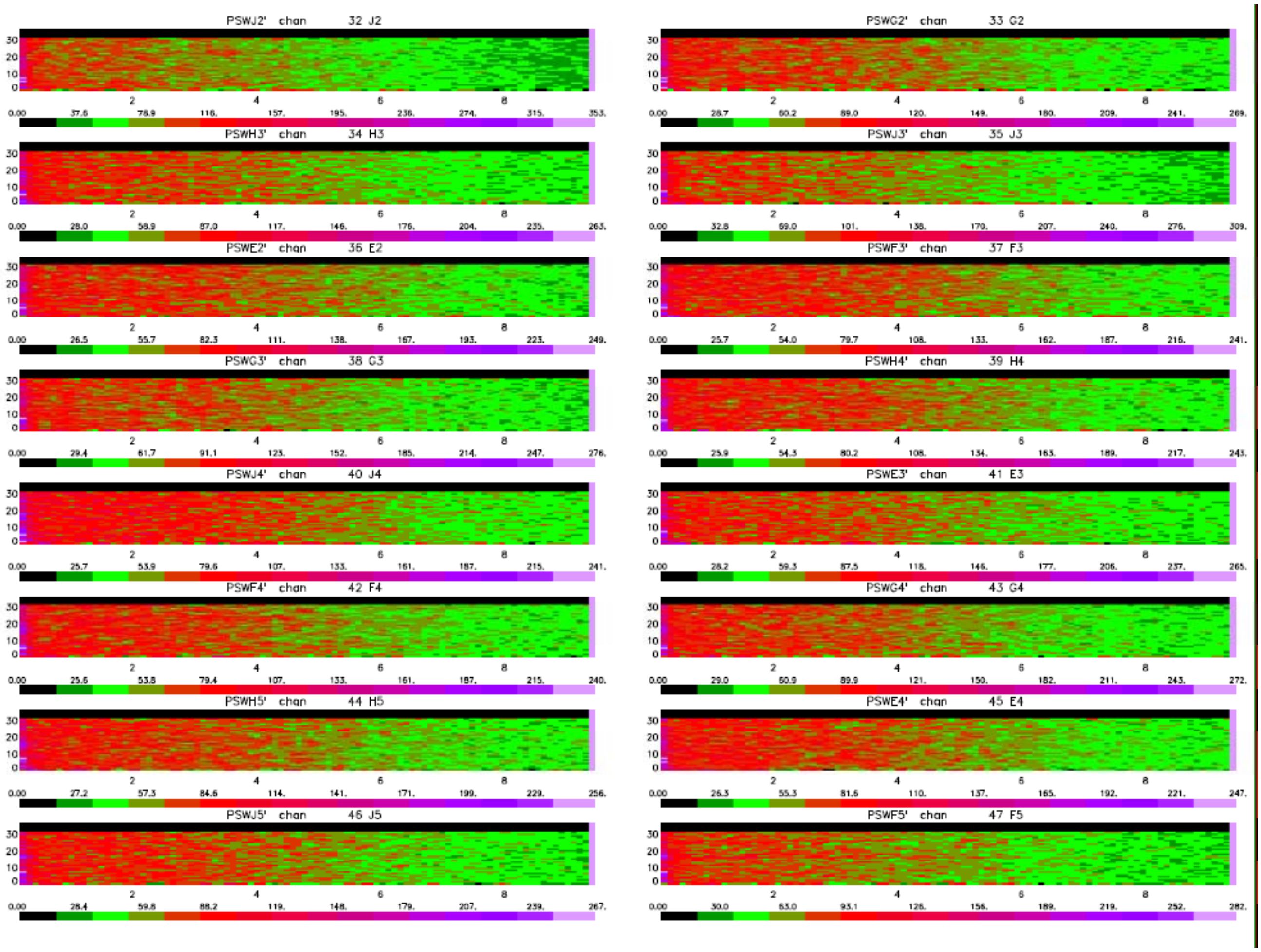
PSWJ2' chan 32 J2
PSWG2' chan 33 G2
PSWH3' chan 34 H3
PSWJ3' chan 35 J3
PSWE2' chan 36 E2
PSWF3' chan 37 F3
PSWG3' chan 38 G3
PSWH4' chan 39 H4
PSWJ4' chan 40 J4
PSWE3' chan 41 E3
PSWF4' chan 42 F4
PSWG4' chan 43 G4
PSWH5' chan 44 H5
PSWE4' chan 45 E4
PSWJ5' chan 46 J5
PSWF5' chan 47 F5

Figure 73

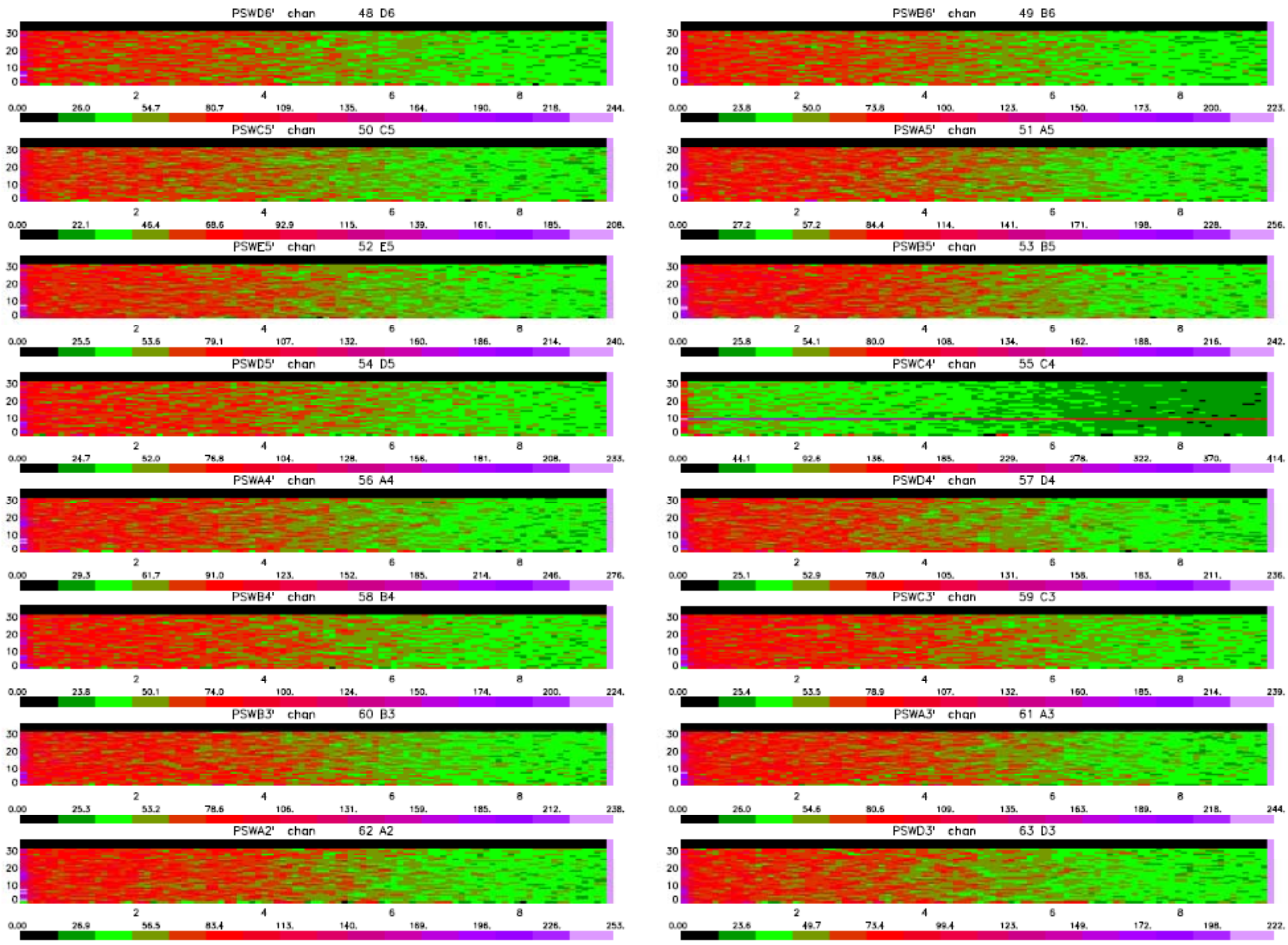
PSWD6' chan 48 D6
PSWB6' chan 49 B6
PSWC5' chan 50 C5
PSWA5' chan 51 A5
PSWE5' chan 52 E5
PSWB5' chan 53 B5
PSWD5' chan 54 D5
PSWC4' chan 55 C4
PSWA4' chan 56 A4
PSWD4' chan 57 D4
PSWB4' chan 58 B4
PSWC3' chan 59 C3
PSWB3' chan 60 B3
PSWA3' chan 61 A3
PSWA2' chan 62 A2
PSWD3' chan 63 D3

Figure 74

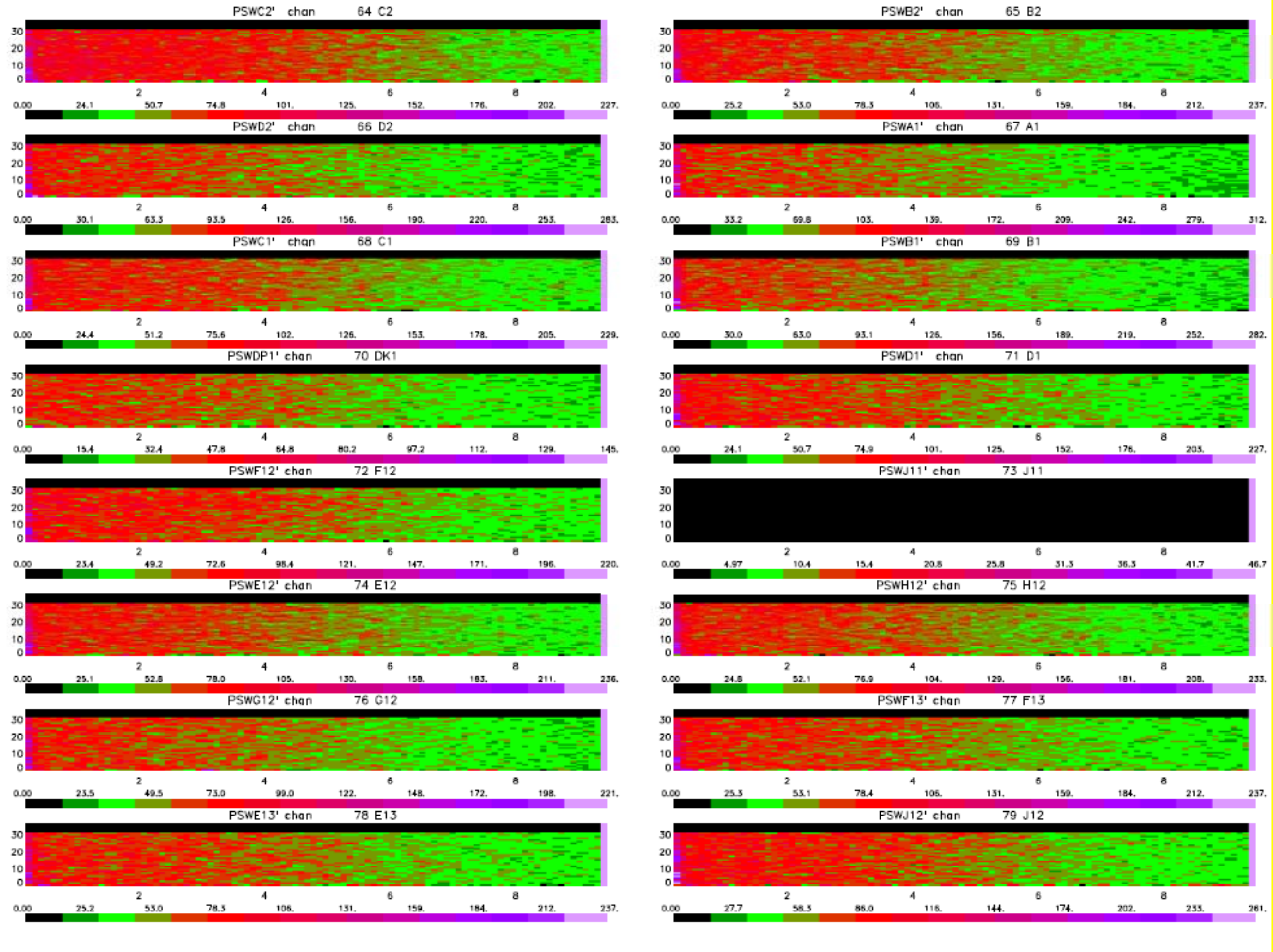
PSWC2' chan 64 C2
PSWB2' chan 65 B2
PSWD2' chan 66 D2
PSWA1' chan 67 A1
PSWC1' chan 68 C1
PSWB1' chan 69 B1
PSWDP1' chan 70 DK1
PSWD1' chan 71 D1
PSWF12' chan 72 F12
PSWJ11' chan 73 J11
PSWE12' chan 74 E12
PSWH12' chan 75 H12
PSWG12' chan 76 G12
PSWF13' chan 77 F13
PSWE13' chan 78 E13
PSWJ12' chan 79 J12

Figure 75

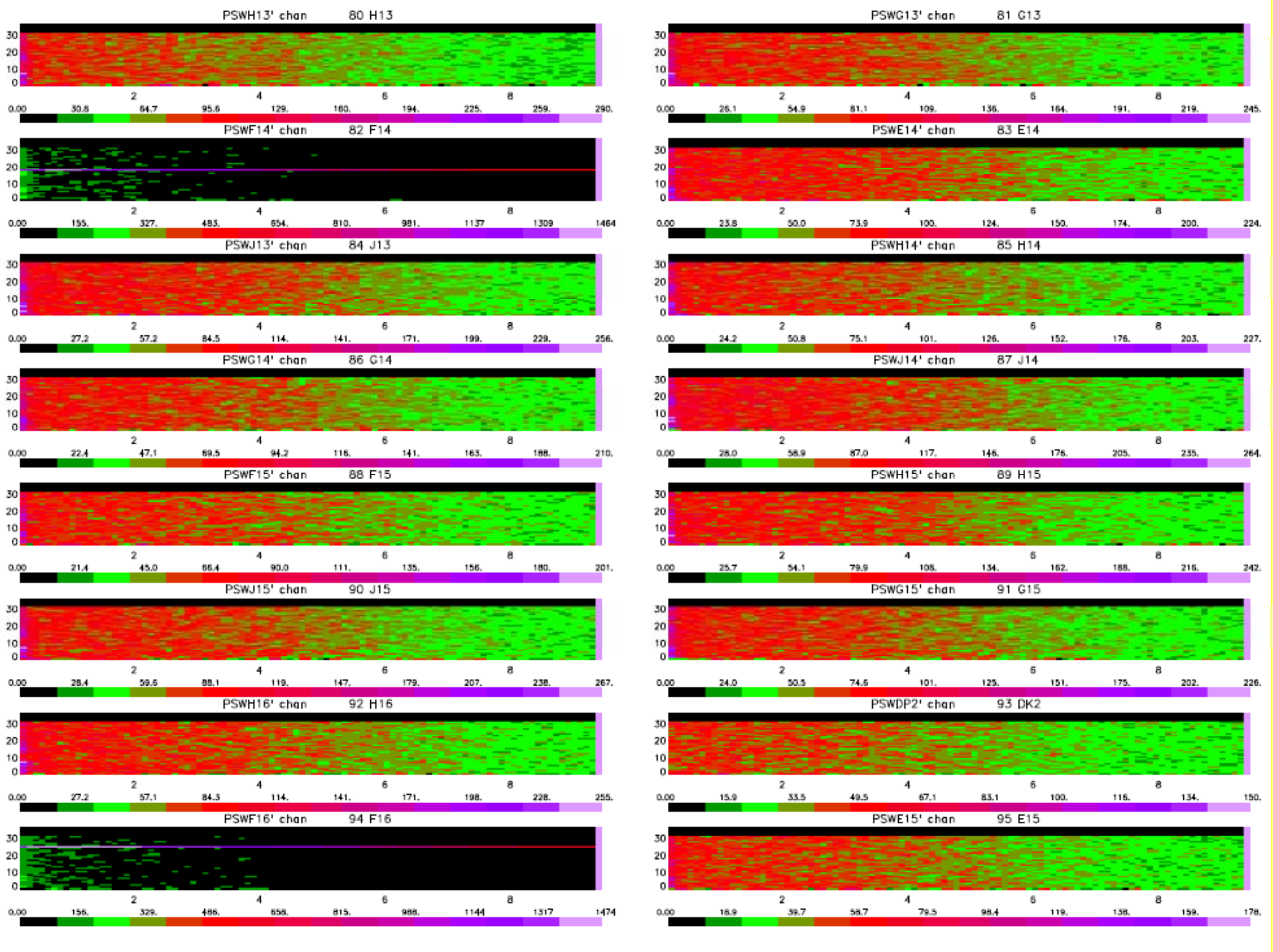
PSWH13' chan 80 H13
PSWG13' chan 81 G13
PSWF14' chan 82 F14
PSWE14' chan 83 E14
PSWJ13' chan 84 J13
PSWH14' chan 85 H14
PSWG14' chan 86 G14
PSWJ14' chan 87 J14
PSWF15' chan 88 F15
PSWH15' chan 89 H15
PSWJ15' chan 90 J15
PSWG15' chan 91 G15
PSWH16' chan 92 H16
PSWDP2' chan 93 DK2
PSWF16' chan 94 F16
PSWE15' chan 95 E15

Figure 76

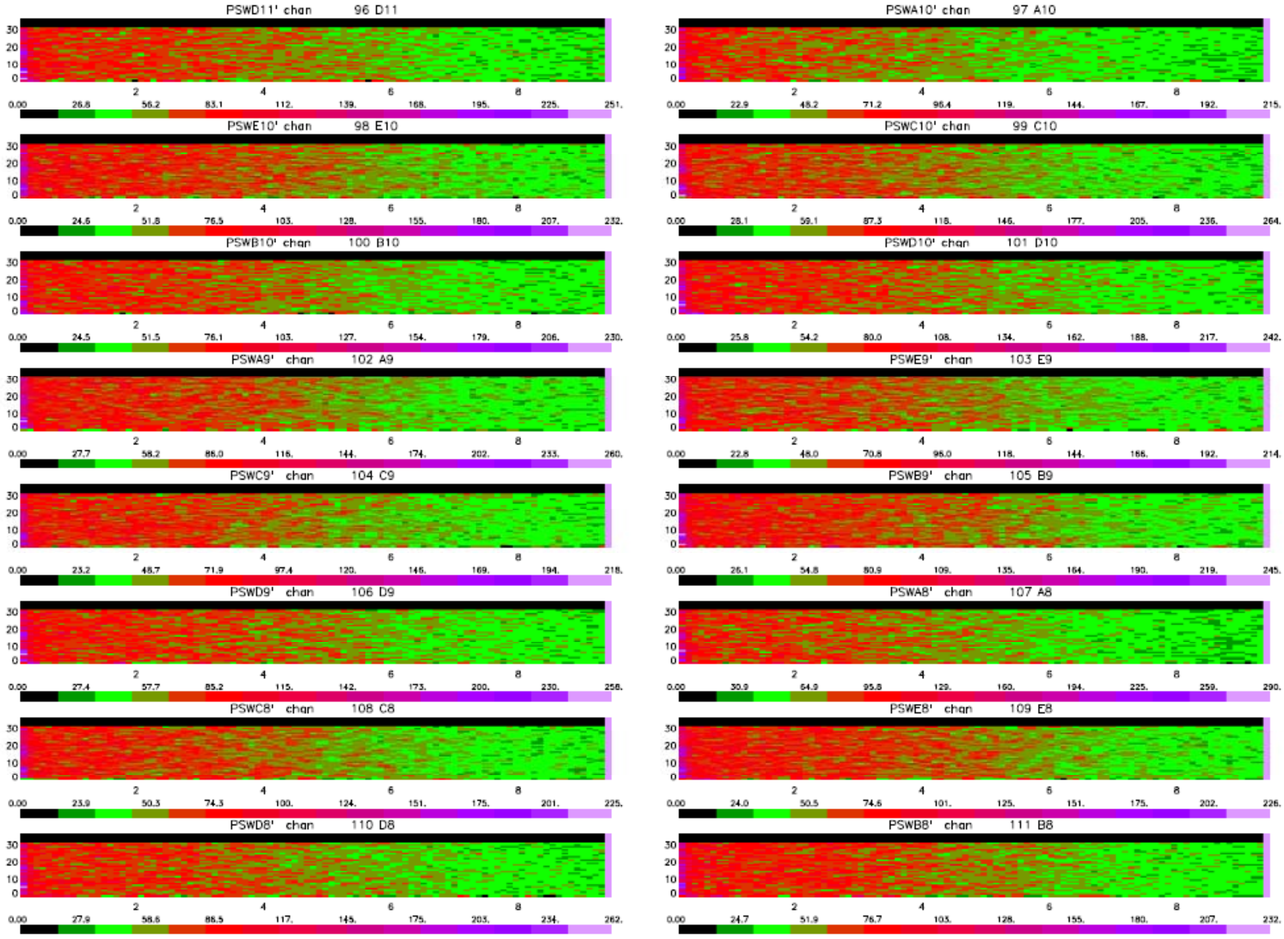

Figure 77

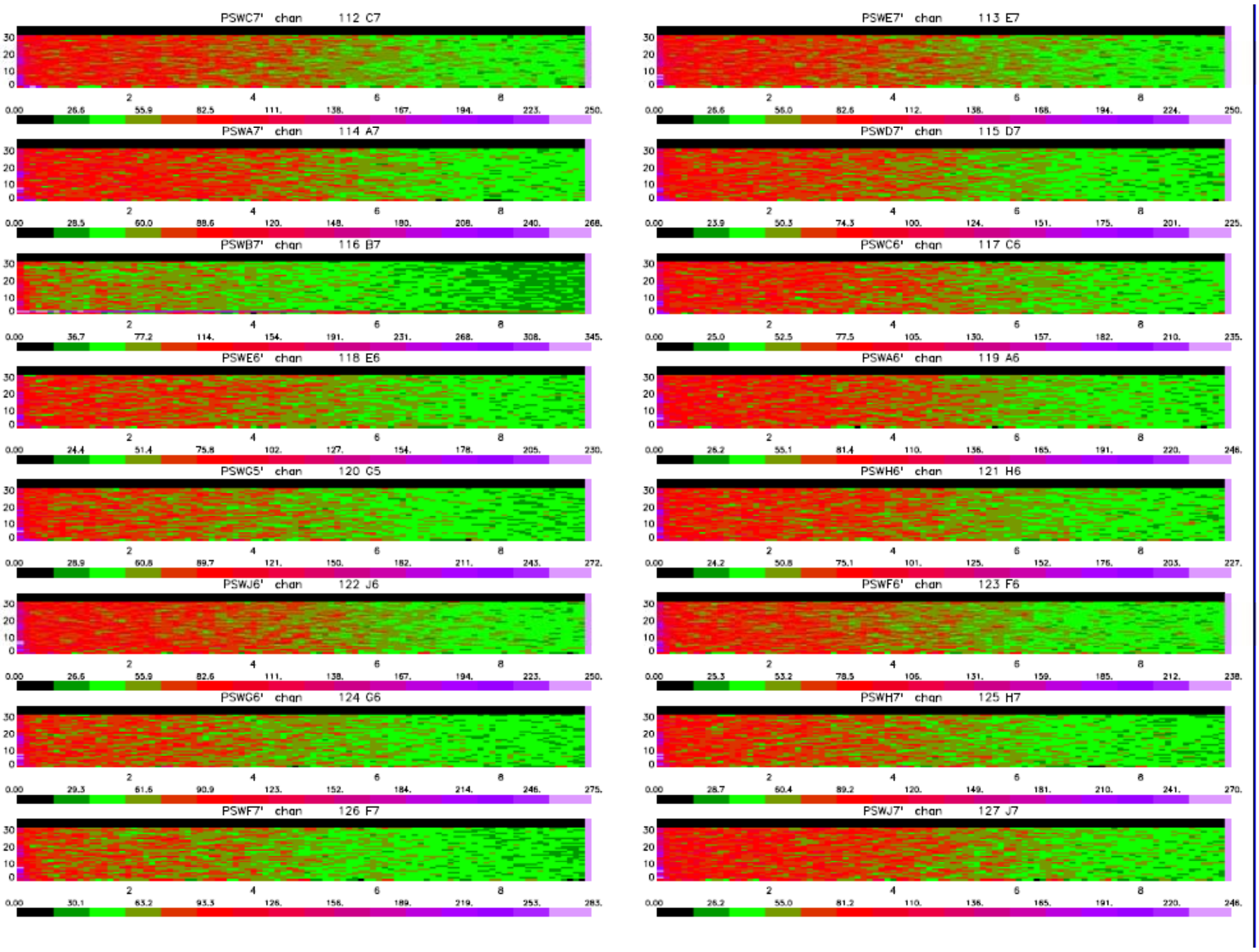
PSWC7' chan 112 C7
PSWE7' chan 113 E7
PSWA7' chan 114 A7
PSWD7' chan 115 D7
PSWB7' chan 116 B7
PSWC6' chan 117 C6
PSWE6' chan 118 E6
PSWA6' chan 119 A6
PSWG5' chan 120 G5
PSWH6' chan 121 H6
PSWJ6' chan 122 J6
PSWF6' chan 123 F6
PSWG6' chan 124 G6
PSWH7' chan 125 H7
PSWF7' chan 126 F7
PSWJ7' chan 127 J7

Figure 78

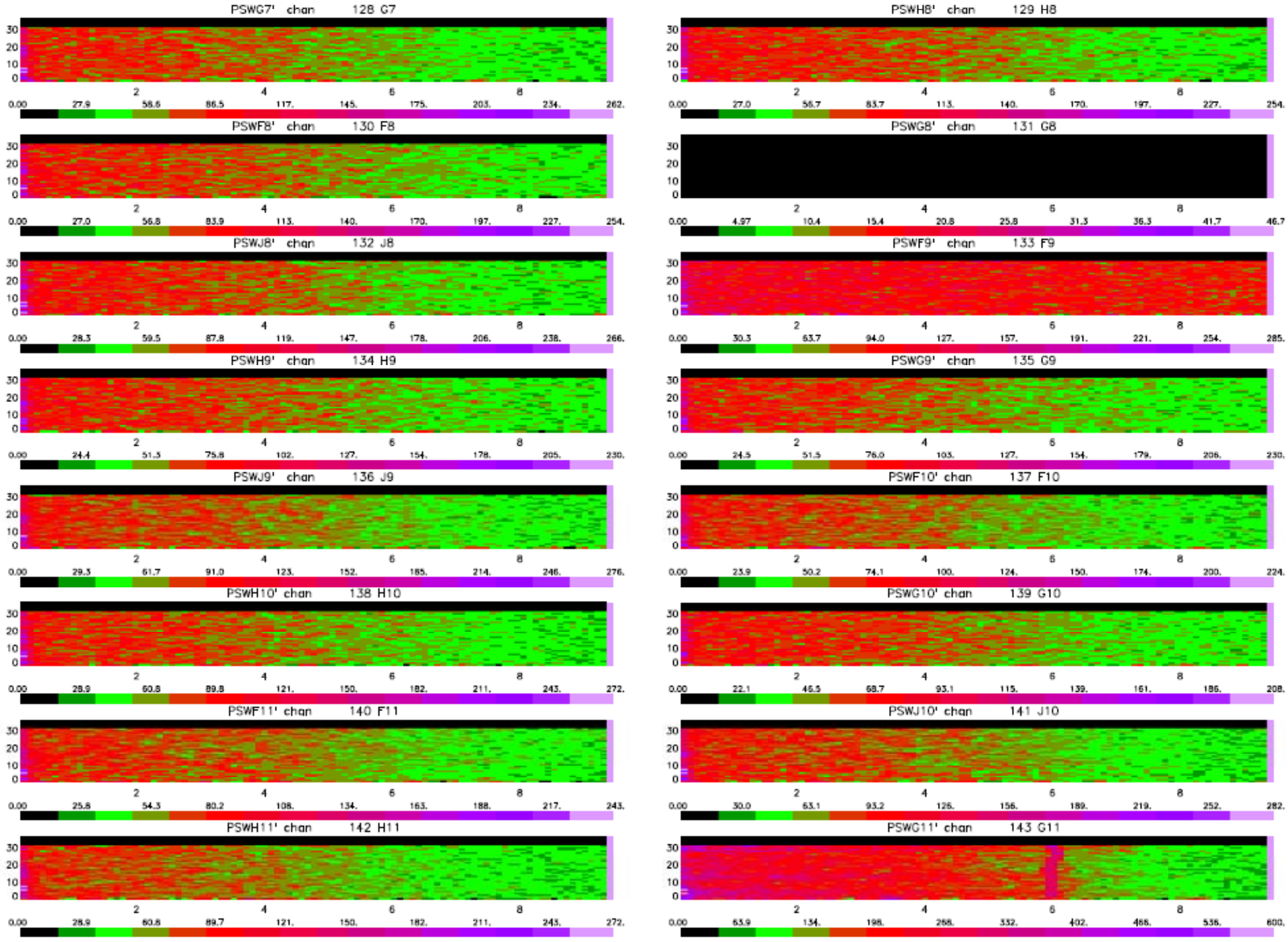

PSWG7' chan 128 G7
PSWH8' chan 129 H8
PSWF8' chan 130 F8
PSWG8' chan 131 G8
PSWJ8' chan 132 J8
PSWF9' chan 133 F9
PSWH9' chan 134 H9
PSWG9' chan 135 G9
PSWJ9' chan 136 J9
PSWF10' chan 137 F10
PSWH10' chan 138 H10
PSWG10' chan 139 G10
PSWF11' chan 140 F11
PSWJ10' chan 141 J10
PSWH11' chan 142 H11
PSWG11' chan 143 G11

Figure 79

8.2.1 PLW Spetrogrammes

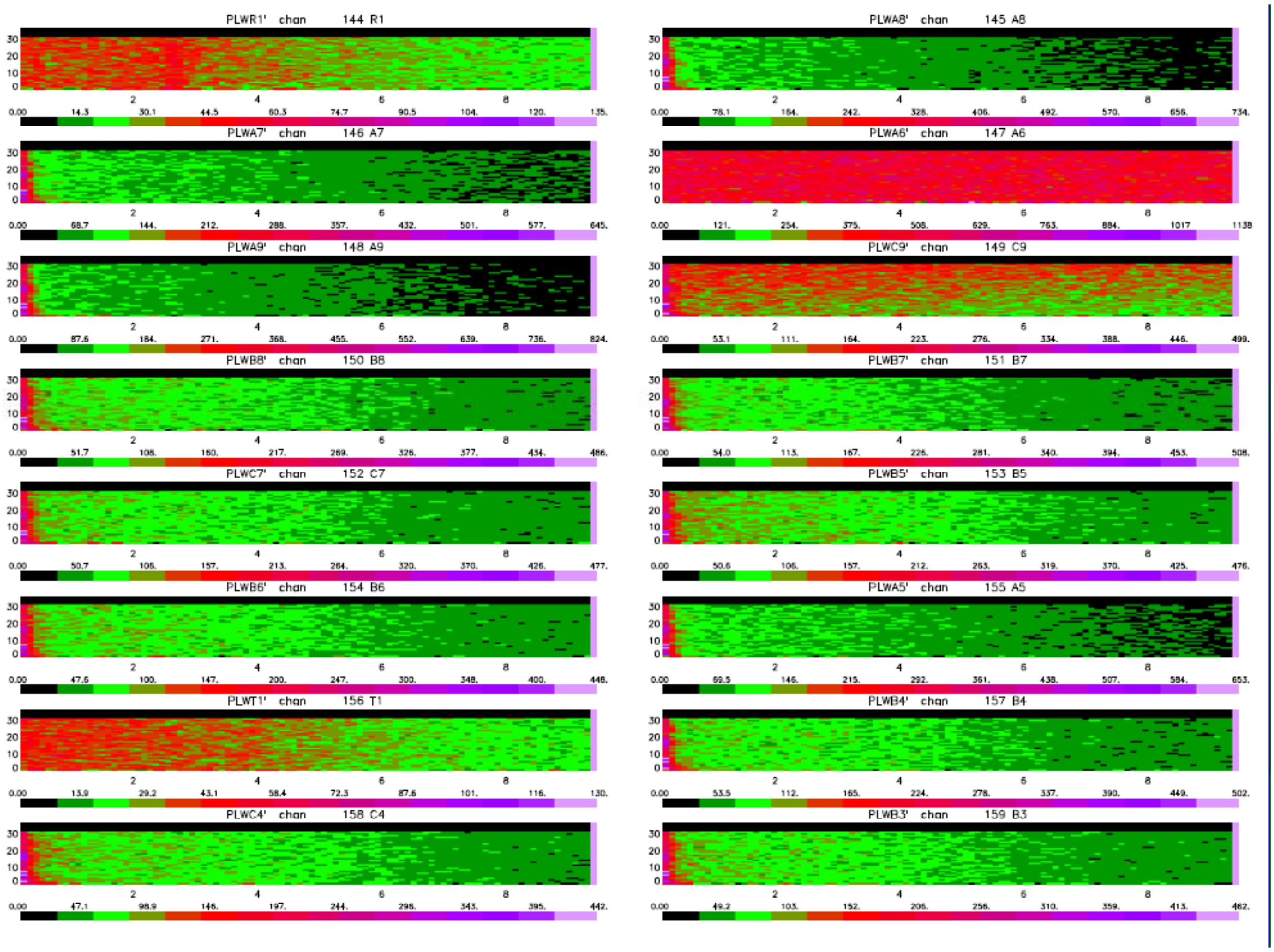

Figure 80

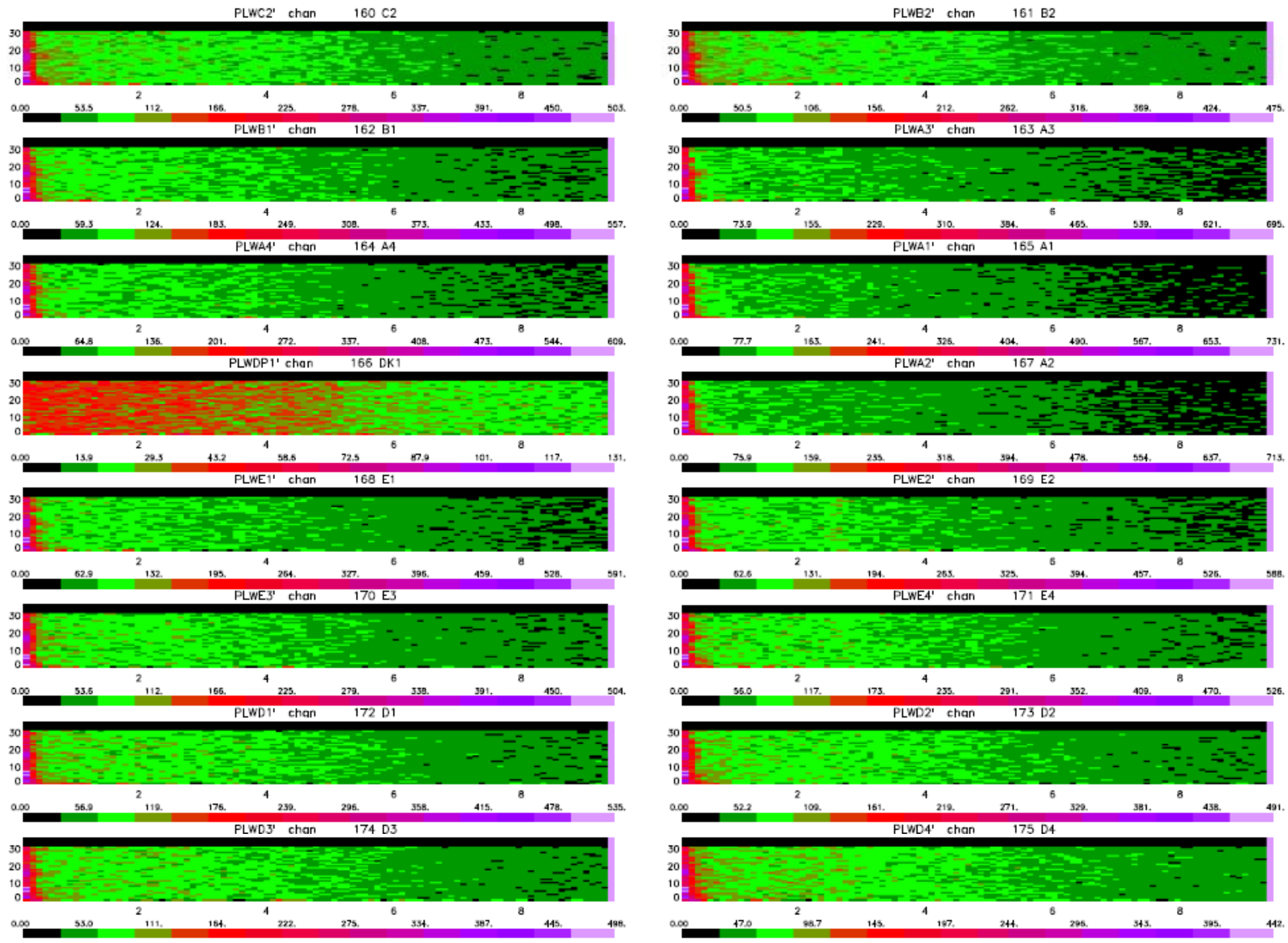
PLWC2' chan 160 C2
PLWB2' chan 161 B2
PLWB1' chan 162 B1
PLWA3' chan 163 A3
PLWA4' chan 164 A4
PLWA1' chan 165 A1
PLWDP1' chan 166 DK1
PLWA2' chan 167 A2
PLWE1' chan 168 E1
PLWE2' chan 169 E2
PLWE3' chan 170 E3
PLWE4' chan 171 E4
PLWD1' chan 172 D1
PLWD2' chan 173 D2
PLWD3' chan 174 D3
PLWD4' chan 175 D4

Figure 81

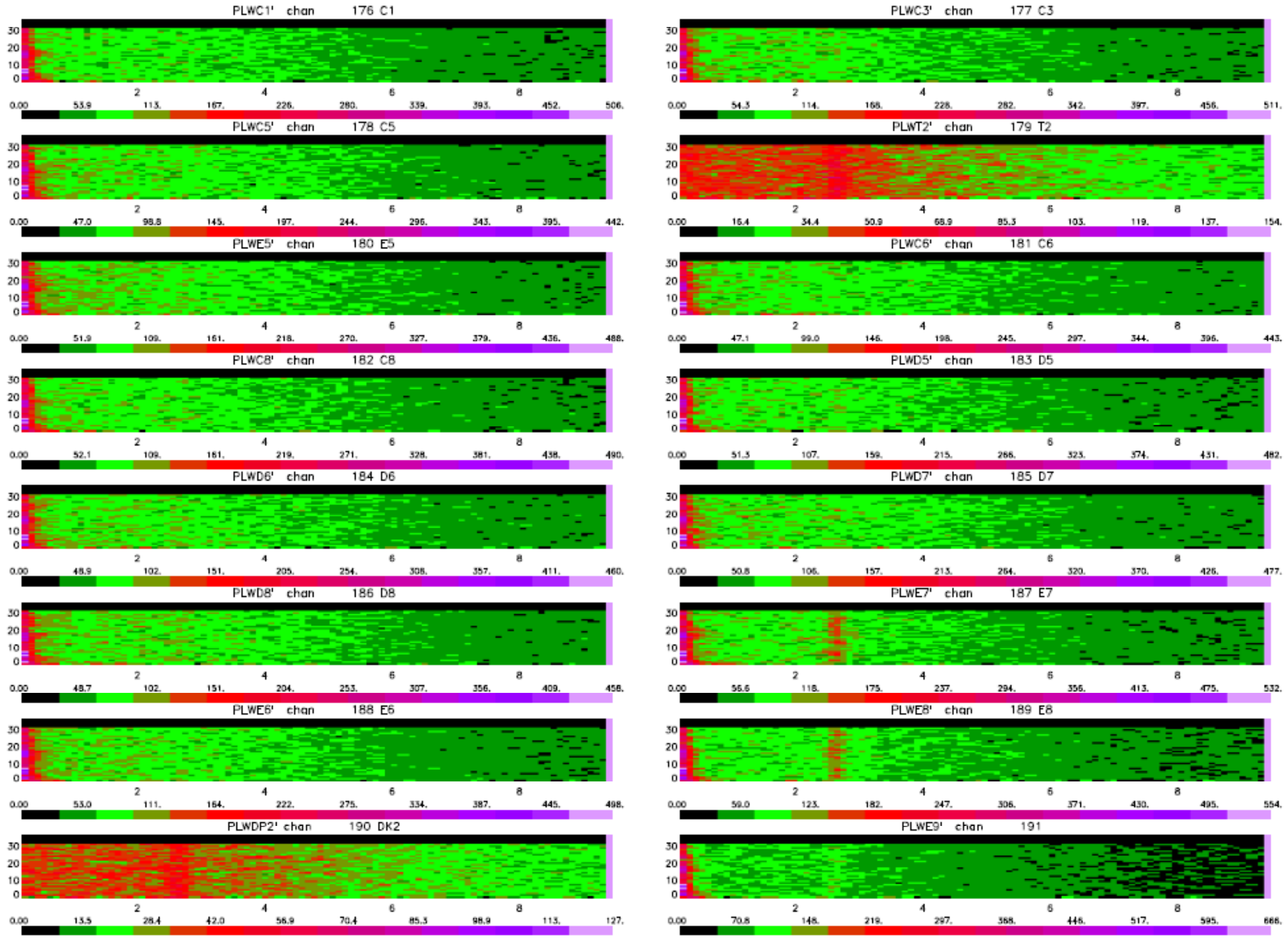

PLWC1' chan 176 C1
PLWC3' chan 177 C3
PLWC5' chan 178 C5
PLWT2' chan 179 T2
PLWE5' chan 180 E5
PLWC6' chan 181 C6
PLWC8' chan 182 C8
PLWD5' chan 183 D5
PLWD6' chan 184 D6
PLWD7' chan 185 D7
PLWD8' chan 186 D8
PLWE7' chan 187 E7
PLWE6' chan 188 E6
PLWE8' chan 189 E8
PLWDP2' chan 190 DK2
PLWE9' chan 191

Figure 82

8.2.2 PMW Spectrogrammes

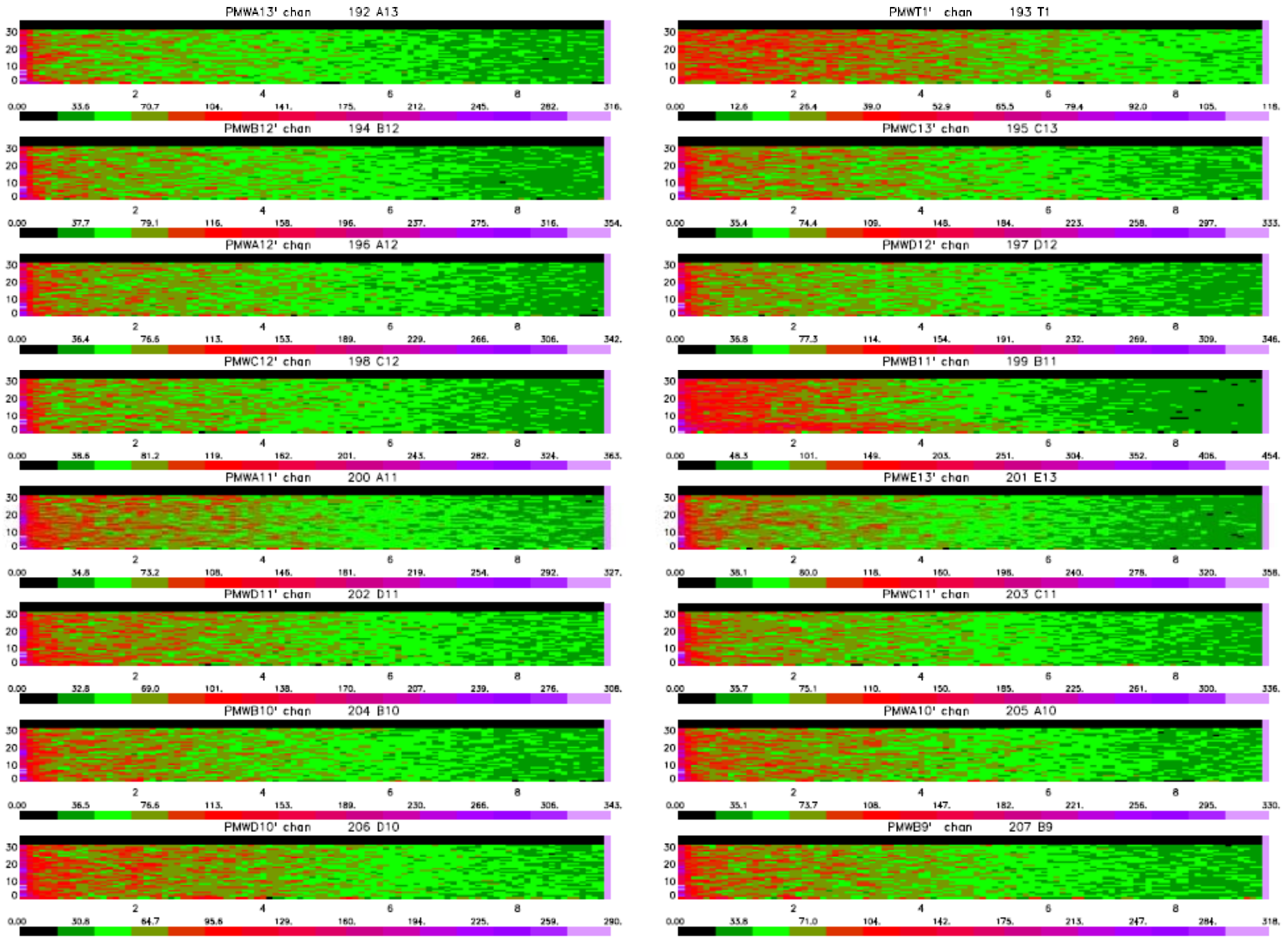

Figure 83

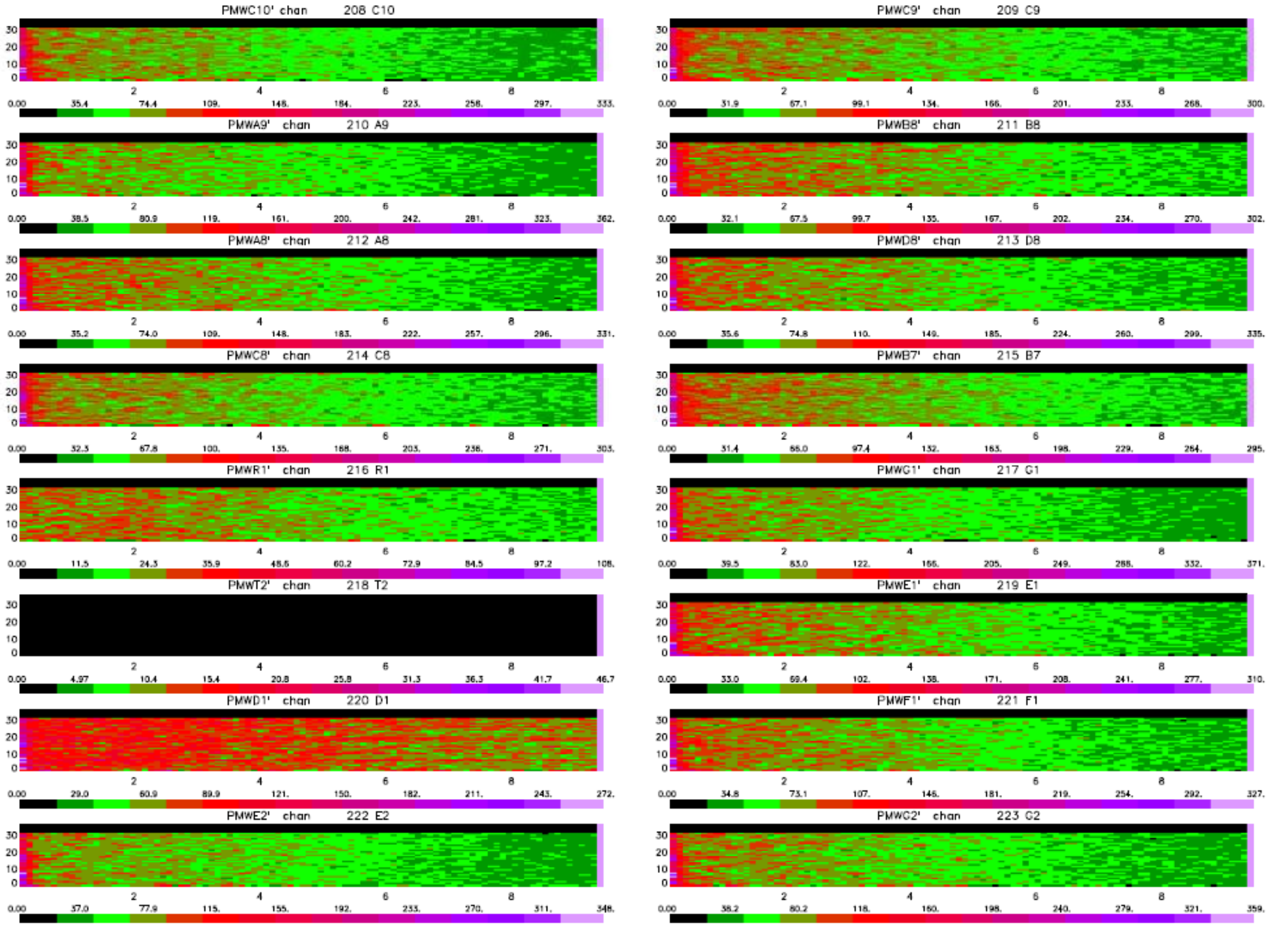
PMWC10' chan 208 C10
PMWC9' chan 209 C9
PMWA9' chan 210 A9
PMWB8' chan 211 B8
PMWA8' chan 212 A8
PMWD8' chan 213 D8
PMWC8' chan 214 C8
PMWB7' chan 215 B7
PMWR1' chan 216 R1
PMWG1' chan 217 G1
PMWT2' chan 218 T2
PMWE1' chan 219 E1
PMWD1' chan 220 D1
PMWF1' chan 221 F1
PMWE2' chan 222 E2
PMWG2' chan 223 G2

Figure 84

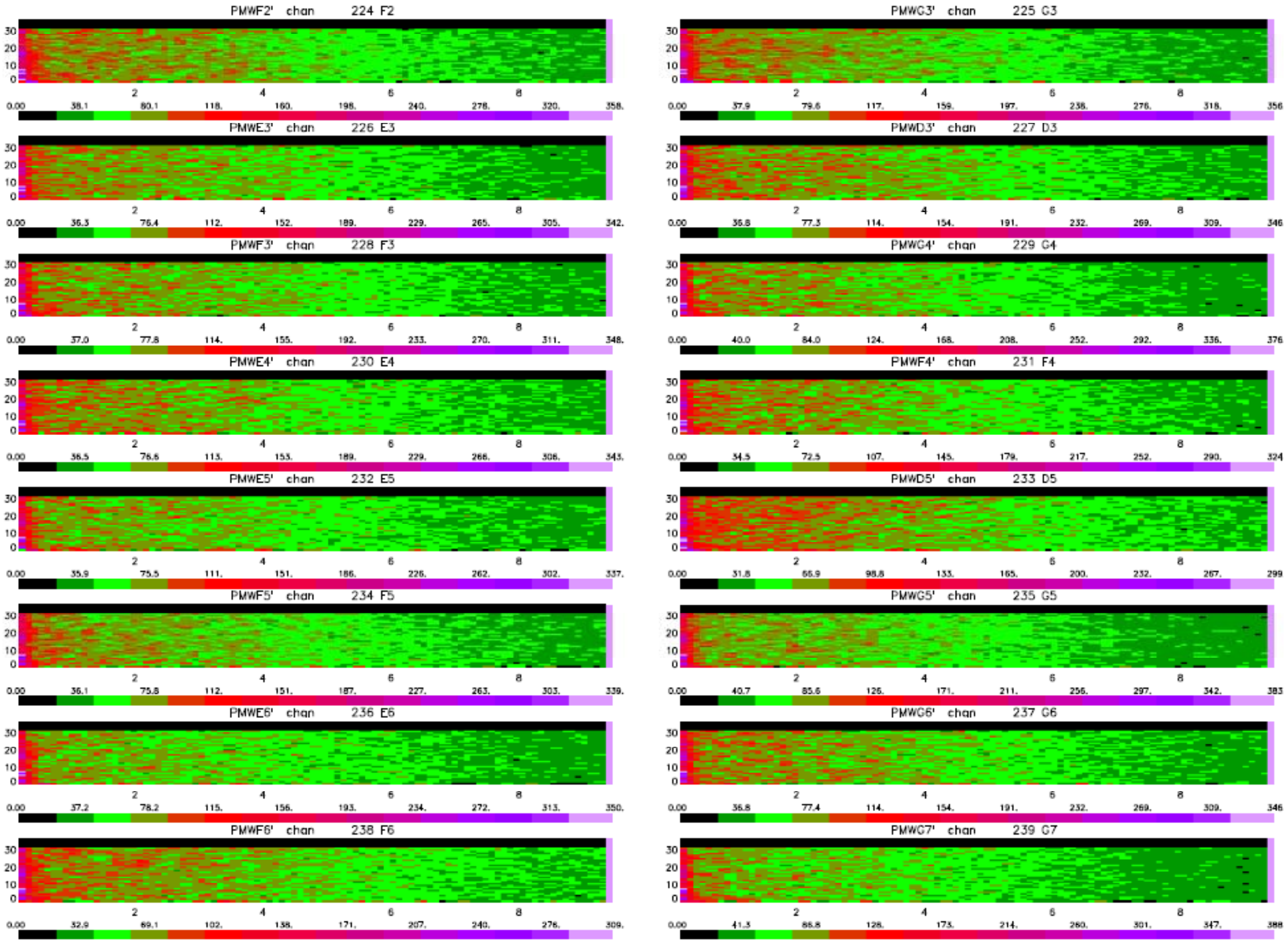
PMWF2' chan 224 F2
PMWG3' chan 225 G3
PMWE3' chan 226 E3
PMWD3' chan 227 D3
PMWF3' chan 228 F3
PMWG4' chan 229 G4
PMWE4' chan 230 E4
PMWF4' chan 231 F4
PMWE5' chan 232 E5
PMWD5' chan 233 D5
PMWF5' chan 234 F5
PMWG5' chan 235 G5
PMWE6' chan 236 E6
PMWG6' chan 237 G6
PMWF6' chan 238 F6
PMWG7' chan 239 G7

Figure 85

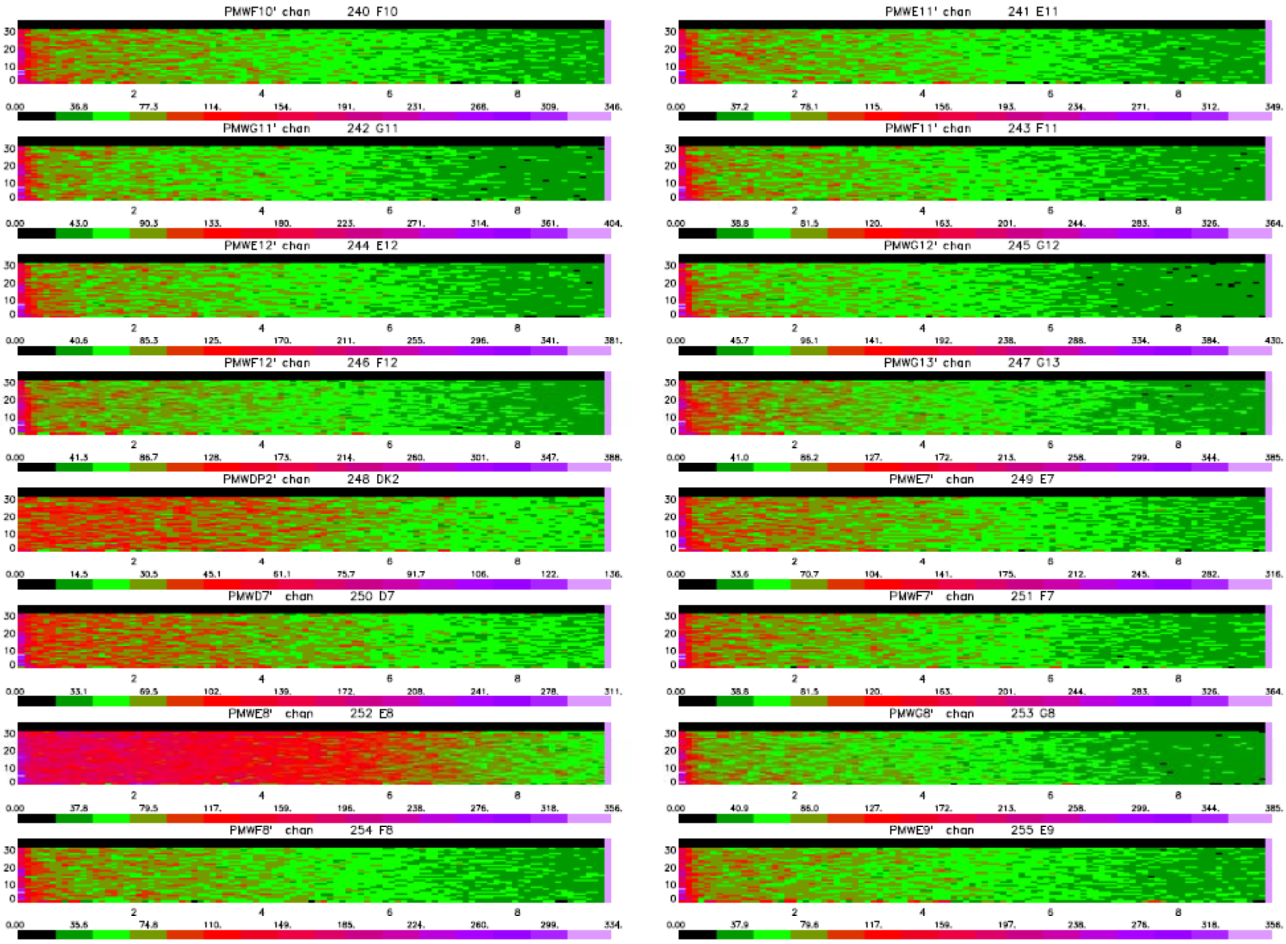
PMWF10' chan 240 F10
PMWE11' chan 241 E11
PMWG11' chan 242 G11
PMWF11' chan 243 F11
PMWE12' chan 244 E12
PMWG12' chan 245 G12
PMWF12' chan 246 F12
PMWG13' chan 247 G13
PMWDP2' chan 248 DK2
PMWE7' chan 249 E7
PMWD7' chan 250 D7
PMWF7' chan 251 F7
PMWE8' chan 252 E8
PMWG8' chan 253 G8
PMWF8' chan 254 F8
PMWE9' chan 255 E9

Figure 86

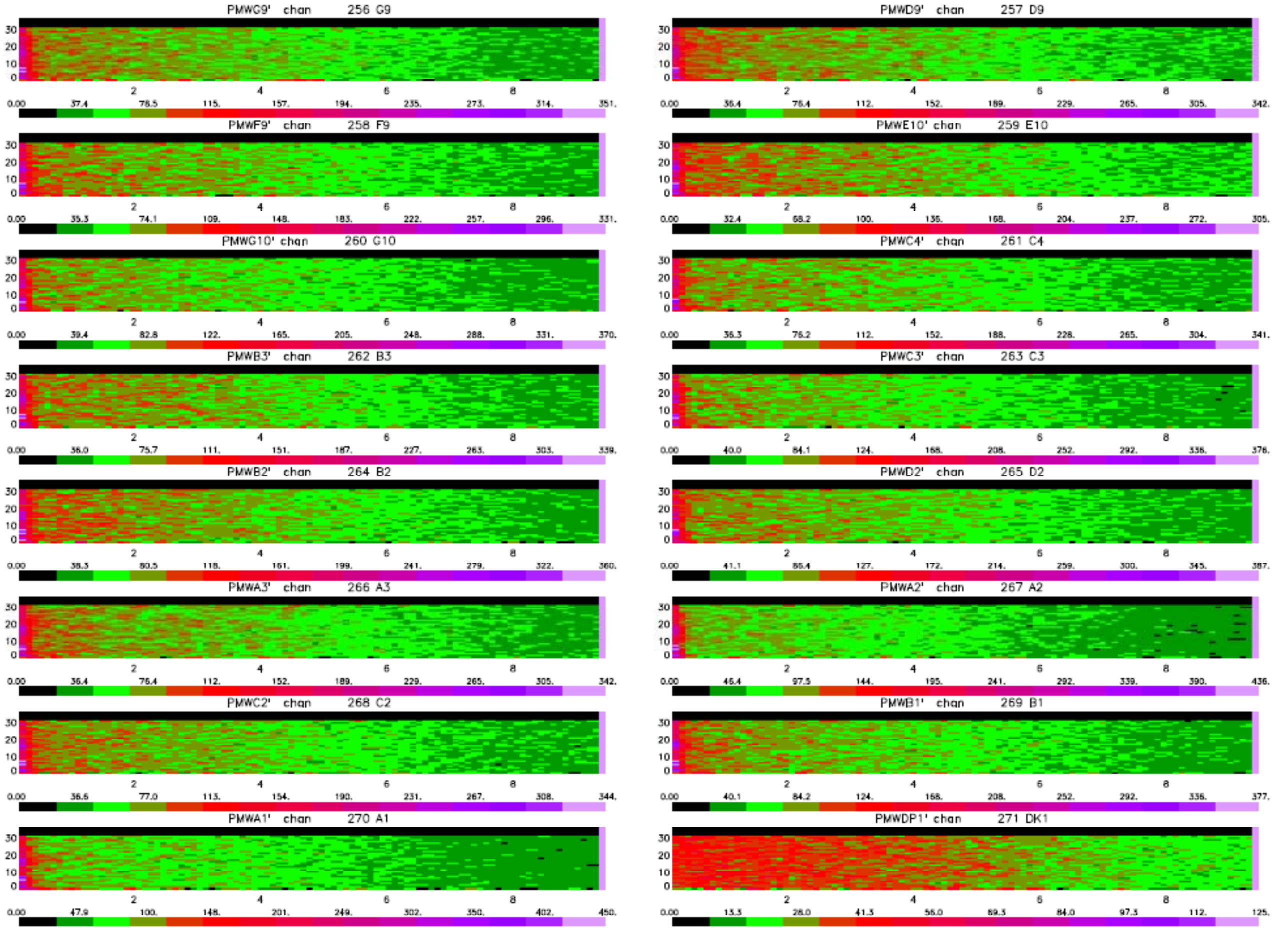
PMWG9' chan 256 G9
PMWD9' chan 257 D9
PMWF9' chan 258 F9
PMWE10' chan 259 E10
PMWG10' chan 260 G10
PMWC4' chan 261 C4
PMWB3' chan 262 B3
PMWC3' chan 263 C3
PMWB2' chan 264 B2
PMWD2' chan 265 D2
PMWA3' chan 266 A3
PMWA2' chan 267 A2
PMWC2' chan 268 C2
PMWB1' chan 269 B1
PMWA1' chan 270 A1
PMWDP1' chan 271 DK1

Figure 87

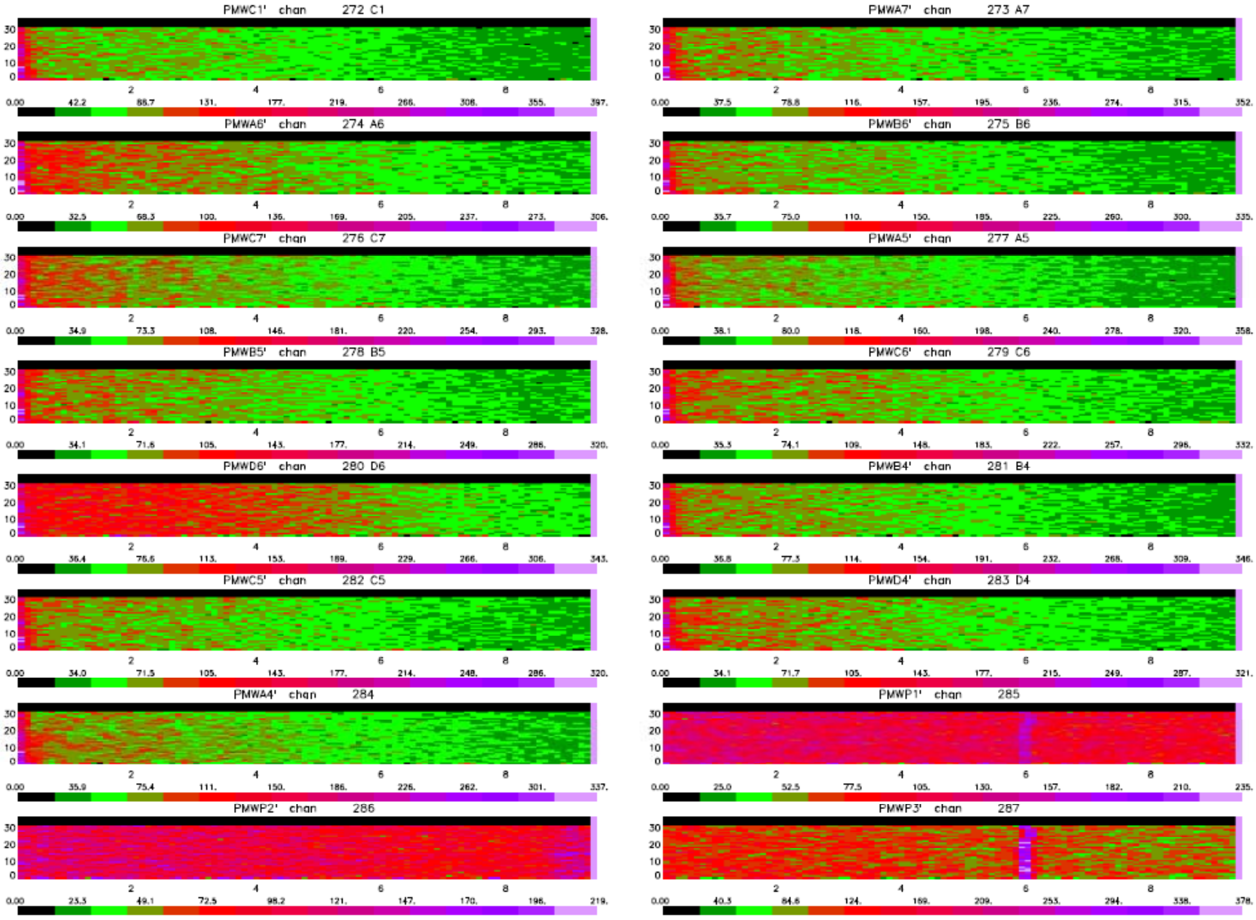
PMWC1' chan 272 C1
PMWA7' chan 273 A7
PMWA6' chan 274 A6
PMWB6' chan 275 B6
PMWC7' chan 276 C7
PMWA5' chan 277 A5
PMWB5' chan 278 B5
PMWC6' chan 279 C6
PMWD6' chan 280 D6
PMWB4' chan 281 B4
PMWC5' chan 282 C5
PMWD4' chan 283 D4
PMWA4' chan 284
PMWP1' chan 285
PMWP2' chan 286
PMWP3' chan 287

Figure 88

8.3 RS – Spectrometer: V-Polarization (0xB00014E3)

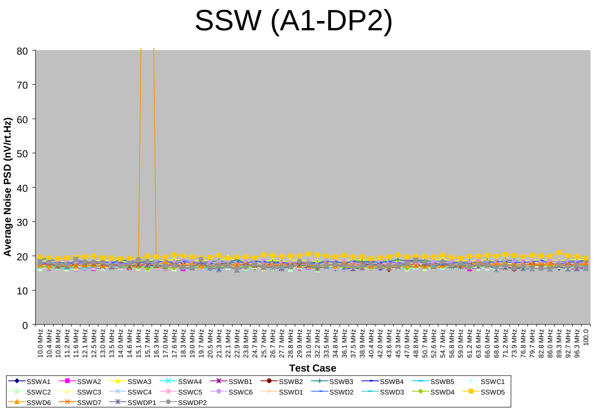

8.3.1 SLW and SSW Spectrogrammes

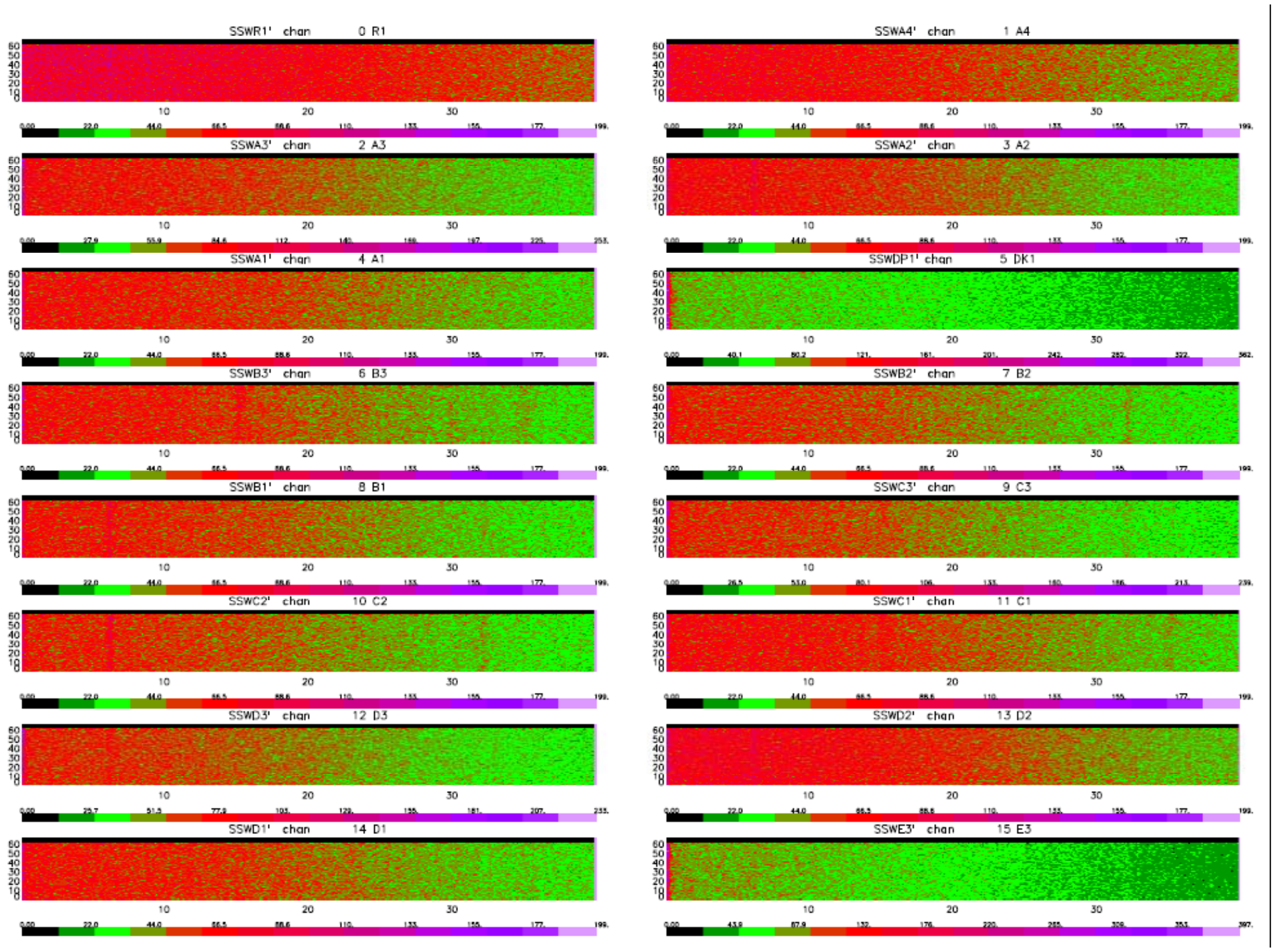

Figure 89

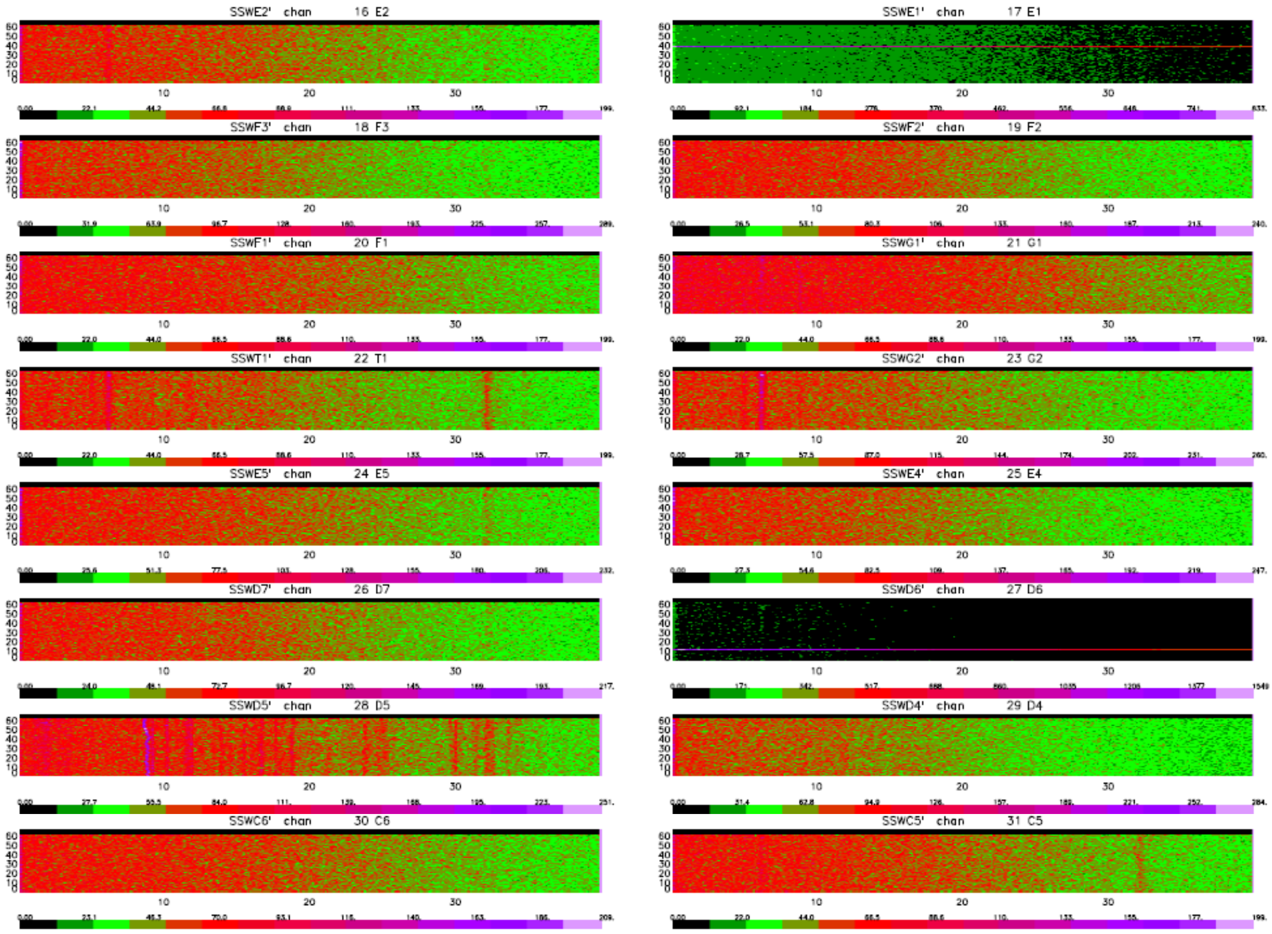

Figure 90

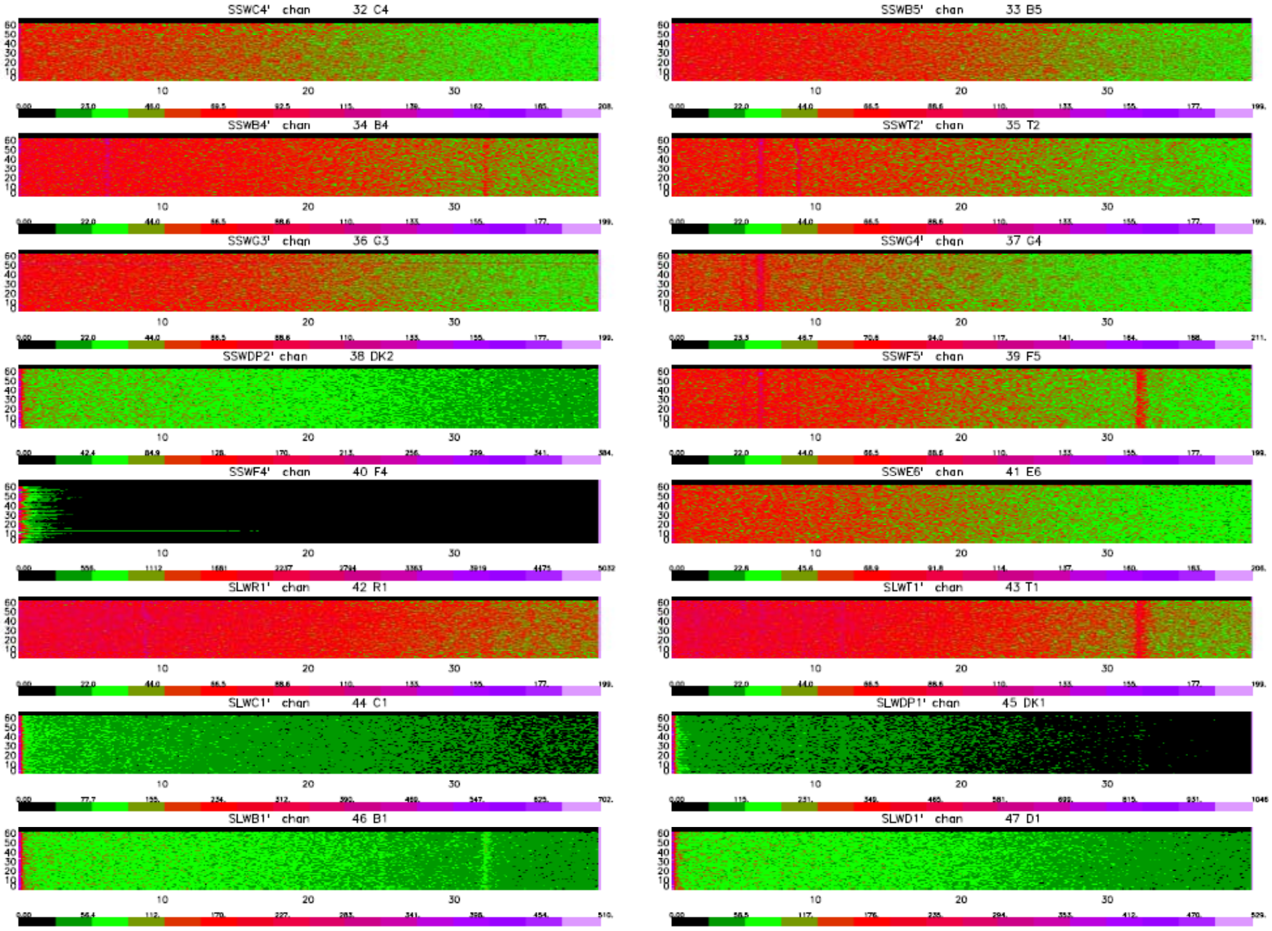
SSWC4' chan 32 C4
SSWB5' chan 33 B5
SSWB4' chan 34 B4
SSWT2' chan 35 T2
SSWG3' chan 36 G3
SSWG4' chan 37 G4
SSWDP2' chan 38 DK2
SSWF5' chan 39 F5
SSWF4' chan 40 F4
SSWE6' chan 41 E6
SLWR1' chan 42 R1
SLWT1' chan 43 T1
SLWC1' chan 44 C1
SLWDP1' chan 45 DK1
SLWB1' chan 46 B1
SLWD1' chan 47 D1

Figure 91

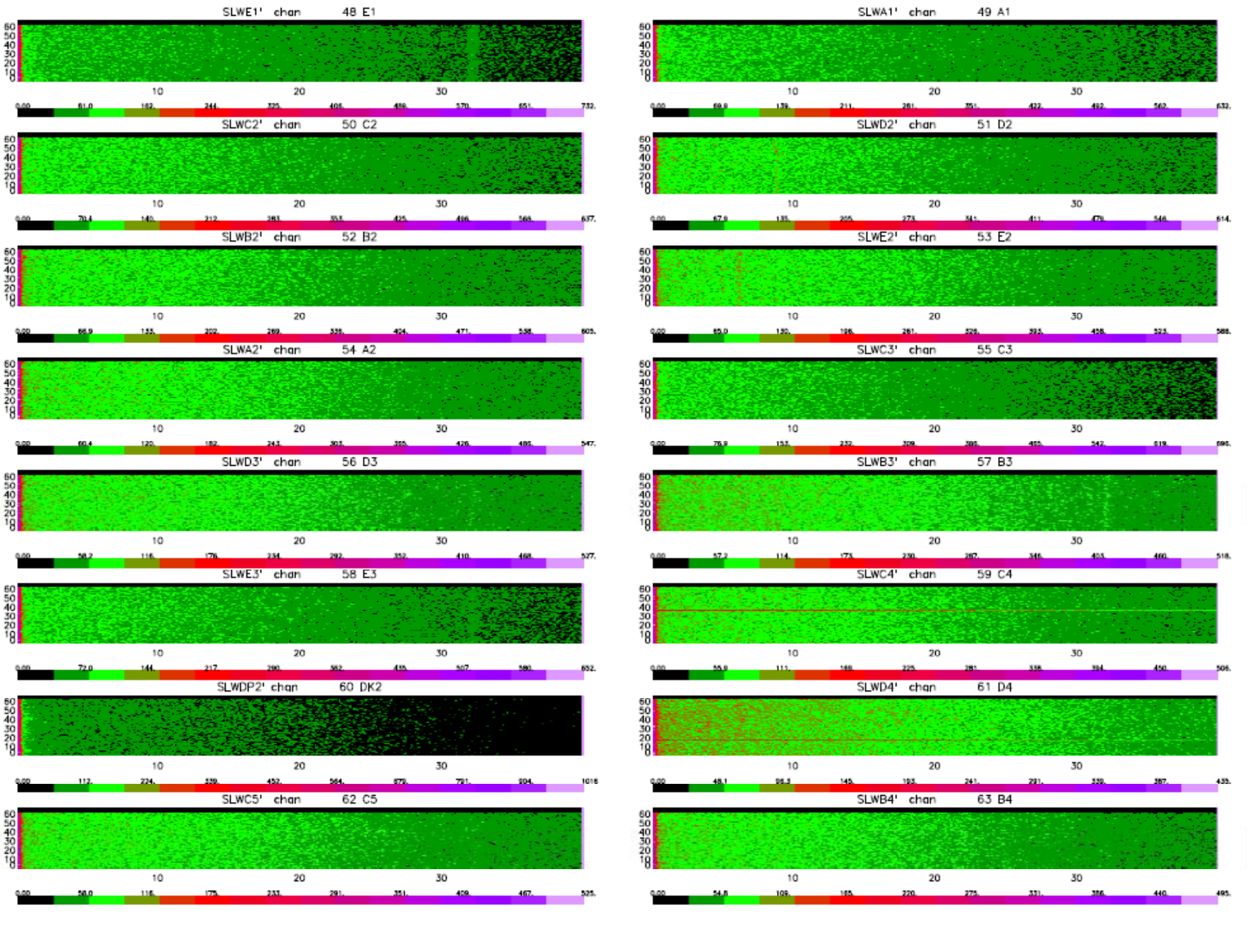

Figure 92

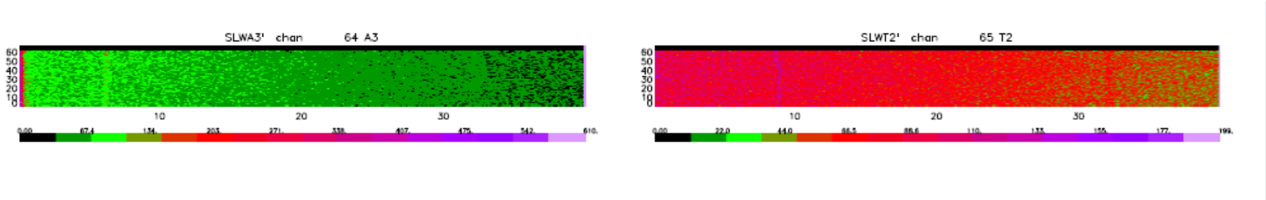

Figure 93

9. Appendix 4: RE Test Data

9.1 Key Spacecraft RE EMC Test results

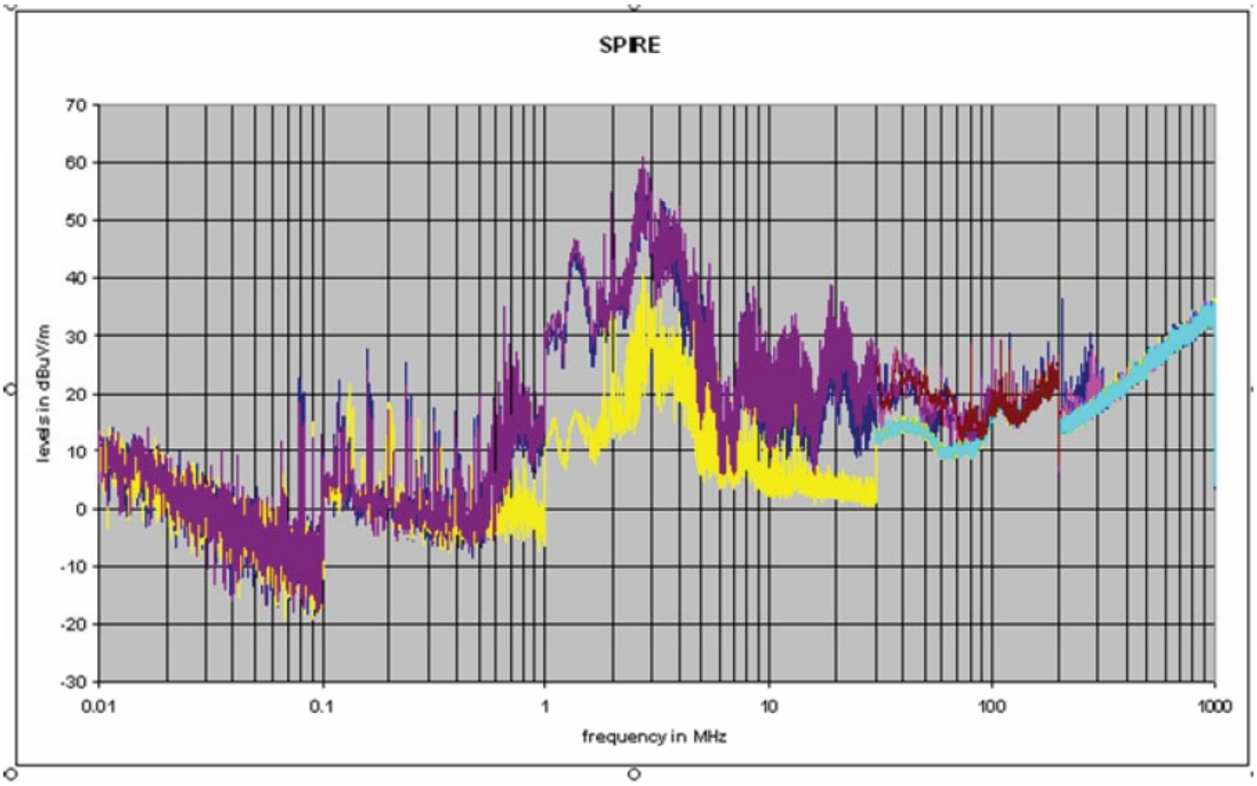

Figure 94 - RE Levels measured during the Herschel RE test in the Maxwell facility. The three traces correspond to three locations/polarizations close to the SPIRE cryoharness.

9.2 Ambient Electromagnetic Environment Monitoring

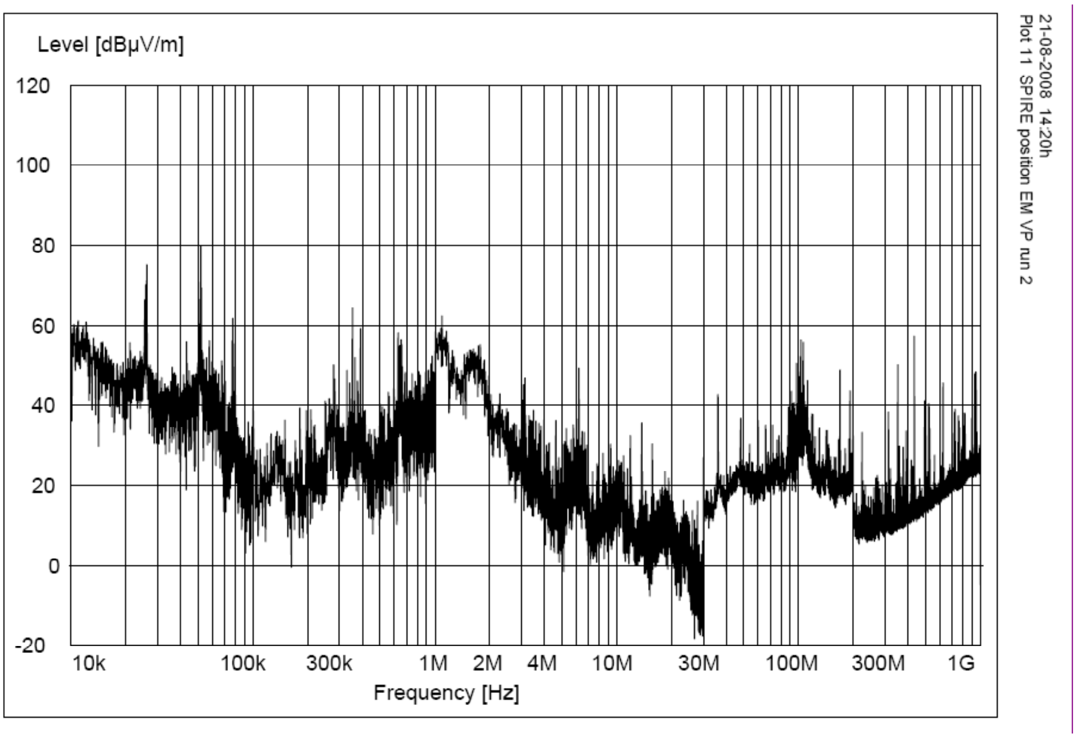

Figure 95 – E-Field ambient levels (Vertical polarization). From RD5.

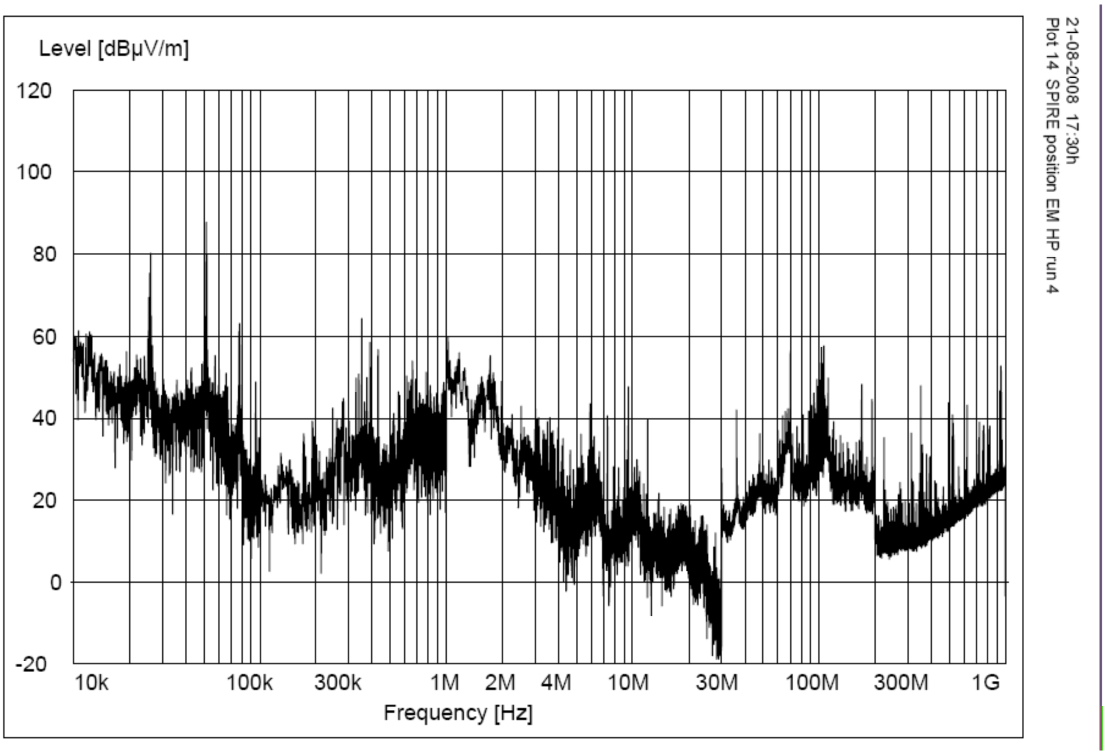

Figure 96 – E-Field ambient levels (Horizontal polarization). From RD5.